

# Re-De-Form

An interactive tool  
for the design and fabrication of  
grid shells structures.



## COLOFON

P5 Graduation Report

Master of Building Technology

July 2021

Delft University of Technology

Faculty of Architecture and the Built Environment

Julianalaan 134, Delft, The Netherlands

Isidoros Spanolios

4846982

1<sup>st</sup> mentor: Serdar Asut

2<sup>nd</sup> mentor: Olga Ioannou

—

## Table of Contents

List of Figures .....	7
Abstract .....	12
Acknowledgments .....	13
1. Introduction.....	16
1.1 Problem Statement.....	16
1.2 Research Question.....	16
1.3 Sub-questions .....	16
1.4 Objectives- Goals.....	17
1.5 Methodology Steps.....	17
2. Freeform Surface Geometry.....	20
2.1 Traditional Surface Classes.....	20
2.1.1 Rotational Surfaces.....	20
2.1.2 Translational Surfaces .....	21
2.1.3 Ruled, HP and Developable Surfaces.....	21
2.1.4 Pipe surfaces.....	22
2.1.5 Offset Surfaces.....	22
2.2 Freeform Surfaces .....	22
2.2.1 Freeform Curves.....	23
2.2.2 Bézier Surfaces.....	24
2.2.3 B-Spline and NURBS Surfaces.....	26
2.3 Meshes .....	26
2.3.1 Chapter Summary .....	27
2.4 Freeform Surface Panelization.....	28
2.4.1 Non-Rationalization.....	28
2.4.2 Pre-Rationalization.....	28
2.4.3 Post-Rationalization .....	28
2.5 Freeform Architectural Examples.....	29
2.5.1 Antonio Gaudi .....	29
2.5.2 Frank Gehry .....	30
2.5.3 Chapter Summary .....	32
2.6 Freeform Design towards the production of a digital workflow .....	33
2.6.1 Freeform Design Definition and Context.....	33
2.6.2 The Shift into Digital.....	33
2.6.3 Freeform Design Challenges.....	34
2.6.4 Chapter summary.....	36
3. The Re-De-Form.....	38



3.1 History and State of the Art on flexible molds .....	38
3.2 Re-De-Form.....	39
4. Timber Gridshell Structures.....	44
4.1 Shells & Gridshells .....	44
4.2 Timber gridshells .....	45
4.3 Timber gridshell examples .....	46
4.3.1 Mannheim Multihalle .....	46
4.3.2 Weald and Downland .....	47
4.3.3 Savill Garden .....	48
4.4.4 Pavilion ZA.....	49
4.5 Computational Form-Finding processes for shells.....	49
4.5.1 Particle Spring Method.....	49
4.4 Timber Gridshell Node Connections and Materials .....	51
4.5 Chapter Summary.....	53
5. Study of a Timber Gridshell Structure with Re-De-Form .....	56
5.1 Form-finding of a gridshell surface.....	56
5.2 From freeform to gridshell.....	60
5.3 Structurally analyzing a timber gridshell .....	65
5.4 Panelization of the freeform surface and Panel Rotational Correction .....	70
5.5 The digital Re-De-Form .....	77
5.6 The Re-De-Form prototype .....	87
5.6.1 Brainstorming.....	87
5.6.2 The Building Weeks.....	89
5.6.3 The Automation .....	98
5.6.4 The final product and its capabilities-limitations.....	103
6.1 Conclusion.....	106
6.2 Reflection.....	108
Bibliography.....	110
Appendix.....	113
Form-Finding (KangarooV2 Physics).....	113
The gridshell model.....	114
Structural Analysis.....	114
Panelization and grid placement.....	115
Panel rotational correction .....	115
Digital Re-De-Form .....	115
Output for Arduino IDE .....	116
Arduino Sketch .....	117

Model Pictures.....	122
---------------------	-----

## List of Figures

Figure 1 Rotational Surface. Curve c rotates around Axis A. Source: own illustration .....	20
Figure 2 (a) Translational Surface, k translates to rail c. (b) Extrusional surface. Source: own illustration .....	21
Figure 3 (a) Ruled Surface. (b) Hyperbolic Paraboloid (HP).. Source: own illustration.....	21
Figure 4 (a) Pipe Surface (b) Offset Surface. Source: own illustration .....	22
Figure 5 A thin birch strip (spline) fixed by hooked weights. Source: Edson International...23	
Figure 6 Bezier, B-spline, Nurbs curves with the same control polygon. Source: Pottmann et al (2007) .....	23
Figure 7 A NURBS curve c and its control polygon. In (a) the weight increases towards point p1 and in (b) the weight increases towards p3. Source: own illustration.....	24
Figure 8 (a) Translational Bezier Surface. (b) Bezier Surface Source:own illustration .....	25
Figure 9 a NURBS surface in different phases: (a) reduced weight at point p. (b) all control point weights are equal. (c) increased weight at point p. Source: own illustration.....	25
Figure 10 Quadrilateral Mesh with 30 vertices (0-29) and 20 faces (A-T). Source: own illustration .....	26
Figure 11 The Fashion and Lace Museum in Calais. (a) The facade consists of double curved glass panels. (b) The panels are joint into a steel structure that followed the panel's profile curves in one direction. Source: < <a href="https://www.moatti-riviere.com/en/projects/cultural-space/cite-internationale-de-dentelle-de-mode-calais">https://www.moatti-riviere.com/en/projects/cultural-space/cite-internationale-de-dentelle-de-mode-calais</a> >.....	28
Figure 12 (a) Triangular Mesh, (b) PQ Mesh. Notice that the triangular mesh nodes are adjacent to 6 beams, whereas the PQ nodes are adjacent to 4 beams. Source: own illustration .....	29
Figure 13 (a) Colonia Guell hanging chain model, (b) the interior Source: < <a href="https://structuresandspans.wordpress.com/">https://structuresandspans.wordpress.com/</a> > .....	30
Figure 14 Two of the freeform works of Frank Gehry: (a) Walt Disney's Concert Hall in Los Angeles California. Source: < <a href="https://www.archdaily.com/441358/ad-classics-walt-disney-concert-hall-frank-gehry">https://www.archdaily.com/441358/ad-classics-walt-disney-concert-hall-frank-gehry</a> > (b) Peix Flish Pavilion in Barcelona, Spain. Source: <a href="https://en.wikiarquitectura.com/building/golden-fish/">https://en.wikiarquitectura.com/building/golden-fish/</a> .....	31
Figure 15 DG Bank Headquarters (Horse's Head). Source: < <a href="https://www.alejandradeargos.com/index.php/en/artp/393-frank-o-gehry-architecture-in-motion">https://www.alejandradeargos.com/index.php/en/artp/393-frank-o-gehry-architecture-in-motion</a> > .....	31
Figure 16 The Guggenheim Museum Bilbao, Frank Gehry Source: < <a href="https://www.guggenheim-bilbao.eus/en/the-building">https://www.guggenheim-bilbao.eus/en/the-building</a> >.....	34
Figure 17 The link between the workflow and the challenges. Source: own illustration.....	36
Figure 18 Different versions of flexible formworks by: (a) Renzo Piano, (b) Spuybroek and (c) Vollers and Rietbergen, Source: Schipper (2015) .....	38
Figure 19 (a) The Former FlexiMold. Source: Asut, Eigenraam and Christidi, 2018, (b) The FlexiMold during the Design Informatics workshop in Poland, Source: Asut and Meijer, 2016 .....	39
Figure 20 The automation workflow as it was originally envisioned Source: Asut, Eigenraam and Christidi, 2018.....	40
Figure 21 (a) Continuous shell: axial and shear forces are visible, (b) Gridshell: the laths carry the axial forces only. Diagonal bracing carries the shear forces. Source: Shell Structures for Architecture (author added the diagonal element).....	44
Figure 22 (a) flat lath grid, (b) grid pushed towards it center, (c) grid lath by crane and self weight drags it to the ground. Source: own illustration .....	45
Figure 23 (a) The Mannheim Multihalle, aerial view. (b) Interior view of the Multihalle. Source: Burkhardt and Bächer (1978) .....	46

Figure 24 Physical model of Multihalle. Source: Burkhardt and Bächer (1978).....	47
Figure 25 (a) Cladding the roof with PVC fabric. (b) Scaffolding with struts. Source: Burkhardt and Bächer (1978).....	47
Figure 26 (a) Weald and Downland Gridshell. (b) Interior view. Source: <a href="https://www.wealddown.co.uk/buildings/downland-gridshell/">https://www.wealddown.co.uk/buildings/downland-gridshell/</a> .....	48
Figure 27 (a) Savill Garden exterior view. Source: <a href="http://www.fourthdoor.org/annular/?page_id=453">http://www.fourthdoor.org/annular/?page_id=453</a> (b) Interior view. Source: <a href="https://alchetron.com/Savill-Building#Interior">https://alchetron.com/Savill-Building#Interior</a> .....	48
Figure 28 Pavilion ZA in Cluj, Romania, Source: Naicu, Harris and Williams (2014).....	49
Figure 29 A simply supported lath modelled with the particle spring method. Note the particles, springs and gravity forces acting on the system. Source: Kuijvenhoven and Hoogenboom (2012).....	50
Figure 30 Single and double layer positioning Source: (Naicu, Harris and Williams, 2014).....	51
Figure 31 Double layer system in plan and section. Source: (Harris et al., 2003).....	51
Figure 32 (a) Slotted hole node, (b) Plate and bolts node. (c) Plate with extended bolts to support diagonal bracing. Source: Harris et al. (2003).....	52
Figure 33 (a) Plate connection with frameless glazing on top. Source: Naicu, Harris and Williams (2014). (b) Interior view of Chiddingstone Orangery. Source: <a href="https://www.glassonweb.com/news/timber-frame-gridshell-historic-orangery">https://www.glassonweb.com/news/timber-frame-gridshell-historic-orangery</a> .....	52
Figure 34 Material selection per project. Source: Based on Naicu, Harris and Williams (2014).....	53
Figure 35 Flowchart for the form finding of a freeform surface. The list of colours on the top left correspond to the different variables used within the flowchart Source: own illustration.....	57
Figure 37 The goals objects. Source: own illustration.....	58
Figure 37 Form-Finding Parameters. Source: own illustration.....	58
Figure 38 A Network Surface of degree 2 is discretized into a U-V Mesh. The example generates 15 laths in each direction. Source: own illustration.....	59
Figure 41 Post and Pre-simulation Length difference. Source: own illustration.....	59
Figure 41 Average lath distance. Source: own illustration.....	59
Figure 41 Output for Structural analysis and Panelization. Source: own illustration.....	59
Figure 42 The different surface options and their control polygon: (a) a flat surface, (b) 2 groups of points pushed inwards, (c) 3 groups of points pushed inwards, (d) 4 groups of points pushed inwards. Source: own illustration.....	60
Figure 43 The script that Evaluates the Surface of the freeform. Source: own illustration.....	61
Figure 44 (a) The intersection points p0, p1, p2 with their respective planes, (b) The NURBS freeform surface the laths create. Source: own illustration.....	61
Figure 45 The cross-section. Source: own illustration.....	62
Figure 46 The Grasshopper definition for the cross section that aligns to the local planes across the freeform surface. Source: own illustration.....	62
Figure 47 The current timber gridshell example with its dimensions in the rest position. Source: own illustration.....	63
Figure 48 The resultant laths. Source: own illustration.....	63
Figure 49 The gridshell in Section. Source: own illustration.....	64
Figure 50 The Offset surface it the cladding of the gridshell. Source: own illustration.....	64
Figure 51 Gridshell structural analysis. Source: own illustration.....	65
Figure 52 The "WOOD" material is chosen from the Karamba3D Library. Source: own illustration.....	66
Figure 53 The " Assemble Model" components contains the parameters. Source: own illustration.....	67

Figure 54 Finding the "Supports". Source: own illustration .....	68
Figure 55 The Assembled Model with the Loads and Supports. Source: own illustration ...	68
Figure 56 Deformation of the gridshell. Source: own illustration .....	69
Figure 57 Axial stresses of the gridshell. Source: own illustration .....	69
Figure 58 The Panelization lines are following the lines of the timber laths. Source: own illustration .....	70
Figure 59 Flowchart for the Panelization of the freeform surface. The list of colours on the top left correspond to the different variables used within the flowchart. Source: own illustration .....	71
Figure 60 The panel network follows the lath network. Source: own illustration .....	72
Figure 61 The panels are numbered and sorted on a grid. Source: own illustration .....	72
Figure 62 The A.13 and A.14 Actual and Hidden panels. Source: own illustration .....	73
Figure 63 Panels A.2 and A.5. Source: own illustration .....	73
Figure 64 Different rotational options. The algorithm finds the similar length of $x$ and $y$ . Source: own illustration .....	74
Figure 65 The first phase of the Rotational Correction Algorithm. Source: own illustration .....	75
Figure 66 The 2nd refinement's 1st part. Source: own illustration .....	75
Figure 67 The 2nd refinement's 2nd part. Source: own illustration .....	76
Figure 68 An overview of the rotated panels and their initial rotations. The corrected panels are marked with a pink colour. Source: own illustration .....	76
Figure 69 Orange is the initial panel and pink is the rotated one. Source: own illustration .....	76
Figure 70 The digital Re-De-Form and some example panels. Source: own illustration ...	77
Figure 71 (a) 7x7 pin Re-De-Form with in-between pin distance 30cm. (b) 10x10 pin Re-De-Form with in-between pin distance 20cm. Source: own illustration .....	78
Figure 72 The extension of the Hidden panels. Source: own illustration .....	78
Figure 73 The extended U and V curve Networks for two different panels. Source: own illustration .....	79
Figure 74 The 3x3 pin Re-De-Form. Source: own illustration .....	80
Figure 75 Scaling the panels to 1:5. Source: own illustration .....	80
Figure 76 Place the pins into their HOME position. Source: own illustration .....	81
Figure 77 Angles of rotation. Source: own illustration .....	81
Figure 78 String to Serial Monitor. Source: own illustration .....	82
Figure 79 Scaling down the gridshell's freeform surface. Source: own illustration .....	82
Figure 80 A patch between the freeform and a Rectangle. Source: own illustration .....	83
Figure 81 1:10 scale of the freeform surface on the FlexiMold. Source: own illustration .....	84
Figure 82 1:15 scale of the freeform surface on the FlexiMold. Source: own illustration .....	85
Figure 83 1:20 scale of the freeform surface on the FlexiMold. Source: own illustration .....	86
Figure 84 The flexible surface of Re-De-Form with respect to the freeform surface it represents. Source: own illustration .....	87
Figure 85 The plan of the Re-De-Form. Source: own illustration .....	89
Figure 86 Re-De-Form in Section. Source: own illustration .....	90
Figure 87 The wooden box and steel rod detail with the magnet on top. (a) in section, (b) in perspective. Source: own illustration .....	91
Figure 88 Ball connection sketch and model. Source: own illustration .....	92
Figure 89 Final ball connection sketch and model. Source: own illustration .....	93
Figure 90 (a) Sketch of the actuator system, (b) The CNC-cut racks. Source: own illustration .....	94
Figure 91 Pinion and rack definition. Source: own illustration .....	95
Figure 92 The guides of the Re-De-Form. Source: own illustration .....	96

Figure 93 The $u_0, u_1, u_2, u_3$ and $v_0, v_1, v_2, v_3$ distances change randomly, (b) The inventive system with the rubber bands. Source: own illustration .....	96
Figure 94 (a)The flexible surface on the grid, (b) The custom depth-cutting tool. Source: own illustration .....	97
Figure 95 Digital to Physical Data Transfer. Source: own illustration.....	98
Figure 96 Circuit Connections. Source:own illustration.....	99
Figure 97 The steps to use the Re-De-Form. (A)Pick a panel number, (B) Copy the values from panel, (C) Paste into the Serial Monitor and hit ENTER. Source: own illustration.....	100
Figure 98 (a) A wooden piece is used for the initial Homing of the pins. (b) he pins of Re-De-Form are Homed. Source: own illustration .....	101
Figure 99 An overview of the Re-De-Form components with their respective number and prices. Source: own illustration.....	102
Figure 100 The Re-De-Form prototype connected to the laptop. Source: own illustration .....	104
Figure 101 Re-De-Form takes the shape of a panel fed from the Serial Monitor of Arduino IDE. Source: own illustration.....	104
Figure 102 Re-De-Form responds to the Freeform Design's challenges . Source: own illustration.....	106
Figure 103 Form-Finding of a freeform surface. Source: own illustration.....	113
Figure 104 Output for Structural Analysis, Panelization and Molding. Source: own illustration .....	113
Figure 105 The gridshell. The cross-section and the pre-panelized surface are defined. Source: own illustration .....	114
Figure 106 The structural Analysis of the timber gridshell. Source: own illustration .....	114
Figure 107 Source:own illustration.....	115
Figure 108 Source: own illustration .....	115
Figure 109 1:1 model. Source: own illustration.....	115
Figure 110 Design in different scales .....	116
Figure 111 3x3 pin Re-De-Form. Source: own illustration.....	116
Figure 112 The output String the Arduino reads. Source: own illustration.....	116
Figure 113 The Arduino Sketch fed into the Arduino Megaboard. Source: own illustration .....	121
Figure 114 The components of the prototype. Source: own illustration.....	122
Figure 115 The prototype before the automation. Source: own illustration.....	122
Figure 116 Tesing posible curvatures with a flexible surface on top. Source: own illustration .....	123
Figure 117 The automated Re-De-Form with the rubber bands added. Source: own illustration.....	124
Figure 118 Me, prototyping. Source: own illustration .....	125

**“De-Form”**

Able to change shape

-

**“Re-Form”**

Able to do it multiple times

-

## Abstract

The thesis focuses on developing a workflow that utilizes an interactive flexible mold as a means of designing and fabricating freeform surfaces. The focus will be on automating a flexible mold (Re-De-Form) and use it to study and fabricate freeform surfaces. Currently, the technology associated with Re-De-Form can produce complex surfaces with double curvature. One of its predecessors, FlexiMold, consists of pins which the user moves manually after reading their position from the digital model of a surface (Asut and Meijer, 2016). The system, however innovative, lacks accuracy, to be realized as a design tool for freeform surfaces. The automation will provide with the precision and accuracy needed for a freeform surface to be produced, as well as reduce the time needed for the digital freeform to be casted onto the physical freeform. The designer is freed from the obligation to place the mold pins each time a minor change in the digital model occurs (Asut, Eigenraam and Christidi, 2018). The validity of the method is tested through the design of a timber gridshell example and its panel fabrication. This includes form finding, structural and cross-sectional study and freeform panelization. A 3x3pin small scale model of Re-De-Form that deforms according to the respective freeform digital model, has been built. Additionally, a Graphical User Interface (GUI) associated with the manipulation of the surface ensures the clarity and intuitiveness of the method to the user. The final product combines physical and digital modelling into a fast, accurate, intuitive and reciprocal freeform design tool.



## Acknowledgments

The Graduation Thesis for me was a challenging process. During the first months, I was trying to structure it and there were times where I was stuck. After P2, both my mentors Serdar and Olga tried to help me so that I can keep on working on it until my P4. Especially with my second mentor Olga, we had a walking talking session right after my P2 that gave me the guidelines on how to approach the topic and how to emphasize on parts that I know that I am capable of accomplishing. I gained a lot of knowledge in topics that I was interested in for some years before starting my Master in Building Technology but never had the proper trigger to start with. Lastly, I would like to thank my parents for their support and also my friends for being there for me during the Corona lockdown.



# 1

## Introduction

# 1. Introduction

## 1.1 Problem Statement

Freeform structures due to their high amount of complexity, pose a number of challenges during their design and fabrication phase, a problem that questions their feasibility as architectural design solutions. In addition, costs from fabrication processes that employ molds to produce free form surface panels, continue to be high and require a lot of material waste. This in turn drives designers to rationalizing freeform surface geometries to minimize the number of molds. One of the technologies related to freeform is FlexiMold, a flexible formwork that adjusts to the shape of the desired surface and used for casting their complex geometry. Flexible molds are not only used as fabrication process but also as a "design to fabrication" mechanism that aims towards realization of freeform surfaces. Freeform design poses architectural, structural and manufacturing challenges, that can be better understood through the example of gridshells. Low accuracy between physical and digital modelling, slow physical modelling production time, difficulty in structural calculations involved and surface panelization are some of the challenges, tackled with the aid of Re-De-Form, an interactive tool for the design and fabrication of gridshell structures.

## 1.2 Research Question

*"Developing a "design to fabrication" workflow that corresponds to the design process and materialization of a timber grid-shell structure, while also establishing an automation process to provide the Re-De-Form with more accuracy/precision in producing freeform surfaces."*

## 1.3 Sub-questions

1. How to study freeform surfaces through Re-De-Form?
2. How can the Re-De-Form be upgraded towards a more fast and accurate mechanism for freeform exploration?
3. How to design a timber gridshell and fabricate its panelization?
4. How can the Re-De-Form be utilized for gridshell design and panel fabrication?

### 1.4 Objectives- Goals

1. Perform an analysis of freeform surfaces and the challenges they pose towards their design.
2. Study the requirements of a timber grid-shell towards its form-finding, materiality, structural analysis, panelization.
3. Relate Re-De-Form to the designing and fabrication process of a grid shell structure.
4. Test the automated workflow using a prototype of Re-De-Form.

### 1.5 Methodology Steps

The Methodology Steps involve the combination of the digital and physical environment of Re-De-Form. These answer the main research question and the sub-questions previously posed.

At first, the Form Finding of a freeform surface is performed and based on that, a timber gridshell geometry is generated. The gridshell is then Structurally Analysed and Panelized to fit Re-De-Form.

Secondly, the automation of Re-De-Form and its link to the freeform timber gridshell structure is implemented. Re-De-Form is designed digitally and linked to the Panelization of the timber gridshell. A scenario of freeform surface physical modelling is discussed too. Then a physical prototype of Re-De-Form designed and assembled in the Faculty of Architecture and the Built Environment, TU Delft. This includes the collection and testing of physical equipment and available technologies from various sources (pins, actuators, details). The next step is to link the positional data of Re-De-Form from the digital to the physical prototype through the use of the Arduino IDE and Rhinoceros-Grasshopper.

(End of chapter)





# 2

## Freeform Surface Geometry

## 2. Freeform Surface Geometry

Freeform architecture is a term linked to architectural forms that are composed of one or more freeform surfaces. It is important to understand the nature of the existent traditional surface classes in order to define the freeform surface as a stand-alone class and not a sub-set of these.

### 2.1 Traditional Surface Classes

The surfaces undergoing this term are mostly characterized by a basic "kinematic" generation because their geometry is the outcome of a smooth sweep performed by a profile curve (Pottmann et al, 2007). These are generated by a geometric family of curves and straight lines and can also be described as a two-dimensional locus of points that define a three-dimensional solid (Ching, 2014). Translational, rotational, helical and pipe surfaces are examples of traditional surfaces and a more detailed presentation of these can be found in Pottman et al (2007).

#### 2.1.1 Rotational Surfaces

Rotational surfaces are generated by rotating a planar or spatial curve  $c$  around an axis  $A$  (Toussaint, 2007). Every point of the curve  $c$  is described by a circle  $C_p$  whose plane is perpendicular to the axis  $A$ . Meridian curves  $m$  are the congruent planar slices of a plane that contains the axis  $A$ , rotates around it and intersects with the surface. A net of orthogonal curves is formed on the rotational surface by the intersection of the meridian curves  $m$  and the parallel circles  $C_p$ . A supporting plane  $S_c$  is perpendicular to the plane  $M$  and contains the circles  $C_p$ .

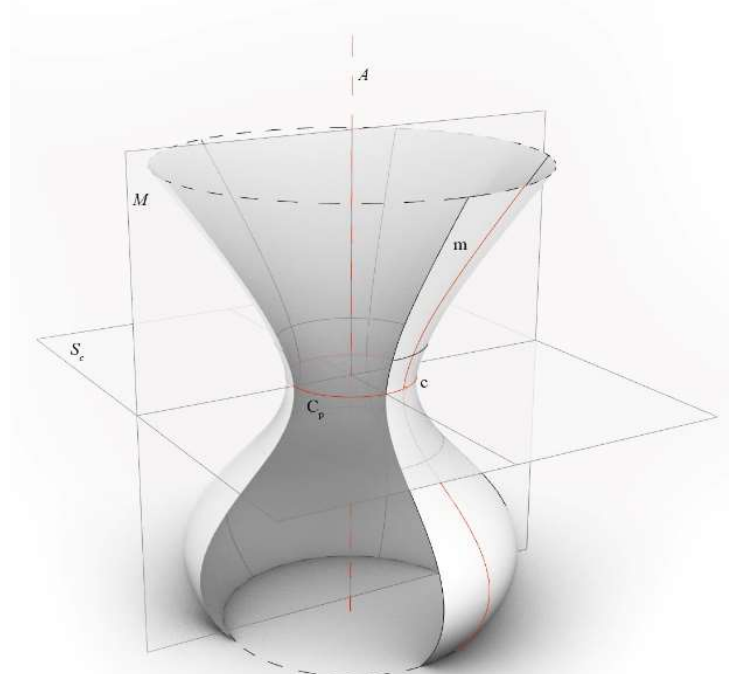


Figure 1 Rotational Surface. Curve  $c$  rotates around Axis  $A$ .  
Source: own illustration



### 2.1.2 Translational Surfaces

Imagine two curves  $k$  and  $c$  which intersect in a single origin point  $o$ . The translational surface is generated by translating the profile curve  $k$  along the path  $c$ .  $k_p$  are curves contained in the surface congruent to the initial curve  $k$ . If the path  $c$  is a straight line then the translation is an extrusion.

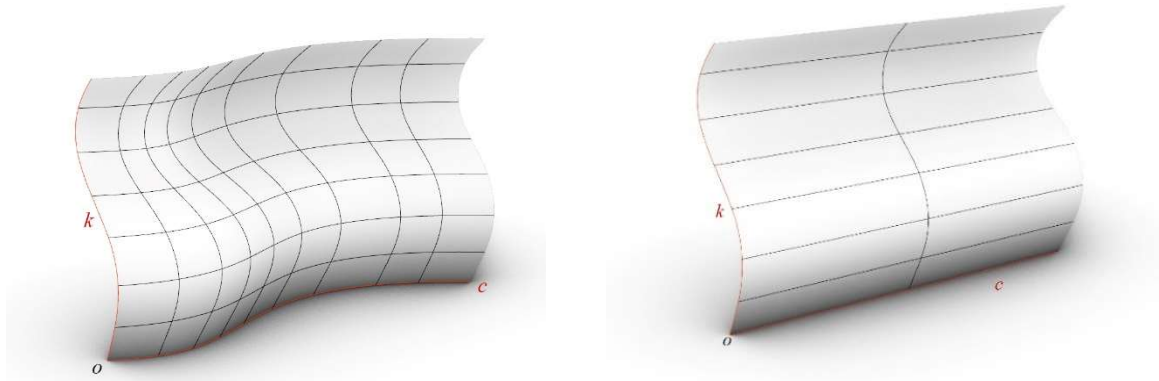


Figure 2 (a) Translational Surface,  $k$  translates to rail  $c$ . (b) Extrusional surface.  
Source: own illustration

### 2.1.3 Ruled, HP and Developable Surfaces

Ruled surfaces contain a continuous family of straight lines named generators or rulings. Examples of these are the cylinder, cones, one-sheet hyperboloids and hyperbolic paraboloids, surfaces that carry families of straight lines. These can also be generated by moving a straight line (Pottmann et al, 2007).

In most cases, ruled surfaces are created by moving a point  $p$  on a straight line (segment)  $k$  along the directrix curve  $c$  (Van de Straat, 2011). The continuous change in the direction of the line  $k$  generates the ruled surface's final geometry.

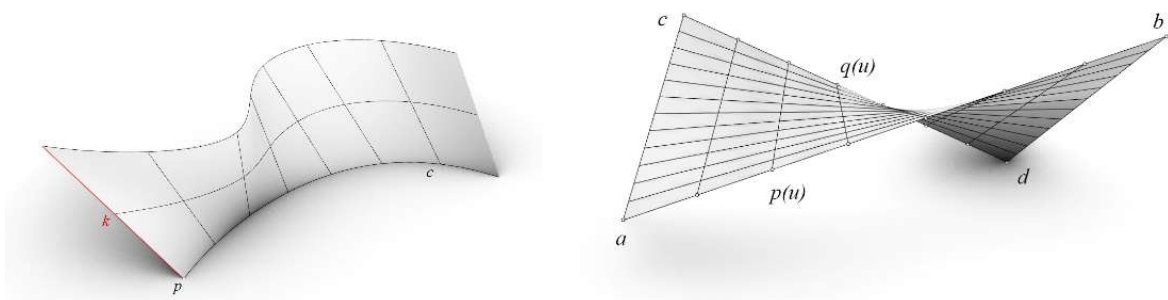


Figure 3 (a) Ruled Surface. (b) Hyperbolic Paraboloid (HP).. Source: own illustration

HP Surfaces (Hyperbolic paraboloids) are excessively used in the area of shells because their positive static properties allow the construction of large spans with a relatively small thickness. (Pottmann et al, 2007). Two skewed vline segments  $ab$  and  $dc$  are equally divided into a number of points  $p$  and  $q$  respectively. Points  $p$  of line  $ab$  and points  $q$  of line  $dc$  correspond to each other. By connecting them an arbitrary ruling of the HP surface is obtained. It is important to state that this type of surface can also be generated as a translational surface.

Developable surfaces are ruled surfaces, but not all ruled surfaces are developable. Their main property is that they can be unrolled onto a flat plane so that the in-surface point's distances are not changed.

### 2.1.4 Pipe surfaces

Pipe surfaces is the envelope of spheres of equal radius  $r$  whose centers lie on a curve  $c$ , named spine or central curve. The pipe surface is determined by a spine curve and a radius  $r$ . They can be created by a family of circles of radius  $r$  that lie on the normal planes of the spine curve.

### 2.1.5 Offset Surfaces

The offset operation is added to the design when the designer wants to add thickness. In the construction of shell structures this is an add-on that makes the final design more realistic. A surface  $S$  is given. The offset surface  $S_b$  is the surface with a constant normal  $b$  distance from the original surface  $S$  (Tomiric, 2013). Both surfaces share the same normals while their tangent planes are parallel to their respective points on the surface. Both surfaces are called parallel surfaces.

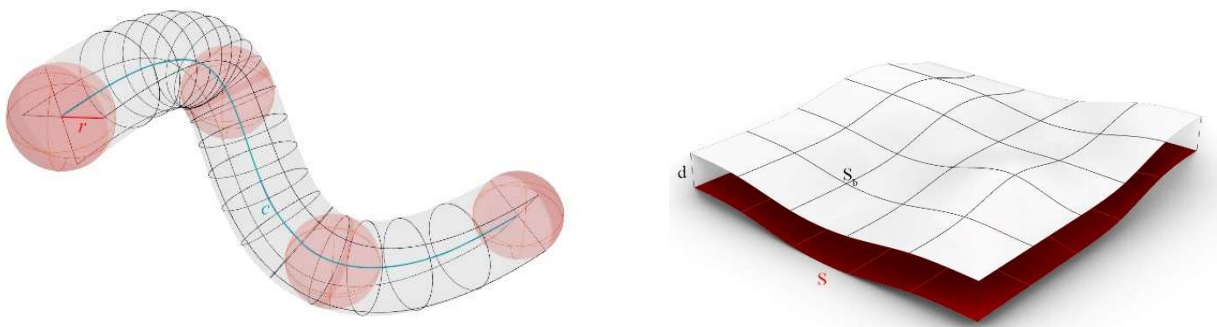


Figure 4 (a) Pipe Surface (b) Offset Surface. Source: own illustration

## 2.2 Freeform Surfaces

Traditional surfaces, such as cylinders, cones spheres, rotational surfaces and ruled surfaces do not always meet sufficiently the demands of designing 3d complex geometries found in contemporary architecture. Freeform surfaces offer more flexibility compared to rotational, translational or ruled surfaces. In this chapter, the types of surfaces discussed are: the Bézier surfaces, B-Spline Surfaces and subdivision surfaces. The latter type overcomes the topological limitations that the Bézier and Spline Method possess (Pottmann et al, 2007).

### 2.2.1 Freeform Curves

Freeform surface modelling requires a fundamental knowledge of the freeform curves. Before the use of computers designers used to draw them by hand with the use of mechanical aids. The curve quality and precision depended on the skill of the designer. Especially for long curves the entire hand had to be kept moving making the curve designing process very demanding and labour intensive. Sometimes mechanical aids called splines were integrated. Their setup consisted usually of a thin bendable wooden or metal rod whose shape follows the curve and is pinned down by weights.



Figure 5 A thin birch strip (spline) fixed by hooked weights. Source: Edson International

Computer Aided Design (CAD) softwares imitate this approach by introducing Bézier, B-spline and NURBS curves. These curve types are defined by a number of control points connected to a control polygon. The control points coordinates are fed into the respective curve geometric algorithm that outputs the final curve

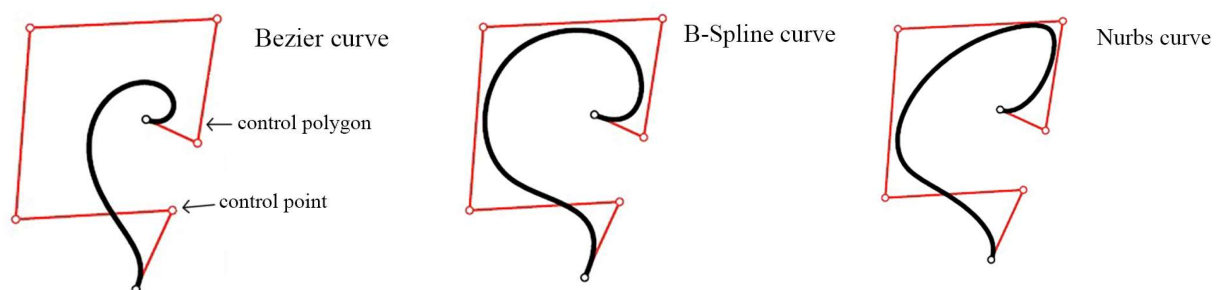


Figure 6 Bezier, B-spline, Nurbs curves with the same control polygon. Source: Pottmann et al (2007)

#### 2.2.1.1 Bézier Curves

The need for more complex curves than parabolas and hyperbolas in the airplane and automotive Bézier curves. They utilize the *Casteljau algorithm* a geometric process based on repeated *linear interpolation* (Tomiric, 2013). While they are totally defined by their control polygon they are the most widespread freeform curves due to their simplicity in use (Pottmann et al, 2007).

#### 2.2.1.2 B-Spline Curves

B-Spline curves consist of Bézier curve segments of the same degree that are connected at their endpoints with the highest smoothness possible (Tomiric, 2013). The B-Spline is defined by the control points  $d$ , the degree  $n$  and the knot vectors. The control points define

the overall curve shape. The degree refers to the degree of its Bézier counterparts and the knot vector identifies the points where the Bézier curves are connected.

### 2.2.1.3 NURBS Curves

NURBS curves are a more sophisticated curve and can generate a wider variety of curves. They utilize an additional parameter associated with the control points, the so-called weights. By increasing the weight of the control point, the curve is driven towards it and by decreasing it the curve moves away from it. B-spline curves are special cases of NURBS curve that all control points share the same weights (Pottmann et al, 2007).

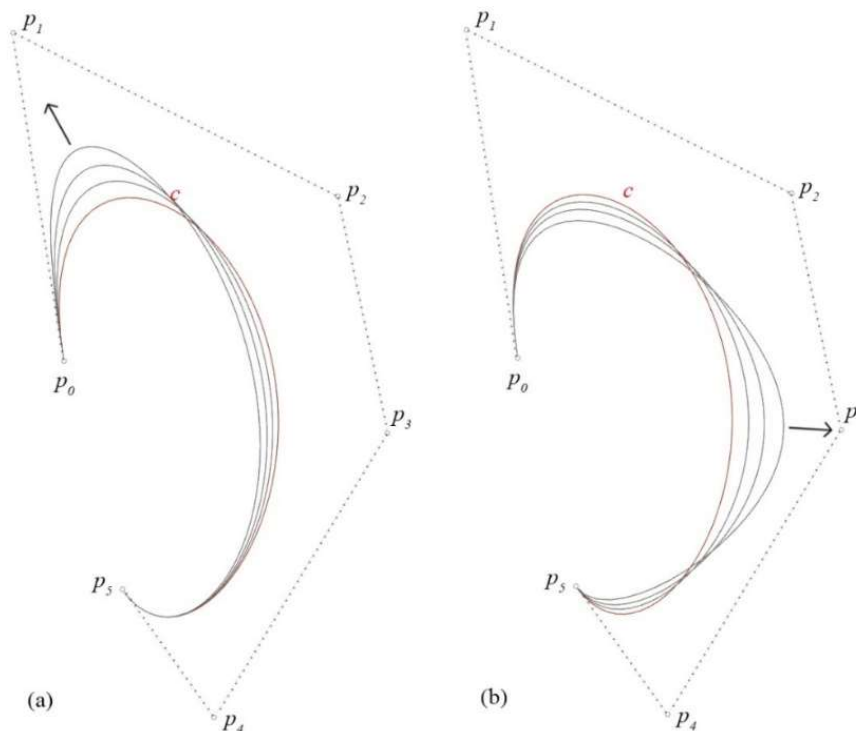


Figure 7 A NURBS curve  $c$  and its control polygon. In (a) the weight increases towards point  $p_1$  and in (b) the weight increases towards  $p_3$ . Source: own illustration

## 2.2.2 Bézier Surfaces

### 2.2.2.1 Translational Bézier Surfaces

Translational Bézier Surfaces are created by Bézier curves. The example illustrated contains two Bézier curves, the first of degree 2 and the second of degree 3. Both curves share the same starting point  $b_{00}$  for the translational surface to be generated. Their control points are displayed with double index notation, thus the quadratic Bézier curve  $b^2$  holds the points  $b_{00}$ ,  $b_{10}$ ,  $b_{20}$  while the cubic Bézier curve  $b^3$  is defined by the  $b_{00}$ ,  $b_{01}$ ,  $b_{02}$ , and  $b_{03}$ .

The translational surface carries a family of quadratic Bézier curves and a family of cubic curves. Distinguishing between those two is needed, so the parameter on  $b^2$  is denoted as  $u$  and the parameter on  $b^3$  as  $v$  (Pottmann et al, 2007)

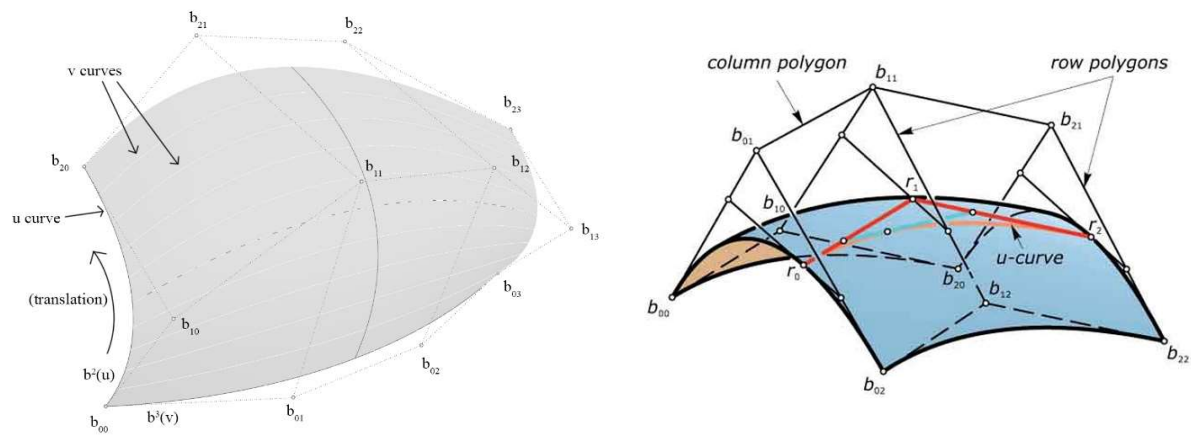


Figure 8 (a) Translational Bézier Surface. (b) Bézier Surface Source:own illustration

### 2.2.2.2 General Bézier surfaces

The General case is a straightforward extension of translational Bézier surface logic. A control mesh is the input of a Bézier surface and it consists of an array of points, represented by a quadrilateral mesh of columns polygons and row polygons. Two indices are used again for each control point. The first index ranges between  $0, 1, \dots, m$  defining the row and the second between  $0, 1, \dots, n$  defining the column. The number of control points is  $(m+1)(n+1)$ . Resembling the translational Bézier surfaces, the surface contains two families of Bézier curves: the first family in  $u$  direction of degree  $m$  and the second family in  $v$  direction of degree  $n$ . Bézier surfaces have a degree of  $(m, n)$  (Pottmann et al, 2007).

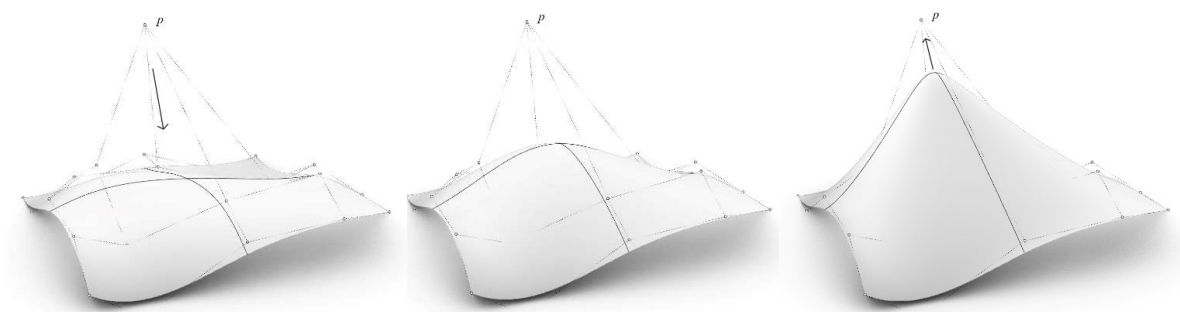


Figure 9 a NURBS surface in different phases: (a) reduced weight at point  $p$ . (b) all control point weights are equal. (c) increased weight at point  $p$ . Source: own illustration

### 2.2.3 B-Spline and NURBS Surfaces

The drawbacks derived from Bézier curves in curve design are inherited in the design of Bézier surfaces too. By increasing the Bézier surface degree the final surface represents the control mesh poorly. The alternative is to change the control point coordinates which changes the overall surface. Bézier surfaces are unable to perform a local control of their points.

On the other hand, B-spline Surfaces overcome this problem by allowing the user to change the degrees for the u and v curves of the surface. They are also defined by a quadrilateral control polygon. To add to that, the NURBS Surfaces can also perform weight control to each one of their control points, enabling local control of the final surface. The B-Spline Surface similar to the B-Spline Curve, is a type of NURBS Surface wherein all control points share the same weight (Pottmann et al, 2007)

### 2.3 Meshes

The types of surfaces discussed above belong to the family of the smooth surfaces and their realization in an architectural scale of a building may not be feasible due to the budget constraints that usually occur. Instead, meshes are being used in many of the freeform examples found in architecture.

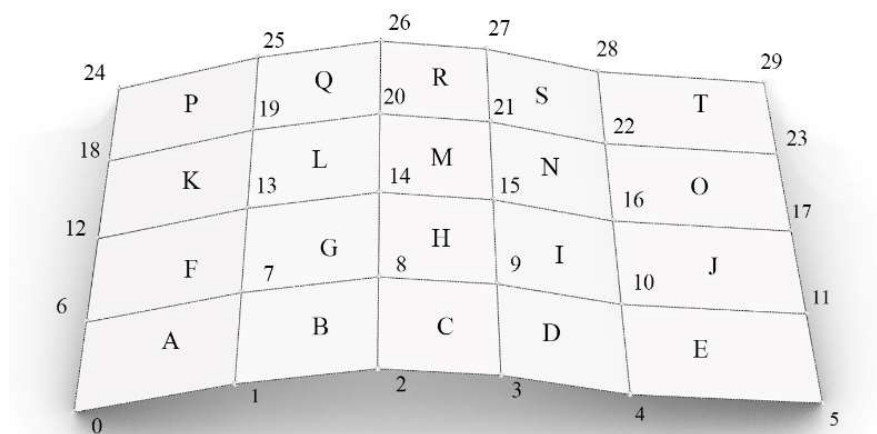


Figure 10 Quadrilateral Mesh with 30 vertices (0-29) and 20 faces (A-T). Source: own illustration

Meshes contain a collection of points (vertices) connected together by faces. Each face is bounded by an individual polygon and the typical types of polygons used are triangular, quadrilateral or hexagon. The collection of polygons is a discretization or else a rough representation of a smooth surface (Pottmann et al, 2007).

Meshes are usually consisted of one type of face. Frequently used face types are triangle, quadrilateral and hexagonal. Meshes are stored in two lists. The first contains the x,y,z coordinates of the polygon's points (Cheng, Zhang and Tang, 2007). The indices of the list contain the x,y,z values of each vertex. The second list contains the faces. The indices from the first list are appended into a sequence regarding the 3D position of the points and the faces. This list displays the connectivity of the vertices in relation to the faces of the mesh.

### 2.3.1 Chapter Summary

Understanding the literature behind freeform geometry is a step towards the creation the digital workflow. Traditional Surfaces will not be used in this case, due to the limited surface complexity, they can represent. Freeform Surfaces and Meshes are utilized instead. The freeform surface is fed into Re-De-Form for the surface study and panel production and the mesh model is fed into the tool used for structural analysis. These are further elaborated in the next chapters.



## 2.4 Freeform Surface Panelization

Freeform surfaces in a building scale need to be segmented into smaller building components to be realized. The process of “panelization” refers to the approximation of a surface by a number of panels that are produced by a certain technology, while maintaining the design intent, aesthetic quality and surface smoothness (Eigensatz *et al.*, 2016). Freeform surfaces depending on the type of panelization are discretized into 3 typical classes, the non-rationalized, the pre rationalized and the post-rationalized (Schiftner *et al.*, 2013). Some projects utilize more than one of the methods described above.

### 2.4.1 Non-Rationalization

In the non-rationalized method the pattern of the structure and panels is chosen freely but in most examples the principle that applies is that the freeform surface is intersected with a regular grid of planes. That technique is subject to the panel size, material, budget and production techniques available at that time. The Cité de la Dentelle et de la Mode in Calais of the Paris-based architects Alain Moatti and Henry Rivière is an example of such method (Cité de la dentelle et de la mode, n.d.). Its double skinned façade is generated by a basic computational model of arc splines. The panels were clamped to a horizontal and vertical grid of steel.



Figure 11 The Fashion and Lace Museum in Calais. (a) The facade consists of double curved glass panels. (b) The panels are joint into a steel structure that followed the panel's profile curves in one direction. Source: <<https://www.moatti-riviere.com/en/projects/cultural-space/cite-internationale-de-dentelle-de-mode-calais>>

### 2.4.2 Pre-Rationalization

Pre-rationalization is achieved by introducing traditional surface classes into the freeform design process, such as translational, rotational or developable surfaces. Frank Ghery's paper and thin metal sheet models are a great example of utilizing these methods into design because of their developability attributes and property-resemblance to the material of steel. Some of his designs are discussed in the next section.

### 2.4.3 Post-Rationalization

The Post-rationalization method uses an ideal freeform surface as a reference. The resultant geometry, after the rationalization, closely resembles the freeform surface and it subjects to typical criteria such as cost, surface manufacturability, size or surface and substructure quality.



Triangulation is one of the most straight forward post-rationalization methods because no restrictions apply on the alignment of panel's seams. One of their disadvantages is that when the freeform triangulated geometry offsets, the nodes and substructure's complexity increases. On the other hand, Planar-Quad Panelization was harder to achieve because the necessary mathematical tools needed to describe them did not exist. Therefore, the main advantages of planar-quads compared to triangles are their ability to offset with reduced geometrical complexity of their formwork, less panel-cutting waste and their decreased joint lengths. The joint complexity of a PQ (Planar Quadrilateral) mesh is less too, considering the fact that one joint has four beams and a triangular mesh joint has 6.

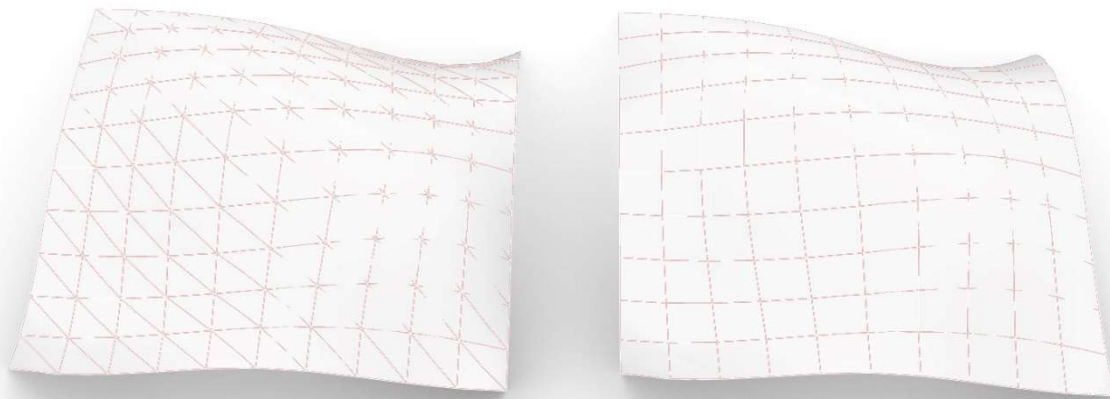


Figure 12 (a) Triangular Mesh, (b) PQ Mesh. Notice that the triangular mesh nodes are adjacent to 6 beams, whereas the PQ nodes are adjacent to 4 beams. Source: own illustration

## 2.5 Freeform Architectural Examples

Freeform surfaces and complex geometry exploration has started before the modern computer age. Examples include dome-like wooden shelters, non-reinforced concrete domes, or prismatic glass domes. With the introduction of reinforced concrete into the building industry in the middle of the 20<sup>th</sup> century, architects and structural engineers started exploring freeform shapes (Henriksson and Hult, 2015). Before computers become available, physical modelling was used in order to define the shape of complex buildings by both architects and structural engineers. Some of the works of Antonio Gaudi and the more contemporary, Frank Gehry will be discussed due to their contribution to the knowledge regarding freeform surfaces.

### 2.5.1 Antonio Gaudi

Antonio Gaudi (1852-1926) a famous Spanish Catalan architect, was driven by the notion that the forms found in nature except for being aesthetical appealing are also structurally functional. By imitating natural forms he believed that his designs would inherit their structural performance too. Forms deriving from funicular lines, move away from geometries such as vertical piers and buttresses that were used in the past and guided him through design solutions due to which he stands out as a well-known architect.



Figure 13 (a) Colonia Guell hanging chain model, (b) the interior Source: < <https://structuresandspans.wordpress.com/> >

Gaudi used three-dimensional scale models during the form finding phase. For the design of Colonia Guell, Gaudi built a 4 meter high, 1:10 scale physical model with the use of weights connected to hanging strings. The resultant catenary curves produced compression-only vaults and arches. Then Gaudi took pictures of the model from different angles and produced the profiles of the catenary curves (Bassegoda Nonell, 2000). In other words, he converted the data generated from physical models with the use of the hanging chain method into architectural data that would help him realize his designs. This is a laborious and time consuming process, but also an inevitable one when the designer wants to gain insight on the complex shape of the building, the structural performance and essential architectural data such as curve profiles, local vault height-span relation, in between arch connections. His design methodology implicitly demonstrates a shift from the physical study of a complex form into information that can be used to realize it.

In later years with the technological advancements, the insight Gaudi tried to gain from his physical models will be available through computer simulations and digital physics engines. With the use of these technologies, optimal structural forms and the structural calculations associated with them are recreated into digital environments. However his contribution into understanding the physics behind the structural behaviour of complex forms needs to be mentioned.

## 2.5.2 Frank Gehry

Another example of freeform architecture is Frank Gehry. His methodology for realizing freeform surfaces utilizes physical modelling with the combination of digital tools. Two of the examples shown are Disney's Concert Hall or the Peix (Fish) pavilion in Barcelona, where the digitization of the large physical models, is performed with the use of mechanical tracking devices. The data captured by the 3D-digitizer are fed into CATIA-3D a design software used mostly in the aeronautical sector during that time. Once digitized the building

can be further computer analyzed and detailed architectural drawings needed for fabrication are created (Hadjri, 2005).

However, this approach brings to light issues that blur the clean relationship between the physical and digital representation. In this case, the geometry of the physical model is a reliable representation of the design intent that the digital model strives to achieve (Shelden, 2002). A great effort is needed to transmute physical data to digital even with the use of highly accurate digitizing technologies. The difficulty lies on the fact that the imperfections and inaccuracies of the physical model need to be removed and that the digital model has to resemble the physical through a geometry that can be manipulated and manufactured.



Figure 14 Two of the freeform works of Frank Gehry: (a) Walt Disney's Concert Hall in Los Angeles California. Source: < <https://www.archdaily.com/441358/ad-classics-walt-disney-concert-hall-frank-gehry> > (b) Peix Flsh Pavilion in Barcelona, Spain. Source: <https://en.wikiarquitectura.com/building/golden-fish/>

That led Frank Gehry into pre-rationalizing his "freeform" designs into classes of traditional surfaces, such as rotational translational or developable surfaces. This limitation is applied due to practical and economic reasons associated with the cost assembly and production of a mold. For each individual surface element a custom mold is needed for the molding or stamping of the surface material on it (Shelden, 2002).



Figure 15 DG Bank Headquarters (Horse's Head). Source: < <https://www.alejandradeargos.com/index.php/en/artp/393-frank-o-gehry-architecture-in-motion> >

In the example of the conference room of the DG Bank Headquarters (Horse's Head) wherein steel is the predominant material, due to its high strength, to be formed it should follow a stamping process that exceeds the typical costs. The study of a flexible formwork that resembles to the surface of each panel would be a good alternative into fabricating the paneling of the structure. Such technologies were not available at that time for mass-production fabrication.

However, the works of Frank Gehry was an initiative for the development of new digital and manufacturing techniques. The standard building components of the modern era could not accommodate the non-standard freeform design current growing at that time, while computer technologies make the designing and manufacturing of complex building forms more common,

### **2.5.3 Chapter Summary**

The chapter showcases through examples the importance of physical and digital modelling when studying free form. In its more primitive phase from Gaudi with the use of photography to Gehry with the utilization of 3D digitizing devices the intention to translate the physical into digital and back is common. The benefits of the connection between these two as well as to the study of the freeform will be given in the next chapter more in detail.



## 2.6 Freeform Design towards the production of a digital workflow

### 2.6.1 Freeform Design Definition and Context

FreeForm design is identified as a new and cross-disciplinary domain and is characterized as representative of the larger scale of impact of digital technologies on building design and production. The term is addressed by two entities, "freeform" and "design". As previously discussed "freeform" is closely related to the geometry and the mathematical algorithms that designers use to simulate curvilinear forms. "Design" is referring both to the architectural object and to the processes that start from the thin world of paper towards the realization of the final product. In other words, freeform design is approached by the computational methods that run towards its generation and not only with its highly curvilinear architectural qualities. Computer-generated freeform surfaces stand as a new architectural language that contains the least repetitive parts possible. (Borgart and Kocaturk, 2008).

The relationship of the emerging digital and technological techniques in design and realization of freeform also needs to be addressed. Zellner (2000) and Kolarevic (2004) have outlined many facts that concern the design practice itself in relation to its emerging technological content and the evolving digital form-generation and manufacturing techniques. Kolarevic argued that the architect has a direct relationship with his/her tools and that the architectural outcome is bonded to the software used during the design phase. He presents many examples of "blob" forms in a way that the reader can understand the fundamentals of digitally-driven generative design and production technologies, rather just mere tools for exploring these forms.

In addition to that, Oxman (2006) carries out a research on the theoretical and conceptual framework of digital design by defining its historical background. She also defines a generic schema of design characteristics with which she classifies digital design in order to conclude to the "digital design thinking" as an upcoming method. From the conceptual process to fabrication digital design is an integral part of freeform architecture.

### 2.6.2 The Shift into Digital

Architectural practice around the world, Franken Architects, Gehry and Associates and Oosterhuis NL has contributed to the emersion of new forms, design thinking, fabrication, organizational methods, design strategies and project management methodologies. Another work of Frank Gehry, the Guggenheim Museum in Bilbao, claims a symbolic importance towards the contextualization of new design directions and methods, New geometric and design qualities "freed from priori formatisms" are launched by the design of this building (Oxman, 2006).

Gehry Technologies, as previously discussed in chapter 2.5.2, established new methodologies towards design, materialization and production that evolve themselves around the field of digital technologies. The digital data gathered from the physical models are used to create point clouds that are interpolated with NURBS curves. These curves are used to create the final 3D surfaces of the model, the NURBS Surfaces. After that the digital model is converted and another physical model is prepared for visual inspection. The process is iterative until the final product is satisfying enough (Borgart and Kocaturk, 2008).

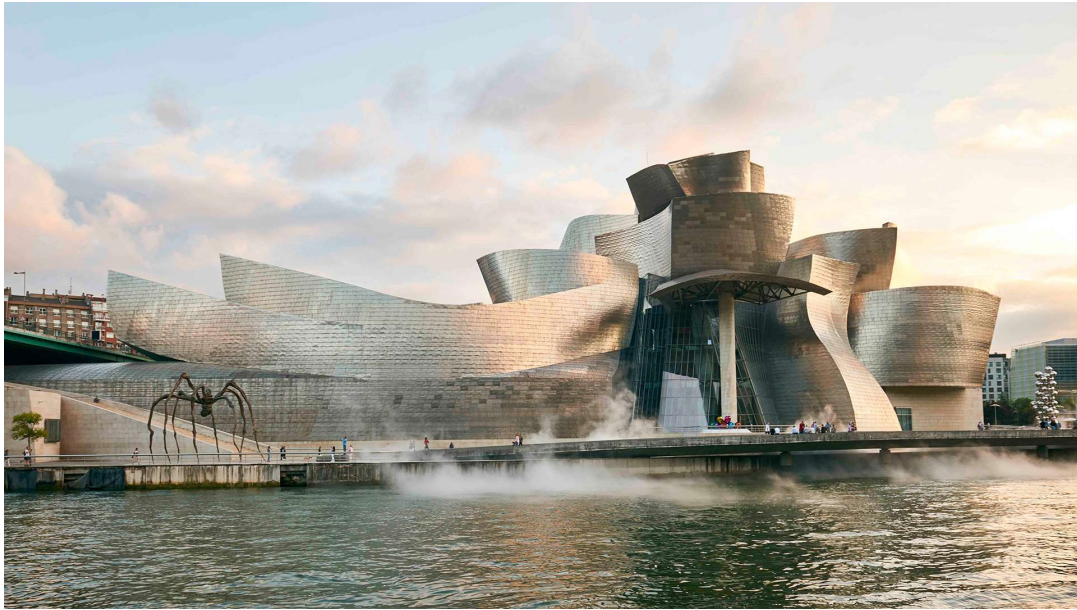


Figure 16 The Guggenheim Museum Bilbao, Frank Gehry Source: < <https://www.guggenheim-bilbao.eus/en/the-building> >

### 2.6.3 Freeform Design Challenges

Freeform design is also characterized by the challenges it entails. These are identified from the viewpoint of three domains: architectural engineering, structural engineering and manufacturing.

#### 2.6.3.1 In Architectural Design

Nowadays, digital design tools have given a variety of possible approaches regarding architectural form. One of them relates to form generation techniques based on computational algorithms. These utilize pre-specified sets of rules that generate forms towards structural or topology optimization and can be used during form finding (Borgart and Kocaturk, 2008). They require mathematical calculations that would be impossible for the human brain to process. At that point computer power is used to solve these tasks while the designer uses his critical ability to decide between the different design options generated.

Moreover, the importance of prototyping as a design thinking mechanism is great when it comes to an architectural product. In the case of the freeform it is an iterative process, that requires the collaboration between the two environments, the digital and the physical. Frank Gehry in his works is a good example of that practice as shown in the previous examples.

Another issue related to the communication between the two environments is accuracy. When translating a 1:50 scale physical model into a 1:1 scale digital model, a small deviation of 1cm becomes 50 times larger. Correcting these mistakes is a time consuming and labour intensive process. The task becomes even harder when designing requires constant iteration between the two environments. Having to correct possible inaccuracies delay the design process.

Lastly, another aspect that touches the field of structural designing too is the communication between the two disciplines. It lies on the fact that digital modelling tools nowadays give the opportunity to the designers to explore more complex forms. However, this does not mean that the resultant geometry is a structurally feasible product and more in depth collaboration between the two disciplines would be required to achieve a buildable result. According to Borgart and Koraturk (2008) in the field of education architects and engineers are not “creatively collaborating” during the designing of complex geometries, despite the fact that throughout history there have been examples that showcase architectural and structural sophistication and integration. They claim that more should be invested into making these two parties communicate towards the design of architecturally and structurally sound building product.

### **2.6.3.2 In Engineering**

The work of the engineer is to prepare the project detailing, structural analysis the static calculations as well as to envision the fabrication and assembly phase of the final product. Once designing starts it is important to know beforehand the influence of the engineer into the evolution of the final product. His/her role has a great impact on the design itself due to the fact that in many cases their approach towards design differs from that of the architect.

Engineers have established their own viewpoint when designing structures. Their design direction inclines towards physical force dependent designing, material properties study and boundary conditions. These principles have proven to be working but when designing freeform it is sometimes necessary to ignore the requirement of physical force dependency as a form finding approach. The principle has worked for Gaudi when building his catenary chain models but contemporary architecture examples can not be restricted by this notion. Instead the two principles should work together to come to a solution structurally feasible that does not deviate from the architectural vision. This could possibly be achieved by constantly feeding the freeform architectural model with information regarding structural attributes such as force distribution and deformation or fabrication attributes such as component number.

What is more, the irregularity of a freeform geometry imposes great difficulty in structural analysis and calculation when compared to regular shapes such as pillars, beams and plates (Qin Peng Li, 2018). While the internal forces can be unreasonably distributed, material waste due to structural miscalculation may occur too. The correct modelling of the structure is a requirement when it comes to accurately representing the real structure. If the data in the Finite Element Analysis (FEA) algorithm utilized for structural analysis are wrong then the resultant computer model while deviate from reality (Borgart and Kocaturk, 2008).

### **2.6.3.3 In Fabrication**

A challenging aspect of the freeform geometry is its fabrication. The manufacturing techniques and materials available can define in a great extend the form itself as well as the geometry of its counterparts. Compared to most standard building structures whose counterparts are products of mass production, complex geometries may include elements that are defined by their uniqueness in geometry. Their curvature may vary along their freeform surface from single to double and vice versa. In return each element due to its geometric uniqueness would require its own formwork for its creation. If, for example, a design needs 100 different counterparts to be realized and each one of them needs a different formwork to be created then the cost for the creation of the formwork would

exponentially increase the overall fabrication cost. Some of the architects try to rationalize their designs to fit the manufacturing techniques available at the time.

On the contrary, if the manufacturing techniques changed to fit the geometric requirements of a design, then the possibilities for future form exploration would increase. In fact, current formworks that support that deviation in curvature along a surface, are able to fabricate these types of elements, but further research still needs to be done into that. Chapter 3 is a research on these types of formworks.

## 2.6.4 Chapter summary

The contextualization of the freeform surfaces in the field of contemporary architecture is important because through the examples developed in Section 2.5 and the analysis of freeform design in Section 2.6 it can be observed that freeform surfaces pose many challenges to be realized in a building scale.

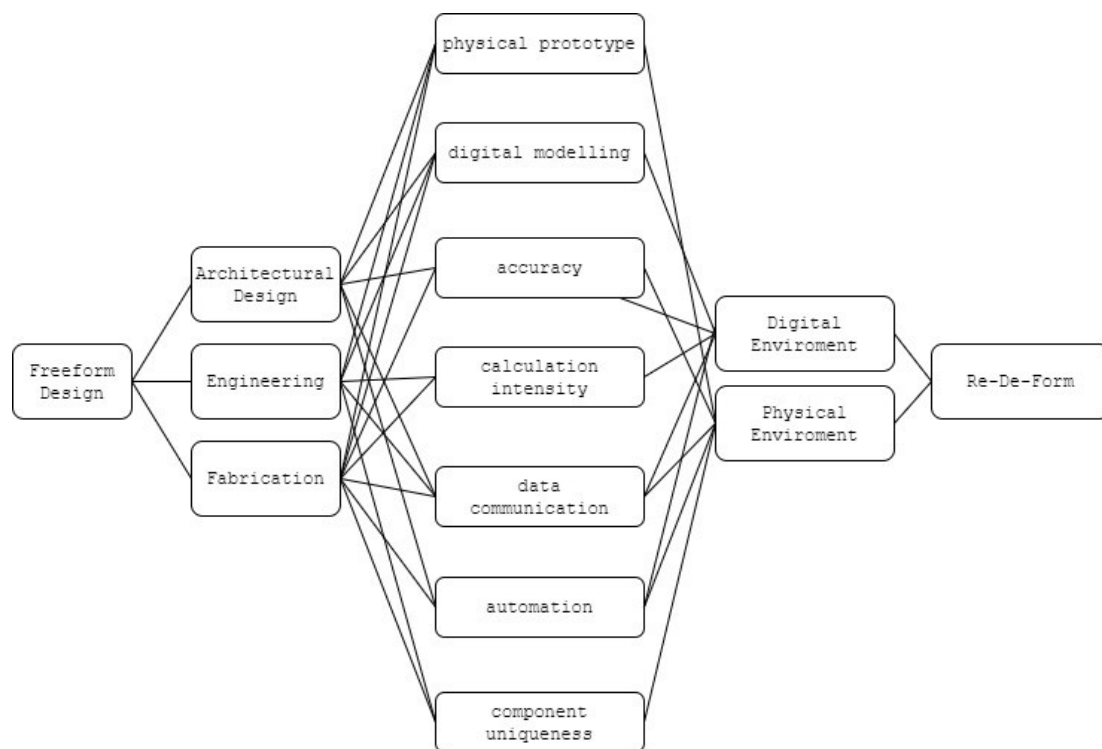


Figure 17 The link between the workflow and the challenges. Source: own illustration

A digital and physical workflow that utilizes a flexible surface as a means of designing process and fabrication, could address those challenges. The graph illustrated below, links the digital and physical environment of the developed workflow to the challenges posed by free form freeform design in terms of architecture, engineering and fabrication. It is noticed that some of the challenges refer to more than one of the three domains.

Later on the report the workflow will be referred to as Re-De-Form. The name of the workflow is the combination of the word "deform", due to its ability to change form and "reform", due to its ability to do it more than once. The workflow includes the digital and physical tools that answer to the challenges posed by freeform design.

(End of chapter)





# 3

## The Re-De-Form

### 3. The Re-De-Form

#### 3.1 History and State of the Art on flexible molds

The concept of using flexible molds to fabricate building components has been studied over the last 60 years. The flexible mold system involves an adaptable formwork of an elastic material that is curved by the use of pistons, actuators or pins (Schipper, 2015). On top of that, the building elements can be shaped by either casting a material that hardens over time such as concrete or by deforming a material that can be softened, such as thermoplastics. After the end of the hardening process the formwork takes the shape of the next component and the process is repeated.

Over the last 60 years several prototypes have been built. One of them is built by Renzo Piano in 1966. The figure displays a method where a part of a scaled freeform surface model is cast into a flexible, 1:1 formwork for the fabrication of a full scale component. The change of scales between the models was realized by a pneumatic device.



Figure 18 Different versions of flexible formworks by: (a) Renzo Piano, (b) Spuybroek and (c) Vollers and Rietbergen, Source: Schipper (2015).

Following the concept of computer-controlled machining techniques, Spuybroek and DeLanda (2004) envisioned an intermediate layer of elastic material between the mechanical system of actuators and the building component that would also protect the electrical mechanisms underneath. The building component would be shaped on top of that. Furthermore, a prototype of Vollers and Rietbergen is used for the fabrication of concrete elements (Schipper, 2015). It consists of computer-controlled linear actuators that deform a flexible surface. The positional values are fed from the computer directly to the physical set-up. However, there were accuracy related limitations inherited by the horizontal displacements of the control points, that occur during the large deformations of the flexible surface.

What is more, there are several examples of formworks utilized in manufacturing of curved elements for facades. Some of them have application in the nautical industry for building boat hulls. Adapa Molds a company situated in Denmark and Curve Works, situated in the Netherlands use large scale adaptable formworks for the fabrication of large-scale single or double curved building components. The concept lies under the production of freeform surfaces with the least amount of molds. Adapa utilizes concrete and composites as a building material (Adapa, n.d.) while Curve Works specializes in composites, wood and Natural Fiber Reinforced Polymers (NFRP).

A more contemporary example in the field of academia that has been the stepping stone for the development of Re-De-Form is the FlexiMold. FlexiMold was developed for the purposes of the course Technoledge Design Informatics in 2016 and is based on the concept of a flexible surface supported by vertical adjustable pins (Asut and Meijer, 2016). The material of the surface is made of High Density Polyethylene (HDPE). The HDPE sheet is able to transform into a complex curved surface due to the square pattern milled on the surface. On the other hand, the material provides with the stiffness required to use the surface as a medium for casting curved forms too.

The curvature of the surface depends on the heights of each pin that support it. A Grasshopper algorithm reads the surface, calculates the height of each pin and prints the output on the computer screen. The pins are adjusted manually on their respective heights and when ready, the designer places the flexible surface on top of the pin bed, to begin with the casting process. Each unique surface requires that process (Asut and Meijer, 2016).

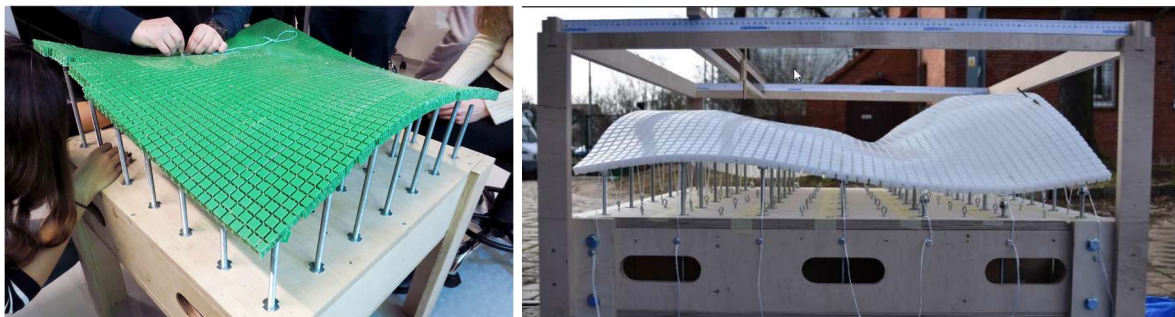


Figure 19 (a) The Former FlexiMold. Source: Asut, Eigenraam and Christidi, 2018, (b) The FlexiMold during the Design Informatics workshop in Poland, Source: Asut and Meijer, 2016

Based on the FlexiMold there is another concept developed in the BK faculty of Architecture, the Reflex. Reflex is about upgrading the manually controlled flexible formwork in two stages. The first stage involves automation of the system. The computer will replace the manual adjustment of the pins to automatic with the use of mechanical and hardware components that will be analysed further in chapter 5. The second stage of the upgrade is the application of Human Computer Interaction (HCI) into the once automated formwork (Asut, Eigenraam and Christidi, 2018). Re-De-Form is a proof of the concept of the first stage of the upgrade.

### 3.2 Re-De-Form

Re-De-Form will provide with the precision, accuracy and control of the freeform's physical geometry. The adjustment of the Re-De-Form to the freeform surface is run almost instantly and should not involve manual adjustments of the pistons as it is done automatically. The goal is to create a mechanism that best represents the surface the designer is currently studying. From a draft freeform surface on a scale of 1:10 or 1:20, depending on the dimensions of the structure, towards its panelization on a 1:1 scale, the automated physical model should be able to generate that curvature. An algorithm feeds positional data from the digital interface to the physical set-up.

On a later stage it could also be used during the form-finding process as a means of physical prototyping mechanism that interacts with the designer. The creation of the Re-

De-Form prototype involves an iterative process that was held in the Modelling Hall of the TU Delft's Architecture faculty, BK.

The manually adjustable actuators of the former FlexiMold are replaced by linear actuators. Their number will determine the detail of the surface curvature, as well as the overall cost of the system. The greater their number, the higher the level of surface detail and curvature possibility but the higher the cost of the overall design. Bigger scales that involve higher levels of detail require more actuators to be placed. Due to low budget the number of actuators is limited to 9, a decision that generates limitations when it comes to surface representation. Thus, an efficient number of actuators needs to be decided.

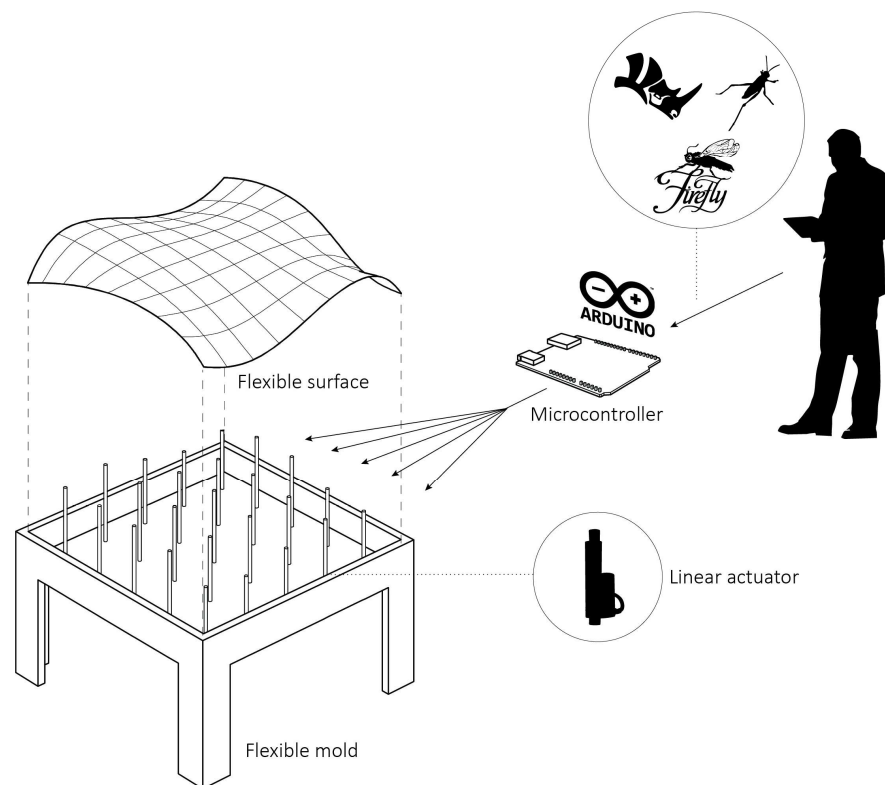


Figure 20 The automation workflow as it was originally envisioned Source: Asut, Eigenraam and Christidi, 2018

As it has been originally envisioned by Asut, Eigenraam and Christidi (2018) the workflow involves the use of Rhinoceros, Grasshopper and Firefly. The hardware components would include an Arduino Microcontroller Board and one linear actuators per pin. These are illustrated in *Figure 20*. The number is limited to the available Input/Output pins of the Arduino Board that is used as a medium for the communication between the digital model and the physical mold. The set up involves 25 actuators on a grid of 40x40cm with a usable surface area of 124x124cm on the XY plane.

The microcontroller Arduino Board consists of 54 digital I/O pins and is connected to the computer through Firefly, a Rhino-Grasshopper plug-in. Each actuator is connected to one input and one output. The input feeds the position of the actuator per second into the computer and the output is used to place the actuator in the correct height every time the designer manipulates the surface in the software.

The advantages of the automation system over the former FlexiMold correspond to the rapid and precise adjustment of the flexible surface. The surface manipulation on the digital mold is directly fed into the physical flexible mold thus making the materialization and fabrication process more accessible and accurate.

On chapter 5 a 1:5 scale variation of the Re-De-Form is developed as part of an iterative process that is ever-developing towards an optimal flexible surface. During the building weeks of the 3x3pin prototype, several challenges and limitations came up. While these were addressed and discussed they provided with useful feedback for the constant improvement of the prototype from the conceptual phase (sketches and computational model) to the final realization of it, the physical model.

(End of chapter)





# 4

## Timber Gridshell Structures

## 4. Timber Gridshell Structures

To reflect upon the use of the automated Re-De-Form and the digital workflow behind that- as a tool for the designing and fabrication of freeform surfaces- a case study is formulated around the design and manufacturing of timber gridshell structures. The study of timber gridshells is gaining popularity in the field of freeform architecture and its practice is used to test the natural limitations of structures (Naicu, Harris and Williams, 2014). They are lightweight, with a small thickness to span ratio and mostly used to cover long spans. Therefore, their use has been limited to some large-scale buildings and some temporary pavilions in the field of academia and experimentation. The goal of the section is to identify the design methods, both physical and computational, used in already existing projects as a foundation for the development of the digital workflow of the Re-De-Form towards the study of those structures.

### 4.1 Shells & Gridshells

Shell structures are used to span long distances with the minimum use of material possible. They are described as curved surfaces with large dimensions in two directions but a small in the third (Williams, 2014). Their double curved geometry provides them with a load bearing efficiency that makes them unique to other structural systems used in the building industry. Their continuous material distribution results in a phenomena called membrane action, a structural state where only normal and in-plane shear stresses occur. The forces are uniformly distributed over the cross section while the bending stresses are negligibly small compared to in plane stresses. The shell can resist in plane and out of plane loads due to its curvature .

On the other hand, gridshells or else lattice shells are defined as "structures with the shape and strength of a double curved shell, but made of a grid instead of a solid surface" (Douthe, Baverel and Caron, 2006). This is partly wrong because in the figure below it can be observed that the gridshell immitates the structural behaviour of a shell. The shear forces though can not be transmitted through the grid, so another form of bracing needs to be implemented to the system. One of the options would be to use a bracing that triangulates the grid and the other one a continuous layer covering the grid that serves as cladding too.

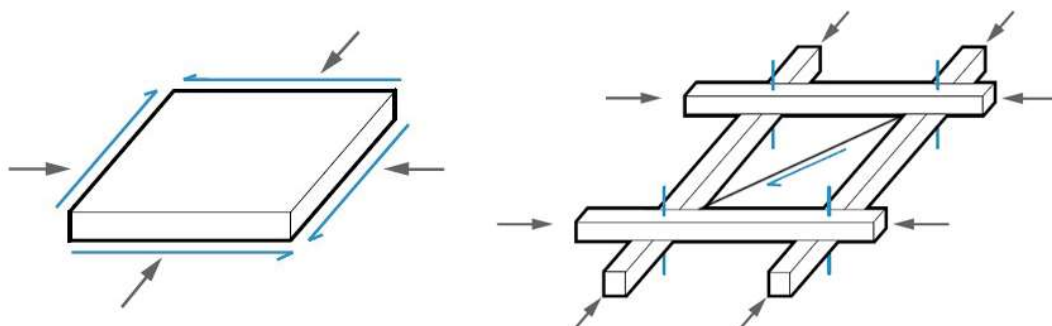


Figure 21(a) Continuous shell: axial and shear forces are visible, (b) Gridshell: the laths carry the axial forces only. Diagonal bracing carries the shear forces. Source: *Shell Structures for Architecture* (author added the diagonal element)



The materials used to construct such structures are steel, aluminium, timber, cardboard and GFRP. With respect to the manufacturing and construction processes and properties of the materials two are the more discreet gridshell categories. The first uses continuous grid members called laths that span across the structure intersecting at the nodes and the second one features smaller straight grid member that connect to each in the nodes (Naicu, Harris and Williams, 2014).

## 4.2 Timber gridshells

Parallel to the growing interest in freeform architecture over the years, is the study of timber gridshell structures. Timber gridshells can deform such that they generate double curved surfaces relatively easy (Harris and Kelly, 2002). The first large scale gridshell was built in Mannheim by Frei Otto, a pioneer in gridshell design and will be further discussed in the next section. It gained much appreciation, however for the next 30 years after its completion timber gridshells lost popularity. The labour intensity during design and construction accompanied with an iterative design and complex form finding process were the main reasons. The computational tools for these processes to happen were introduced 25 years later and were used in the construction of the Weald and Downland Museum. Also, by taking into account the construction processes that were introduced the resultant building was far more sustainable from its predecessor. With respect to the minimum material usage due to the shell action and the use of timber laths, a material harvested from renewable energy resources.

The construction phase of timber gridshells has two variations (Naicu, Harris and Williams, 2014). Both involve a flat bi-directional grid of laths that connect at their intersections using pin connections. The first variation involves deforming the quadrangular flat mat by pushing the laths towards the center while the other variation involves placing to grid to its final height and use gravity to push its boundaries to the ground. For both methods when the desirable shape is reached, the pin connections are tightened and the boundaries of the gridshell fixed to their position. The application of timber during this process is optimal due to its light weight material properties, bending possibility and enough strength to resist loads and moments.

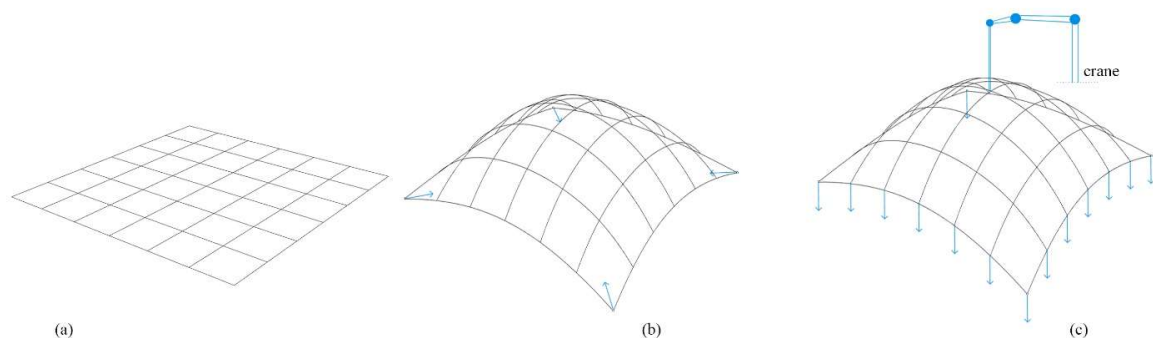


Figure 22 (a) flat lath grid, (b) grid pushed towards its center, (c) grid lath by crane and self weight drags it to the ground. Source: own illustration

### 4.3 Timber gridshell examples

Timber gridshells are mainly used as roofs that cover large-scale building spans and can host a variety of functions underneath. Large-scale gridshell types can accommodate theaters, exhibition spaces and other recreational activities. More contemporary examples are raised as methods of experimentation with material behaviour and computational form-finding processes. They are used as small-scale pavilions able to function as cultural venues.

#### 4.3.1 Mannheim Multihalle

The winning design for the space of the Multihalle in Mannheim was the gridshell of Frei Otto in collaboration with Ove Arup & Partners. The complex consists of several functions, a multipurpose hall, spaces for exhibition, entertainment, theaters sports activities and concert while the idea behind the design was to unify these spaces by spanning a roof that would cover them all as one entity.

The roof touches the ground in a way that it leaves the impression that it is a continuation of the surrounding garden. Covering a space of 3600m<sup>2</sup> and with a maximum longitudinal span of 85m, a PVC coated fabric is the cladding material used. The grid consists of a double layer lath mat of 50x50mm in cross-section and a spacing of 50cm. Hemlock Pine was the timber material selected for its straight grain and availability in long lengths. To increase in-plane stiffness the double layered section is supported by 6mm cables every 4.5 meters in both directions (Happold and Liddell, 1975).

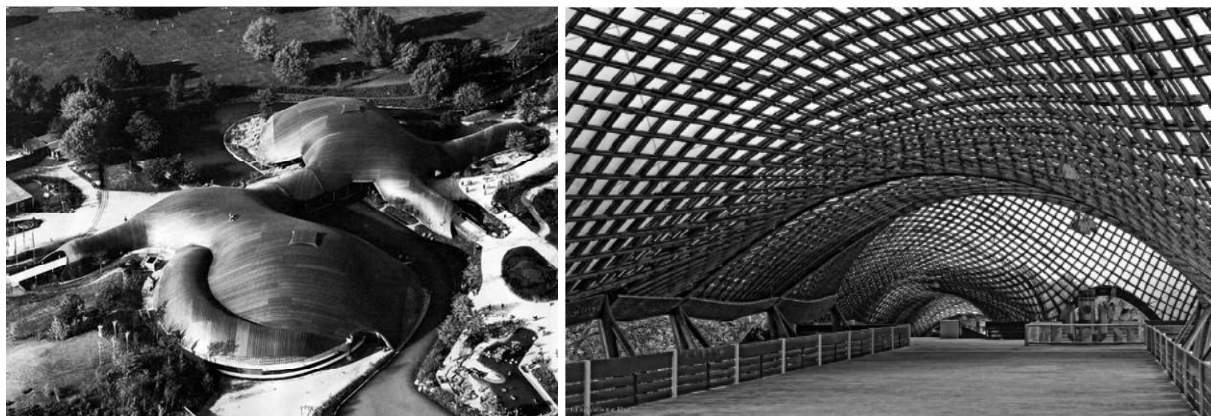


Figure 23 (a) The Mannheim Multihalle, aerial view. (b) Interior view of the Multihalle. Source: Burkhardt and Bächer (1978)

The physical modelling performed for the initial form finding, involved hanging chain models. The accuracy of the nodes had to be increased because when transferred from the 1:98 model to the building scale the mistakes occurred would be tremendously enlarged, almost 100 times. The node coordinates were documented using stereo photography in order for the exact position to be monitored for the upcoming structural calculations. Due to model inaccuracy though not all members were in tension but this problem was tackled with the use of the force density method of a net structure.

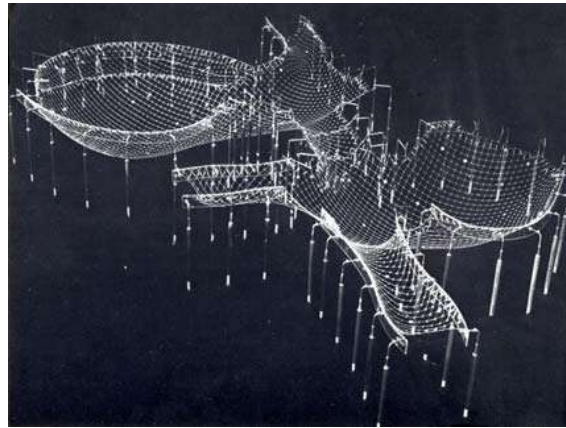


Figure 24 Physical model of Multihalle. Source: Burkhardt and Bächer (1978)

During the construction phase, the initial plan was to lift the gridshell into shape with the use of cranes. This proved to be cost-effective so the contractors had to come up with other options. Instead, the gridshell was pushed to shape from the boundary edges. To reduce costs a minimum amount of scaffolds were placed to hold it into shape. Each scaffold supported a unidirectional strut to increase the span effect of the scaffold. After the erection the structure was covered by a hot-welded, PVC coated fabric.

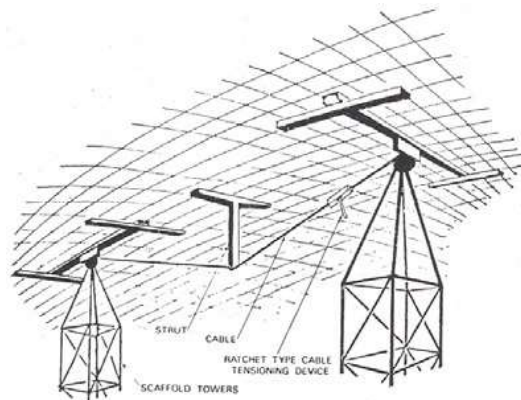
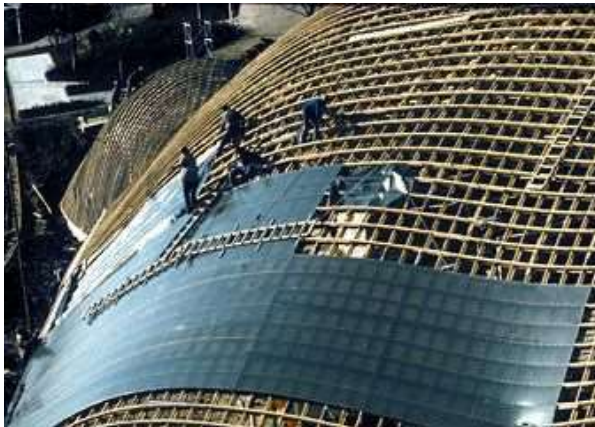


Figure 25 (a) Cladding the roof with PVC fabric. (b) Scaffolding with struts. Source: Burkhardt and Bächer (1978)

#### 4.3.2 Weald and Downland

The Weald and Downland gridshell was built at the Weald and Downland Open Air Museum in the UK in 2002 by Edward Cullinan Architects, Buro Happold and Green Oak Carpentry (Harris and Kelly, 2002). The roof has a longitudinal span of 48m and between 11-16 wide with a clear height between 7-10m. The roof is cladded with Red Cedar boards and polycarbonate glazing. The gridshell consists of a double layer mat of 50x35mm oak laths. The same layering technique was used in Mannheim to provide out of plane resistance. The in-between lath distance varies from 500mm in areas where extra resistance is needed and 1000mm in other areas. Computational methods were utilized to minimize the grid density locally and provide with cost reduction and less complexity in assembly. Diagonal bracing is added too.



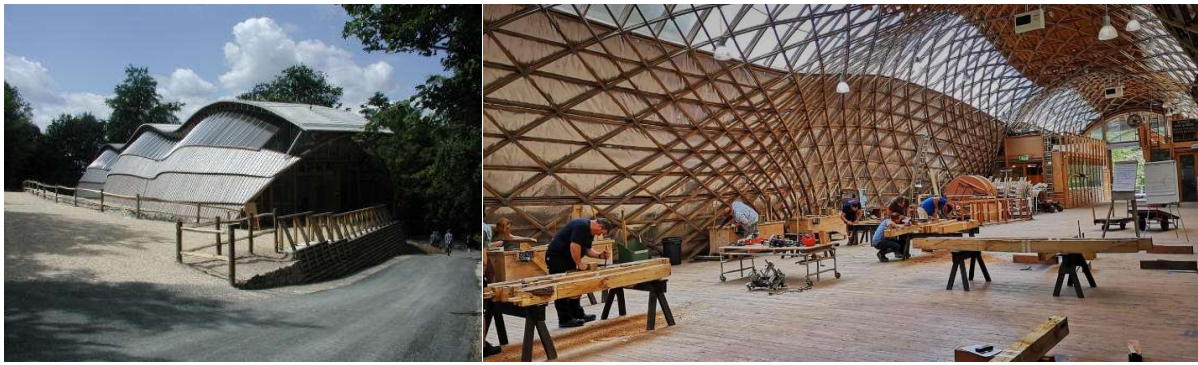


Figure 26 (a) Weald and Downland Gridshell. (b) Interior view. Source: <https://www.wealddown.co.uk/buildings/downland-gridshell/>

The form finding process involved the creation of several physical models, while the computational methods towards it used the dynamic relaxation technique which will be elaborated in the next section. The structure was designed according to Eurocode5 with a timber grade of D30 and a bending strength of  $30\text{N/mm}^2$ .

#### 4.3.3 Savill Garden

The Savill Garden gridshell was built in 2005 by Glenn Howells Architects in collaboration with HRW, Buro Happold and Green Oak Carpentry to cover the new visitor's Center of the Royal Landscape. The gridshell is a double layered timber construction with a longitudinal span of 98 m and a lateral of 28m and its height varies from 4.5 to 8.5m. The mesh size is 1m and the laths in cross-section are 80mm wide and 50mm high, connected by shear blocks of  $80 \times 120 \times 300\text{mm}$ , resulting in a cross-section of 190mm (Source: <https://www.e-architect.com/oxford/48savill-building>). The roof cover contains blocks of Birch Plywood covered with insulation and aluminium for rain-resistance.



Figure 27 (a) Savill Garden exterior view. Source: [http://www.fourthdoor.org/annular/?page\\_id=453](http://www.fourthdoor.org/annular/?page_id=453) (b) Interior view. Source: <https://alchetron.com/Savill-Building#Interior>

Modelling the structure was a time-consuming process and to prove its structural integrity many prototypes were built to be tested. Larch was used for its natural strength and durability, adding to the environmental value of the overall structure. Also one of the clients demanded that wood should be harvested from the royal garden and be used as much as possible. The structural larch laths, block pieces and oak cladding are harvested locally (Tang, Chilton and Beccarelli, 2013).

#### 4.4.4 Pavilion ZA

A contemporary gridshell example built in 2013 in Cluj, Romania as part of a student workshop is the Pavilion ZA. It is a small scale structure consisted of double layer lath system and a general dimensioning of 18x13x4 meters. The material of the laths is Siberian Larch with a cross-section of 70X20mm per lath. The form finding process was executed computationally with the use of the Kangaroo Live Physics, a plug-in supported by Rhinoceros-Grasshopper (Naicu, Harris and Williams, 2014).



Figure 28 Pavilion ZA in Cluj, Romania, Source: Naicu, Harris and Williams (2014)

#### 4.5 Computational Form-Finding processes for shells

Form-Finding methods for shells are classified into three discrete families: Stiffness matrix methods, geometric stiffness methods and dynamic equilibrium methods (Adriaenssens, Block, Veenendaal and Williams, 2014). The first is the oldest family among the three and utilizes matrices of standard elasticity and geometric stiffness. It has been adopted from structural analysis methods such as finite element analysis. The second group contains methods widely used such as the Force Density Method (FDM) and Thrust Network Analysis (TNA). These methods are material independent because they only utilize force densities and trajectories. The last group constitutes of the Dynamic Relaxation Method (DR) and the Particle Spring Systems (PS) (Michiels, Adriaenssens and Dejong, 2019). These methods solve the problem of a system's dynamic equilibrium, by applying static equilibrium. The geometry is manipulated by modifying the particle's mass, spring lengths and stiffnesses. The method of Particle Springs System will be introduced to the computational workflow of this thesis due to the manipulation possibilities that the user has with the surface geometries he/she is investigating, the accuracy of the form generation and the material properties that the freeform case surface can receive.

##### 4.5.1 Particle Spring Method

As an alternative to physical modelling that famous architects such as Frei Otto and Isler did for their hanging chain models and tension membranes, architects and engineers have begun to create these examples in simple digital simulations by utilizing particle-spring systems. At first, these methods were used in the animation and gaming industry, to model arbitrary topologies of cloth and hair while in recent years these tools are becoming increasingly available for architectural and engineering form finding purposes (Kotnik and Weinstock, 2012).

A particle springs system comprises of particles with certain mass and position that are connected with springs of certain stiffness and rest length. Anchor points and gravity forces are introduced too. When the simulations runs the particles move through space until the forces acting on the system reach a static equilibrium similarly to the Dynamic Relaxation method (Lewis, 2003). This method aids the user towards creating a valid structural form while he/she interacts with the system in real time by altering parameters, as anchor point positions, gravity loads or spring stiffness values. A structurally optimized finished form, saves the designer from waiting until the end of the design process to optimize it structurally (Kilian, 2004).

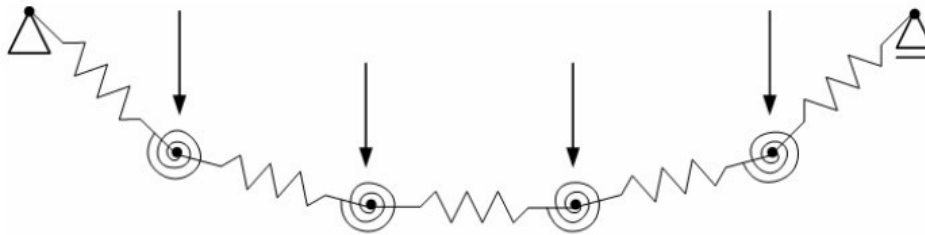


Figure 29 A simply supported lath modelled with the particle spring method. Note the particles, springs and gravity forces acting on the system. Source: Kuijvenhoven and Hoogenboom (2012)

Kuijvenhoven and Hoogenboom (2012) used the particle-spring system method during the Form-Finding phase of a gridshell consisting of flexible members. In their method the particle spring systems were used to simulate the behaviour of the gridshell during construction. Also, based on their work, the initial shape does not need to be specified in detail by the designer which makes it an intuitive and easy-to-use tool for the formfinding of a gridshell.

#### 4.4 Timber Gridshell Node Connections and Materials

Regarding the connection systems, the timber gridshell examples mentioned above and some other contemporary examples use 4 sets of bi-directional laths. Due to this arrangement timber gridshells can support axial stresses, (both compressive and tensile stresses) in two directions, as well as out of plane loading (Naicu, Harris and Williams, 2014). Cross ties, rigid bracing or active covering systems are implemented to provide in-plane shear strength and stiffness.

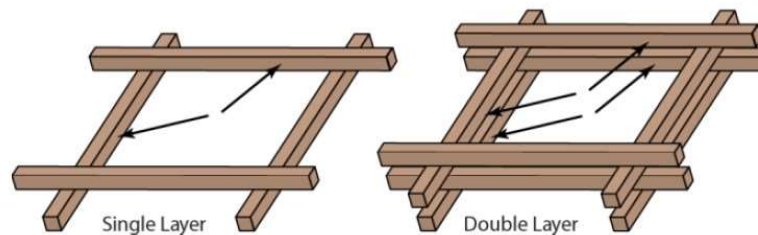


Figure 30 Single and double layer positioning Source: (Naicu, Harris and Williams, 2014)

Also, in order to benefit from the double layer system, the laths need to stay connected so that the shear forces can be transferred from top to bottom (Happold and Liddell, 1975). Nodal connections located in the intersection of the adjacent layer and shear blocks inserted between the laths are responsible for the shear force transfer. Thus, a "composite section that has a significantly greater strength than the individual laths" is achieved (Harris *et al.*, 2003).

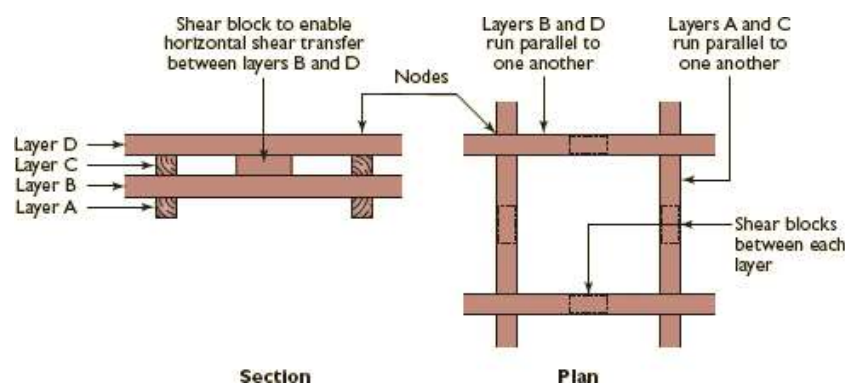


Figure 31 Double layer system in plan and section. Source: (Harris *et al.*, 2003)

Identical nodal connections are used all over the structure. The high amount of repetition leads to less complex detailing and a drop in the overall cost effectiveness. Therefore, the layered structure and the fact that for the post-forming process of the system requires freedom in movement and rotation of the nodes make the overall construction process, challenging.



The Multihalle in Mannheim, features nodes that allow local movement in the plane direction through the slotted holes in the top two layers of the detail. In the center of the node connection a bolt runs through all 4 timber layers. When the final freeform shape is achieved during construction, the 4 layers are clamped together by tightening the bolt. However, extracting material, required an expensive and time-consuming process as well as reduced the cross-sectional resistance to buckling (Harris *et al.*, 2003).

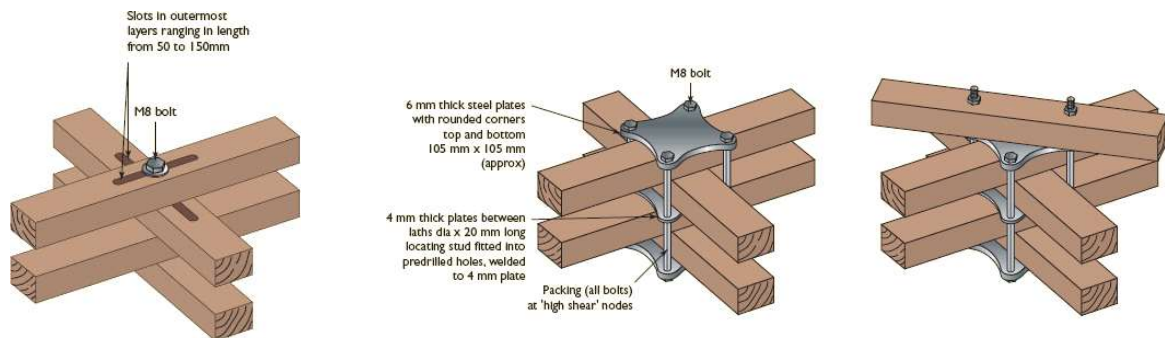


Figure 32 (a) Slotted hole node, (b) Plate and bolts node. (c) Plate with extended bolts to support diagonal bracing. Source: Harris *et al.* (2003)

More recently, in the Downland Gridshell an alternative method was invented. Instead of a bolt and a slit in the middle, the layers are clamped together with a system of 3 plates and 4 bolts per node. The bolts are clamping the plates externally without the need to cut-out material while the two top layers are free to slide and rotate before tightening (Harris *et al.*, 2003). In the connection displayed above two of the bolts were extended for the application of stiffeners. In the case of the Chiddingstone Castle gridshell the node connection supports frameless glazing (Naicu, Harris and Williams, 2014).

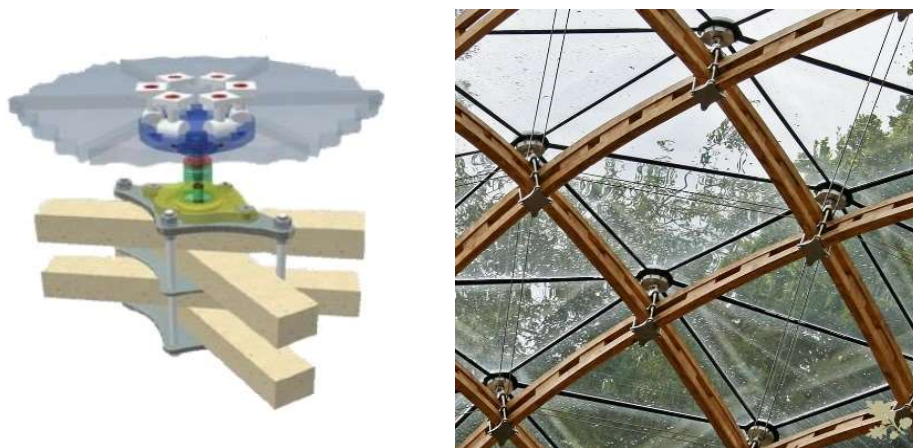


Figure 33 (a) Plate connection with frameless glazing on top. Source: Naicu, Harris and Williams (2014). (b) Interior view of Chiddingstone Orangery. Source: <<https://www.glassonweb.com/news/timber-frame-gridshell-historic-orangery>>



The materials chosen per different design as well as the reasons behind their choice are summarized under *Figure 34*.

	Materials	Reason
Mannheim Multihalle	Western Hemlock	Long Length availability
Weald and Downland	Oak	Durability and local availability in the UK
Savill Garden	Larch	Availability to the client's own wood source
Pavilion ZA	Siberian Larch	Availability from supplier, durability and aesthetics

Figure 34 Material selection per project. Source: Based on Naicu, Harris and Williams (2014)

## 4.5 Chapter Summary

The chapter sheds light into timber gridshells and their application into contemporary building construction. Critical design aspects elaborated such as materiality, nodal connections detailing, structural systems and form finding methods, provide with the necessary information for the development of the computational method and physical environment.

Remarkable is the double layer lath system that is used in all the 4 examples mentioned. Different sizes are used for the cross-section and the lath in-between distance. In the Mannheim Multihalle, physical modelling was used as a formfinding method, whereas in the more contemporary Pavilion ZA, computational formfinding methods were used. The Nodal connections per example varied but the logic of fixing the structure into place once the final shape is given is the same for all 4 examples. In all the examples different types of Wood material are used mostly depending on the availability.

In the next chapter the information acquired is put into practice during the study of a timber gridshell example through Re-De-Form.

(End of chapter)





# 5

## Study of a Timber Gridshell Structure with Re-De-Form

## 5. Study of a Timber Gridshell Structure with Re-De-Form

The focus of this chapter is to provide with an in-depth understanding of the methods and tools utilized in the digital workflow with respect to freeform surface and gridshell study, panelization and FlexiMold application. The creation of the Re-De-Form prototype, its automation and its link to the digital workflow is also included as an ever-developing iterative process..

### 5.1 Form-finding of a gridshell surface

Physical modelling is a critical part of the freeform design process. In the case of the wooden gridshell, form study starts from assembling a physical flat sheet of wooden laths and ends by pushing all or some of its edges inwards. The process repeats and several "push scenarios" take place until the final form is decided. Aim of the digital workflow is to recreate this concept in a digital environment, in a way that the designer benefits from the computational processes the digital has to offer into studying complex structures, such as the gridshells. Freeform study, structural analysis, panelization and panel fabrication are some of the processes offered.

In *Figure 35* the computational process is explained step by step. The method used for Form-Finding is the Particle Spring Method mentioned in chapter 4.5.1. As the name suggests it requires the use of particles as vertices or points and springs defined as line segments. These two types of Geometry are fed into the Physics Engine KangarooV2 developed by Daniel Piker.

The script executes deformation of an initially flat rectangular surface. Firstly, a surface is created and then meshed into U and V values that the user can change accordingly. The U-V number defines the number of points-particles of the system and also the complexity of the primitive freeform surface. The more control points the greater the complexity of the deformation, due to that, a value of 8 is set by default. The script automatically connects each point to its adjacent one in one direction with a line segment. The 2 resultant lists "Segments in U" and "Segments in V" include the simulation's springs.

Later, the lists of points and lines are fed into KangarooV2, as Goal Objects alongside with other user input colored by orange in the flowchart of *Figure 35*. Axial and Bending strength are defined, while the spring lines need to remain in the same length once the simulation ends. A small upward force is also defined because the freeform has to deform upwards as a wooden gridshell would normally do. What is more the user should define the Anchor Points, which in the case of this form study are the points that are pushed inwards to shape the geometry. In other words, a geometry is defined by its control polygon, given physical properties and manipulated through the use of the Kangaroo Physics Engine.

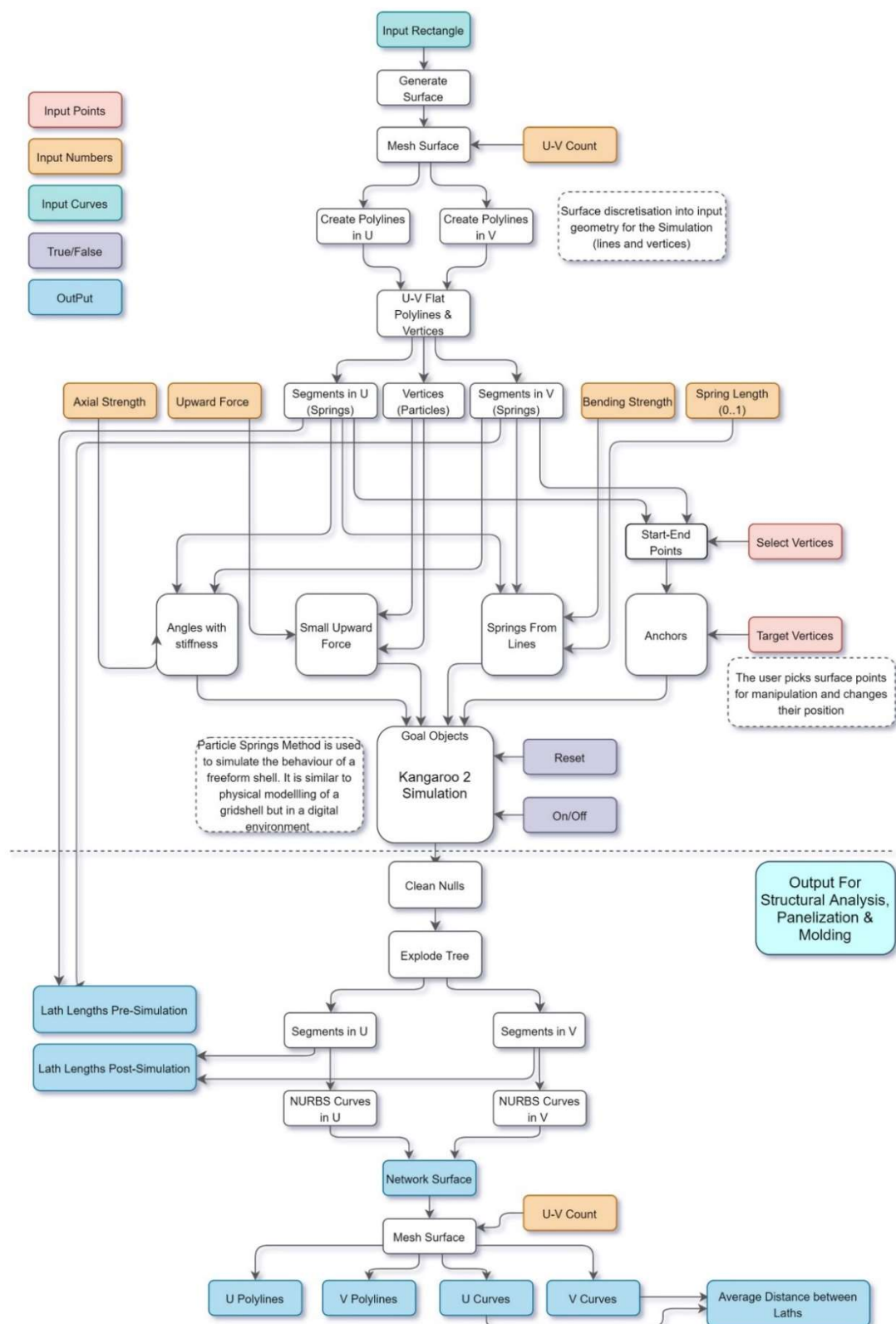


Figure 35 Flowchart for the form finding of a freeform surface. The list of colours on the top left correspond to the different variables used within the flowchart Source: own illustration

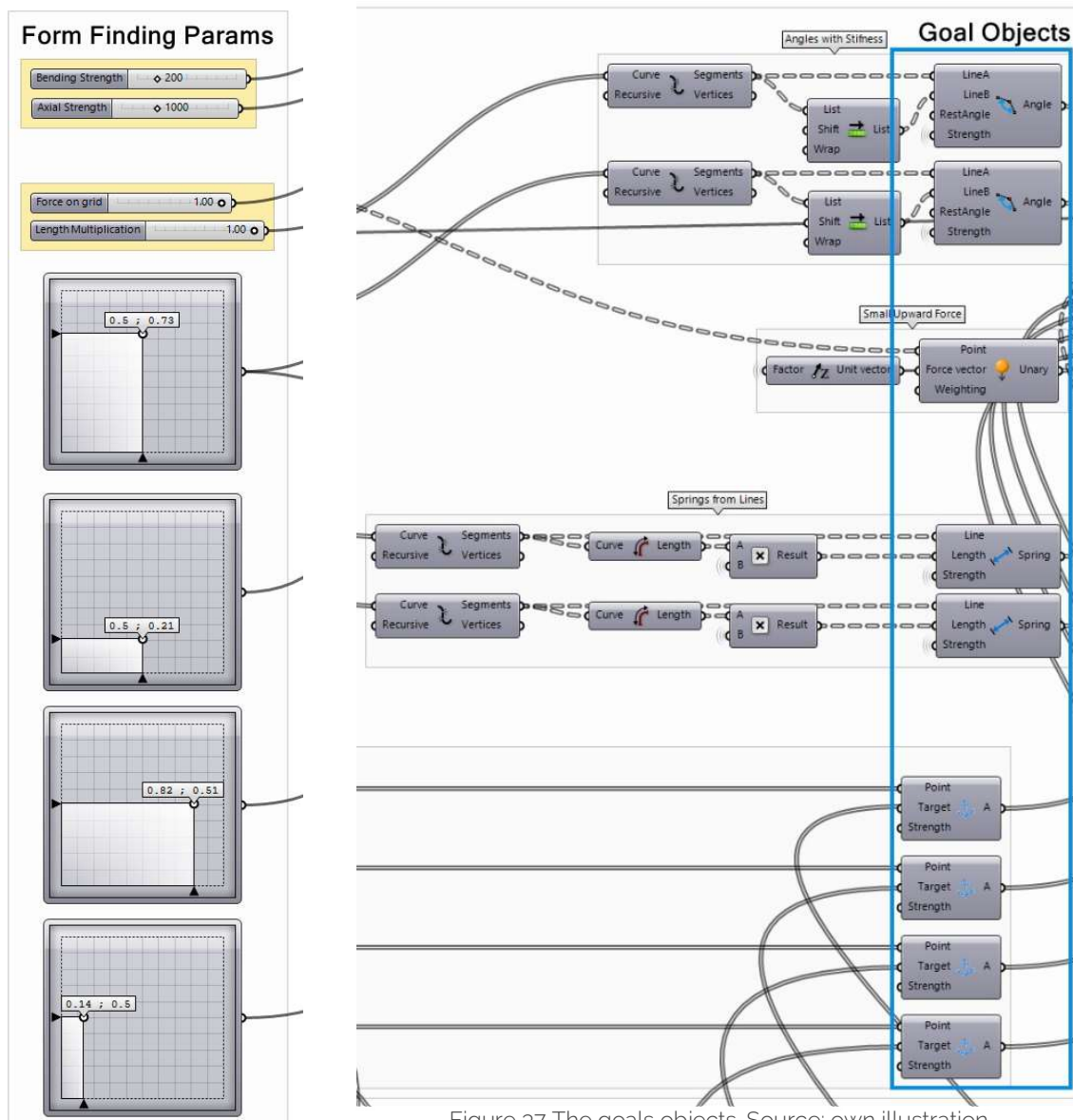


Figure 37 Form-Finding Parameters. Source:own illustration

Figure 37 The goals objects. Source: own illustration

In *Figure 37* and *Figure 37* the Parameters and Goal Objects are illustrated respectively. Bending Strength Slider connects to the Kangaroo's Angle component whereas Axial Strength and Length Multiplication Sliders to the Length (Line) component. The Force on Grid connects to the Unary Force. In *Figure 38* the output surface is meshed to be used later in the algorithm.

The freeform example studied contains 4 anchor groups of points that are pushed inwards. Each group is linked to one of the MD Sliders illustrated in *Figure 37*. The MD sliders controls the group's position on the x-y plane with respect to their rest position. The points move inside the "hidden" rectangle set by the MD Slider and their rest position is the 0.50 ; 0.50.

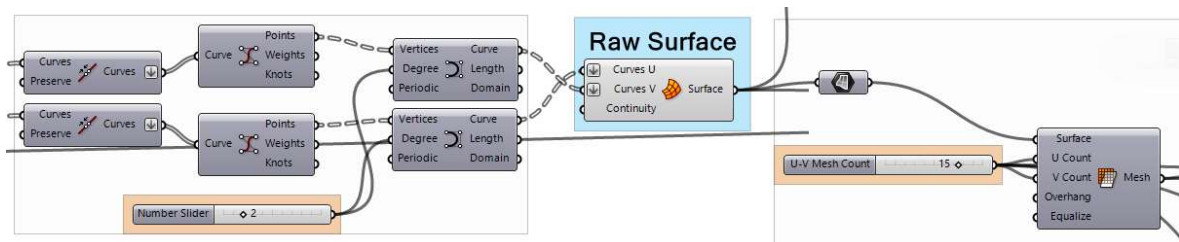


Figure 38 A Network Surface of degree 2 is discretized into a U-V Mesh. The example generates 15 laths in each direction. Source: own illustration

After the Form-Finding simulation the Null outputs are cleaned from the output list and the line segments of the control polygon are replaced by NURBS Curves in the U and V direction. A Network Surface generated by these curves is discretized into a Mesh and its U-V count represents the number of laths of the gridshell. The structural analysis will require U-V Polylines and the panelization and molding U-V Curves. These are displayed in Figure 41. Lastly, the average distance between the laths is calculated in Figure 41 as well as the lengths of the laths pre and post-simulation are compared in Figure 41.

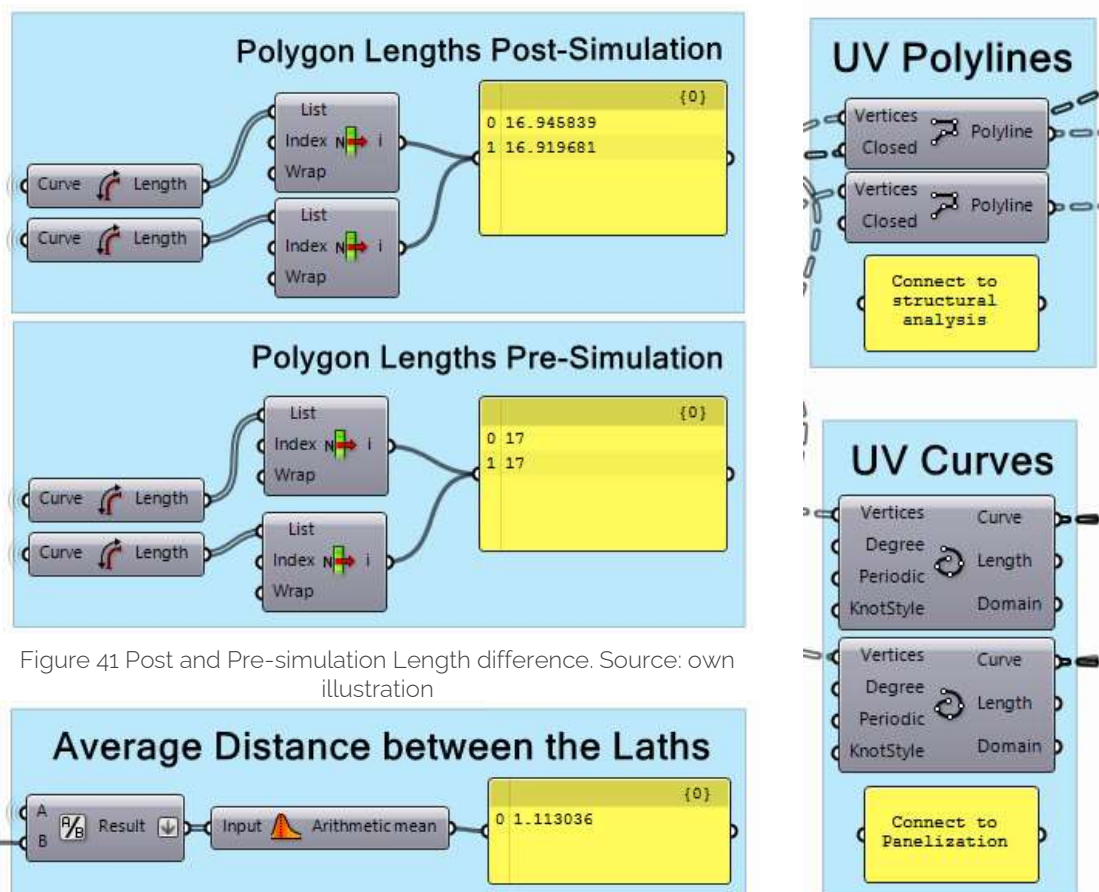


Figure 41 Post and Pre-simulation Length difference. Source: own illustration

Figure 41 Average lath distance. Source: own illustration

Figure 41 Output for Structural analysis and Panelization. Source: own illustration

In *Figure 42* different design options are displayed based on the number of control points pushed inwards. Note the control polygon per freeform changes accordingly. Option (d) is to be developed further towards generating the timber gridshell.

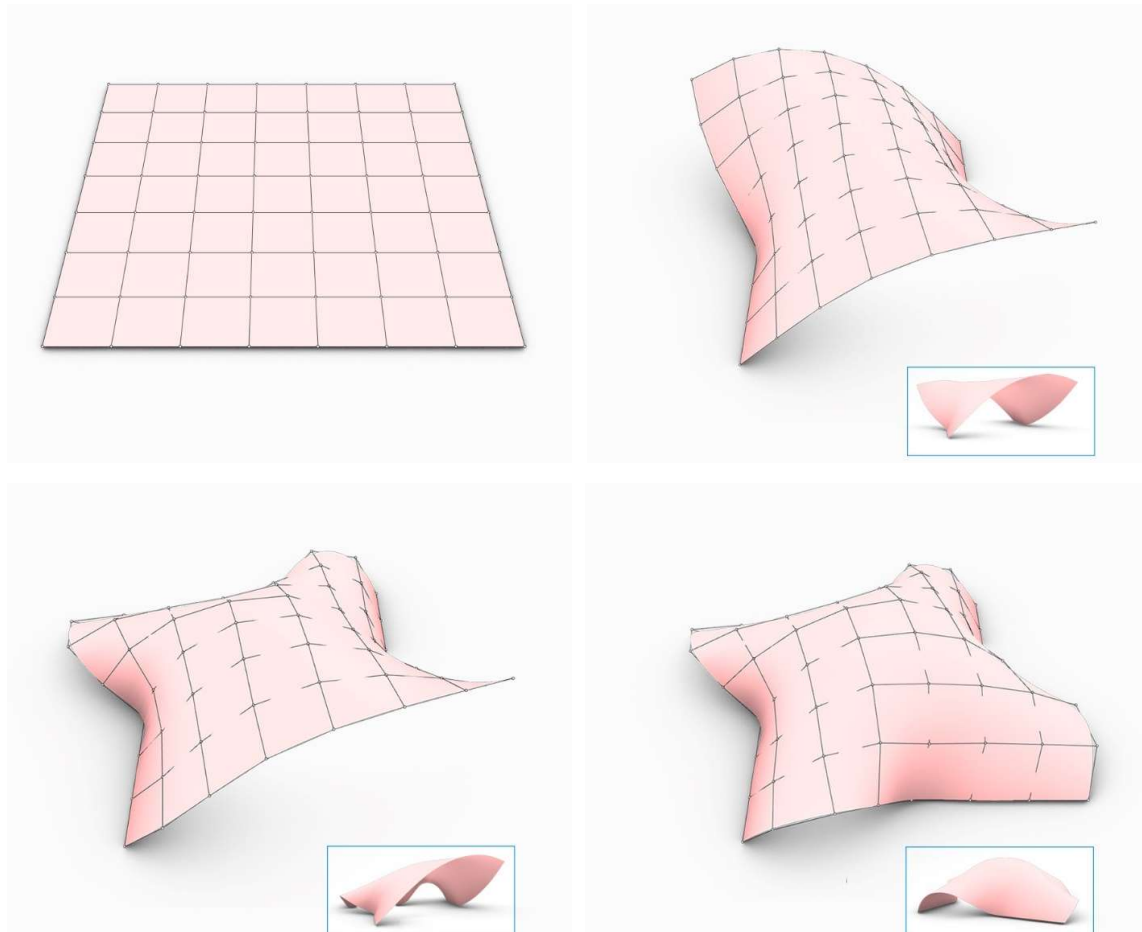


Figure 42 The different surface options and their control polygon: (a) a flat surface, (b) 2 groups of points pushed inwards, (c) 3 groups of points pushed inwards, (d) 4 groups of points pushed inwards. Source: own illustration

## 5.2 From freeform to gridshell

The chapter gives an overview of the computational method involved in generating the gridshell digital model from a freeform surface. Its cross-section and cladding surface will be discussed too. The UV curves created post-simulation are used as input in this chapter. The number of laths that run through the primitive freeform surface had already been decided and the surface is discretized accordingly.

The computational challenge faced in this part of the script is that the cross-section once decided needs to be applied along each curve with its long face parallel to the freeform surface. The main idea is to align the gridshell's cross-section profile multiple times across each curve so that when lofted the laths are shaped. Since the curves are not planar, but free in the 3D space the 2D profiles applied were found rotated without following the curvature of the freeform surface. This generated twisted laths that poorly represented the gridshell.



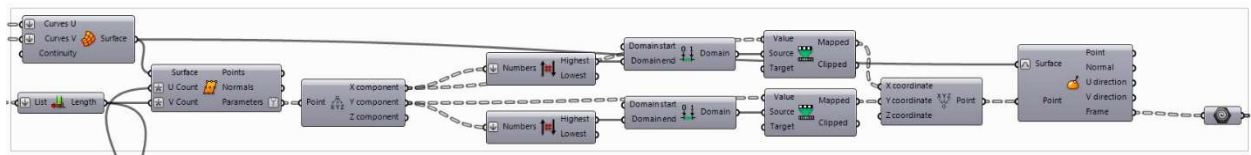


Figure 43 The script that Evaluates the Surface of the freeform. Source: own illustration

The solution to overcome this problem was that the profiles were not aligned to the tangents of the curves. Instead, they are aligned perpendicular to the normals of the surface where the curves intersect. By using the Evaluate Surface Component the surface normals were located and for each point a local plane is assigned. *Figure 44* displays 3 points and their respective planes. The Orient component places the "Source" object, the cross-section to the "Target" geometry, the local plane. Then the profiles are lofted and the final laths are displayed.

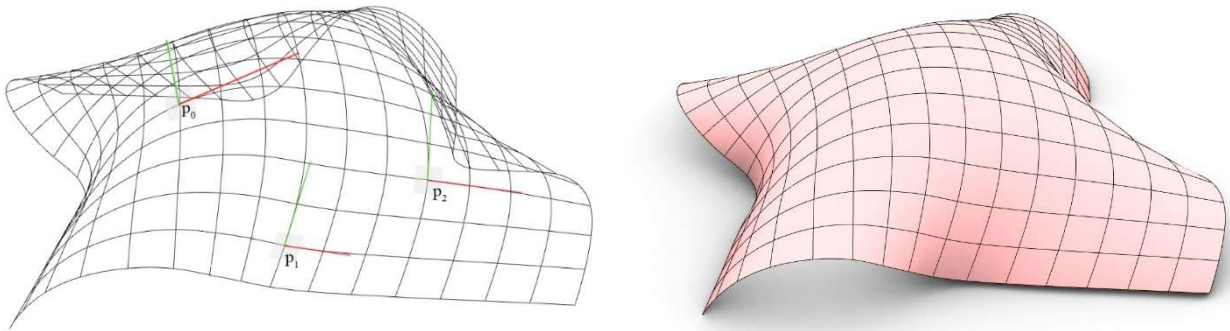


Figure 44 (a) The intersection points  $p_0$ ,  $p_1$ ,  $p_2$  with their respective planes, (b) The NURBS freeform surface the laths create. Source: own illustration

The cross-section chosen for the gridshell is the double layer system found in most of the gridshell examples demonstrated in chapter 4. In theory, nodal connections exist in the intersection between the adjacent laths but are not studied further in this paper. Also, in between the laths shear blocks who are responsible for the shear transfer are added too. Both elements create the "composite connection" that Harris was referring to in chapter 4.4.

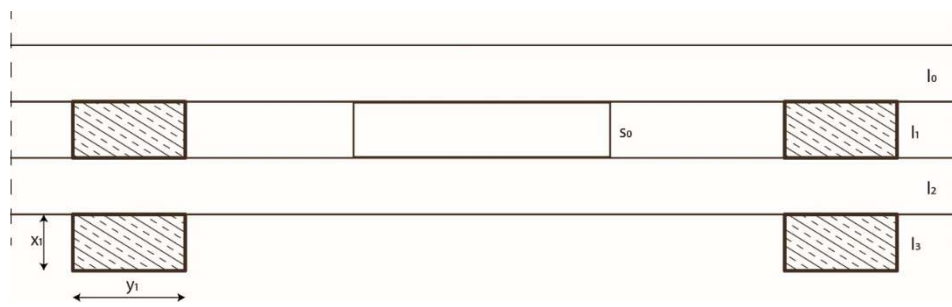


Figure 45 The cross-section. Source:own illustration

In *Figure 45* the cross-section is displayed. The laths are indicated as  $l_0$ ,  $l_1$ ,  $l_2$ ,  $l_3$  and the shear block as  $s_0$ . The values  $x_1$  and  $y_1$  are the width and height of each lath and can change accordingly by the user. Later on the structural analysis the height of the cross-section is not considered to be the  $x_1$  but the height addition of 3 laths due to the fact that once the shear block is placed in between the two adjacent top laths the system is considered solid and the beam height becomes  $3 \cdot x_1$ . Smaller lath height allows for less material use and less cost while maintaining the structural performance.

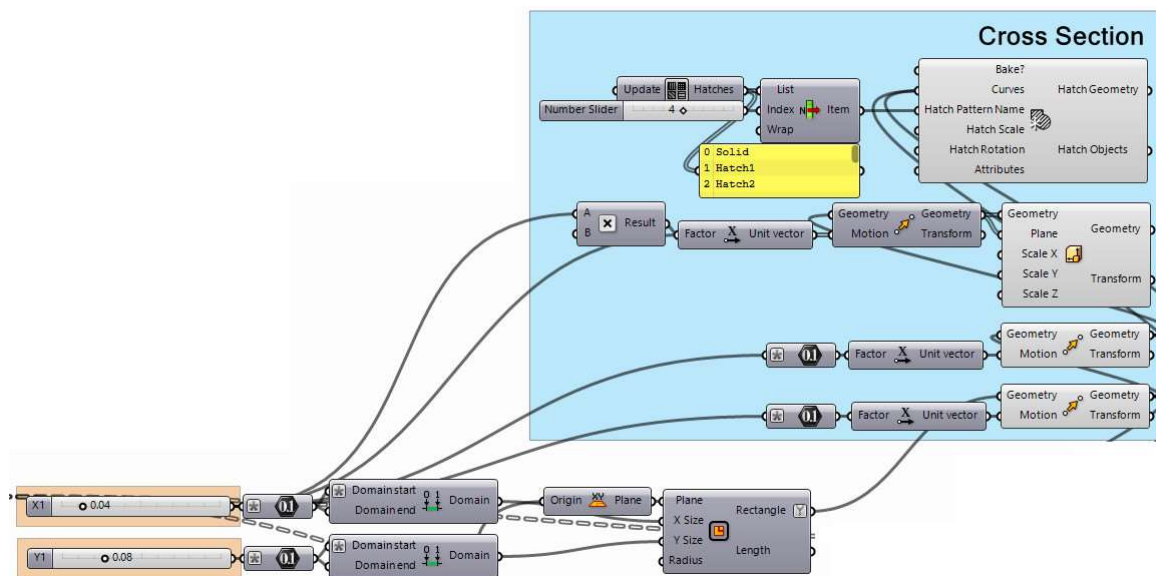


Figure 46 The Grasshopper definition for the cross section that aligns to the local planes across the freeform surface. Source: own illustration

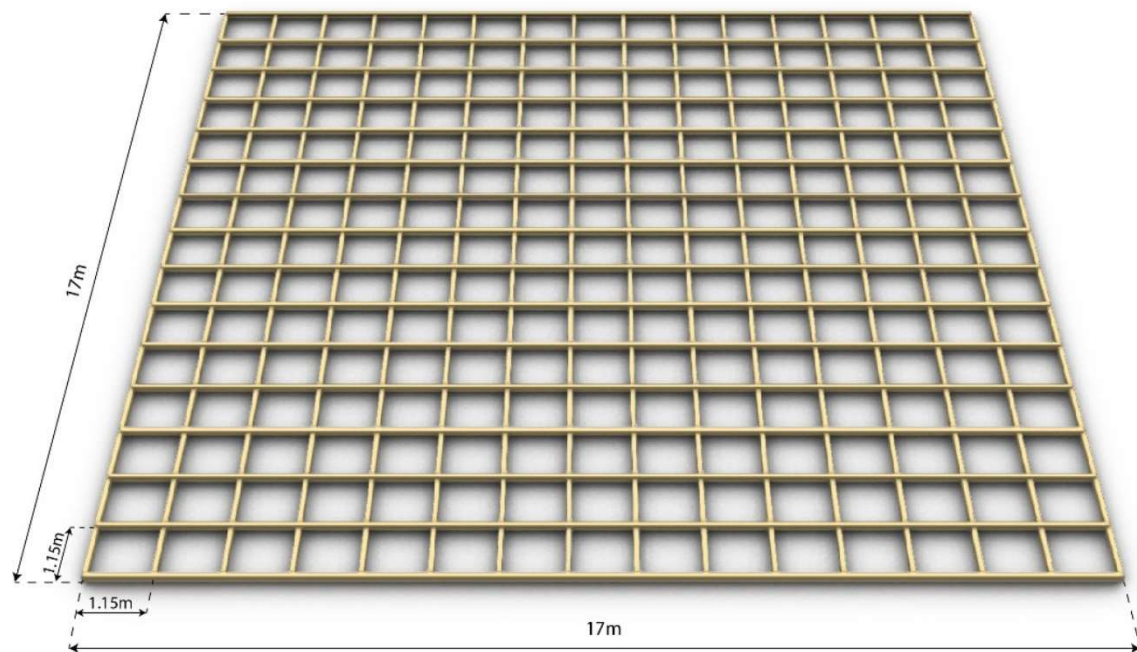


Figure 47 The current timber grishell example with its dimensions in the rest position. Source: own illustration

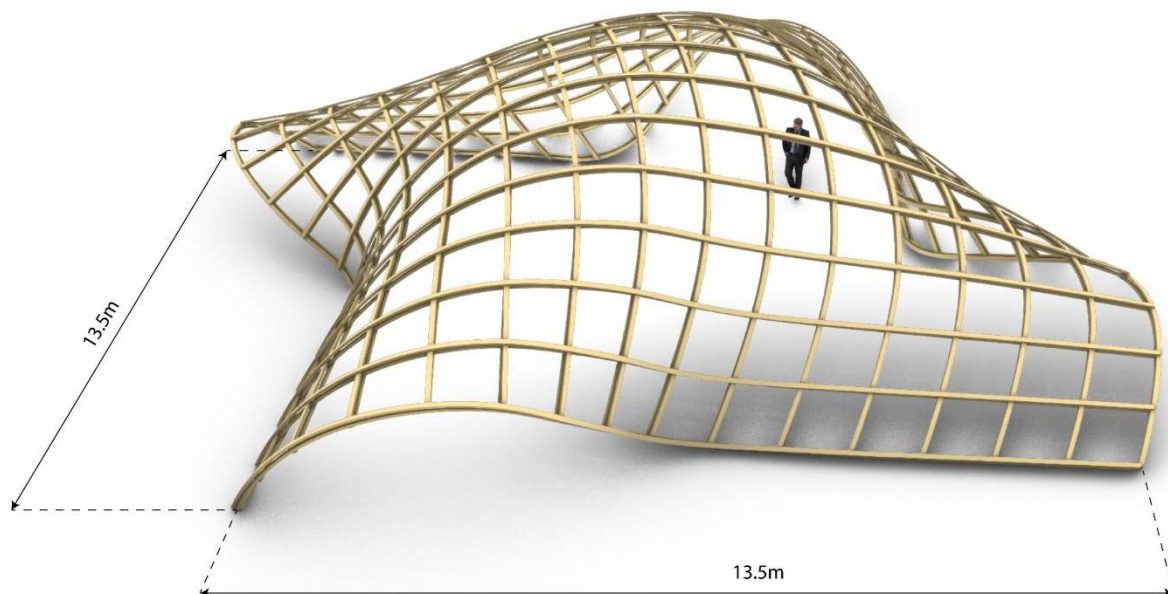


Figure 48 The resultant laths. Source: own illustration

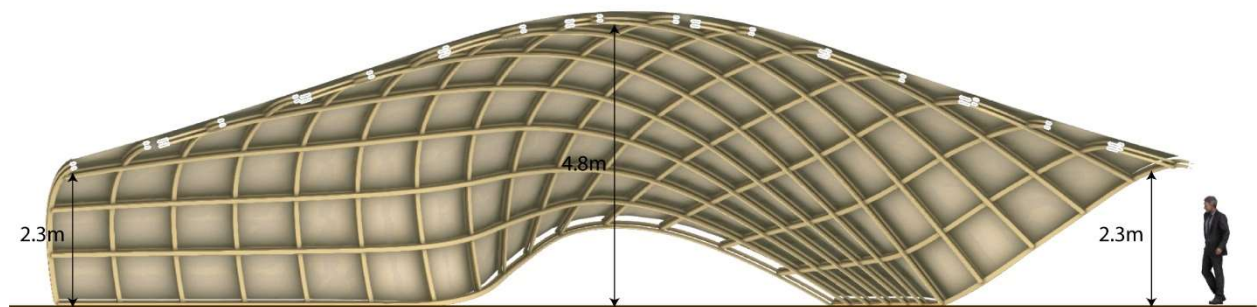


Figure 49 The gridshell in Section. Source: own illustration

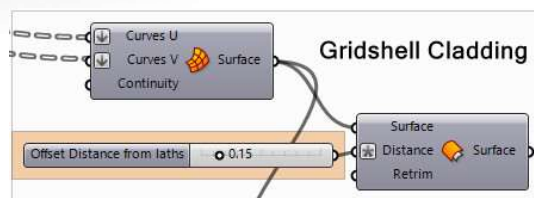
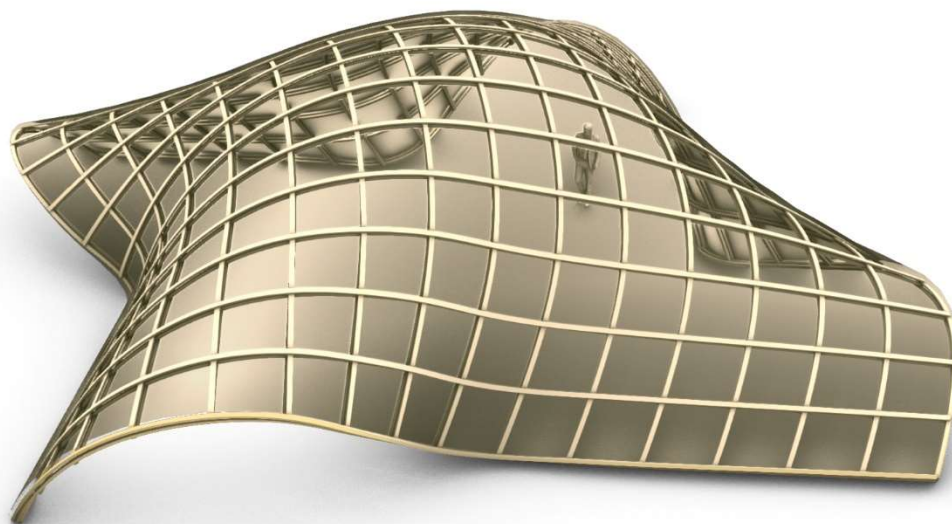


Figure 50 The Offset surface it the cladding of the gridshell. Source: own illustration

From a flat grid of laths 17x17m the maximum dimensions decrease to 13.5x13.5m when pushed inwards. However, the lengths of the laths remain the same and the dimensioning of the of the cladding' panelization follows that rule. Lastly, the cladding is a freeform surface "Offset" from the original freeform NURBS surface displayed in *Figure 44**Figure 46(b)*. Further details are given in chapter 5.4 about the panelization.



### 5.3 Structurally analyzing a timber gridshell

In this chapter the possibility of integrating a structural analysis into the study of a timber gridshell is demonstrated. The Karamba3D Grasshopper plug-in is used as a structural engineering tool which provides an accurate analysis of shells. The Algorithm used is the first order theory for small deflections and the results demonstrated in *Figure 51* are the Axial Forces acting on the gridshell and the Displacement.

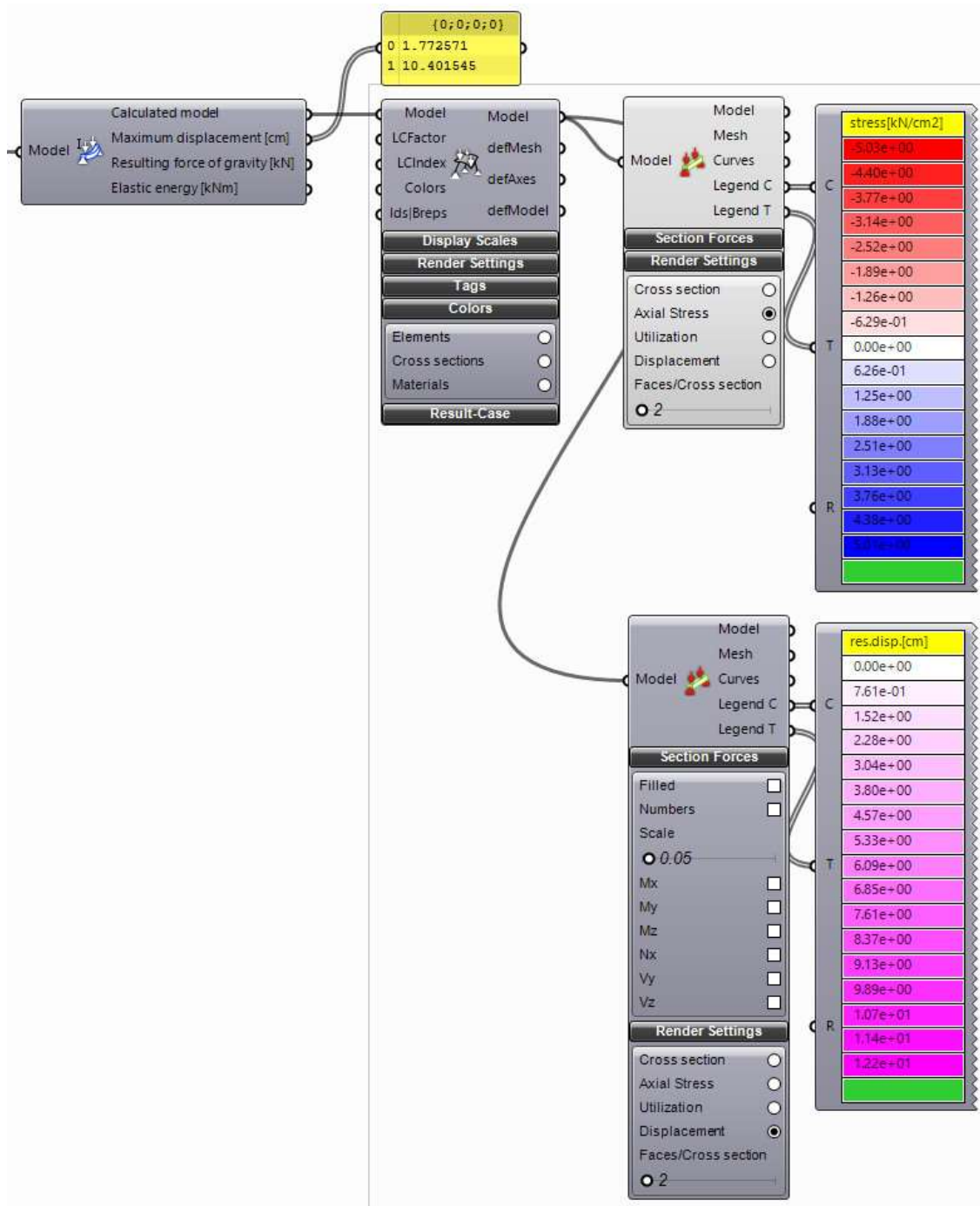


Figure 51 Gridshell structural analysis. Source: own illustration

Due to the fact that the type of timber and the panel material were not decided, specific numbers regarding the material's mechanical properties were not decided too. Custom materials could not be created. Instead, for the timber the "WOOD" material available in the library of Karamba3D is used. The "Disassemble Material" component indicates the mechanical properties of it. Its properties are comparable to the other materials found in the library such as Steel, Aluminum and Concrete and can result in different structural behaviours. These can be viewed in *Figure 52*

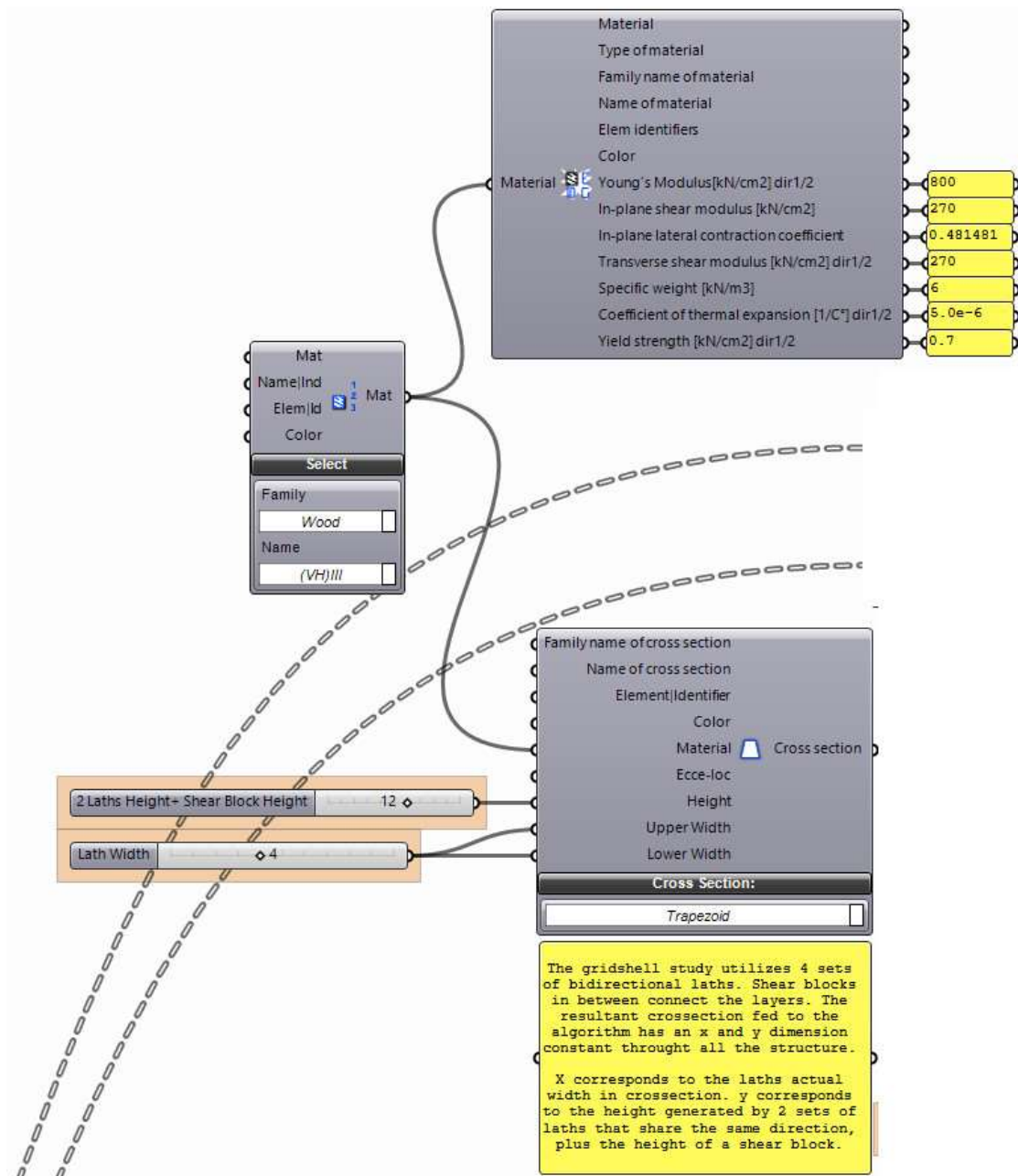


Figure 52 The "WOOD" material is chosen form the Karamba3D Library. Source: own illustration

The "Assemble Model" component gathers the 3 critical data for the structural simulation. These are the "Elements", "Supports" and "Loads" which can be seen in *Figure 53*.

The "LineToBeam" component contains the "Elements" which in this case are the U-V polylines obtained from the previous phase. A label-name "Lath" and the cross-section is assigned to it. As stated in chapter 5.3 the height of the cross section is equal to the addition of the 3 consecutive lath heights due to the shear blocks added in between. The width remains the same.

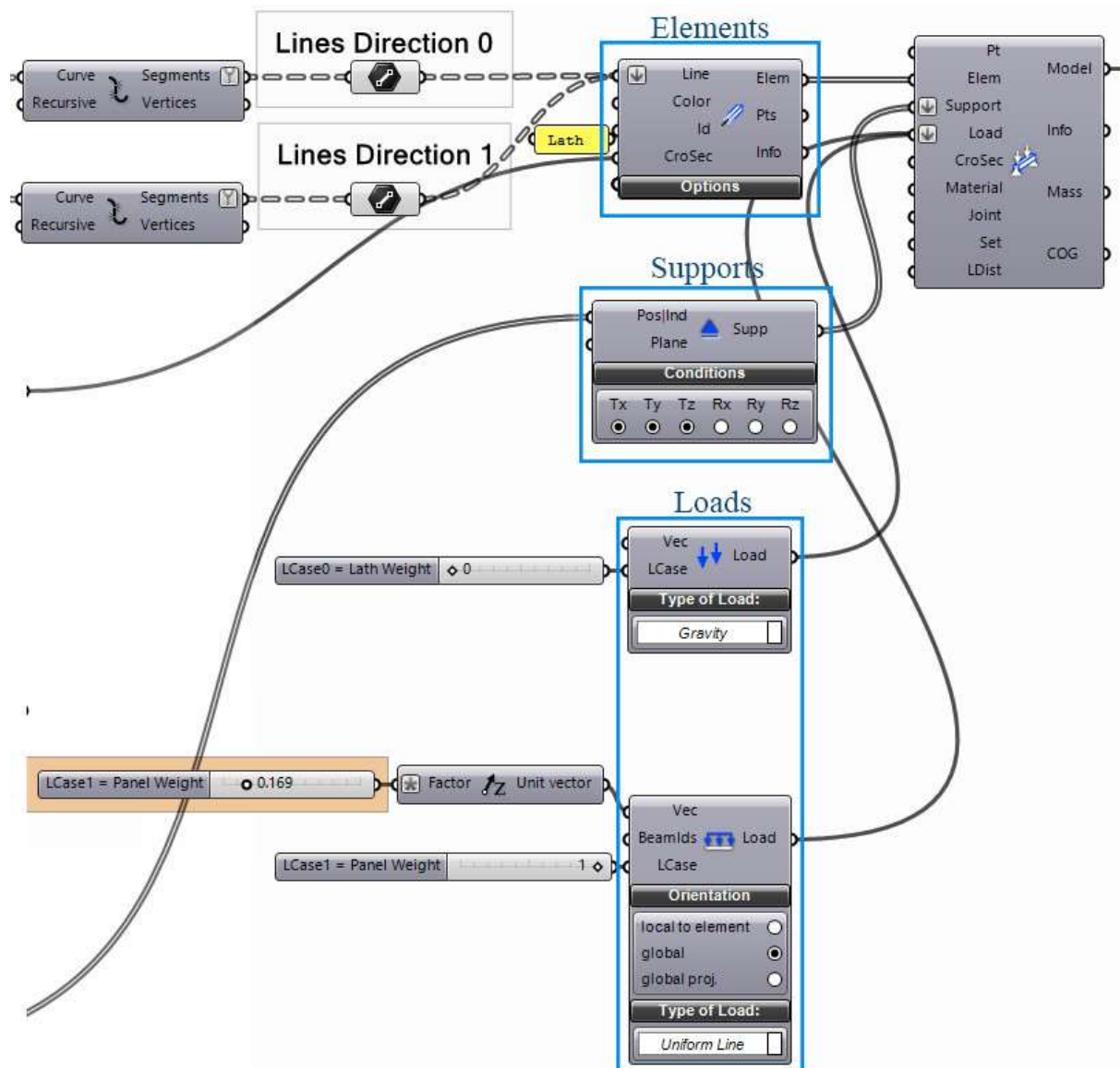


Figure 53 The "Assemble Model" components contains the parameters. Source: own illustration

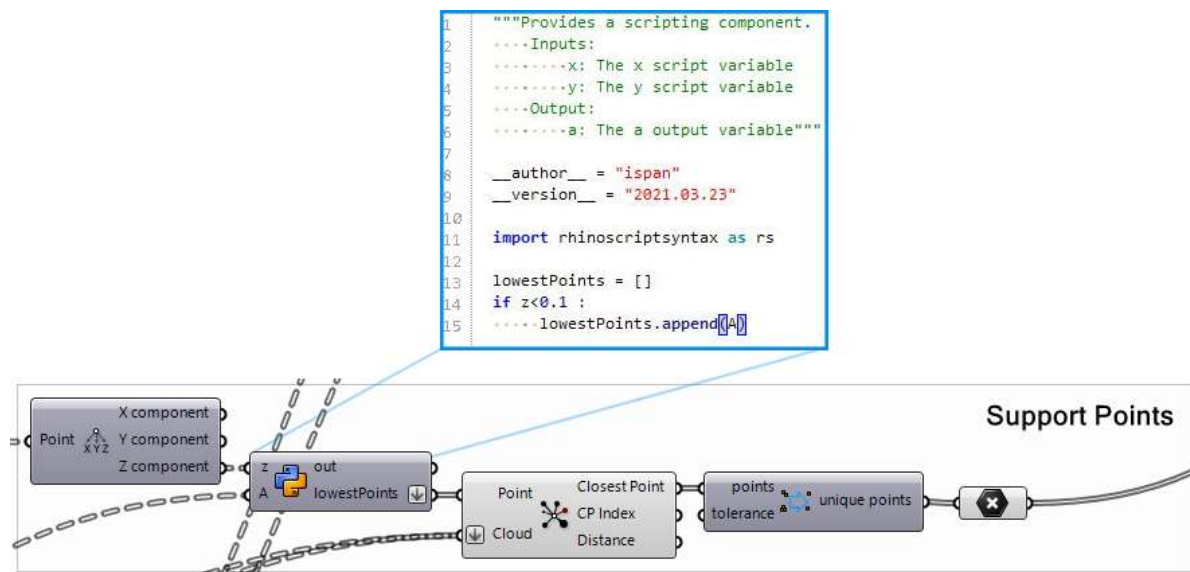


Figure 54 Finding the "Supports". Source: own illustration

The "Supports" are defined computationally in *Figure 54*. The z value is extracted from each point on the list of points where the laths intersect. A GhPython component checks for each z value if it is smaller than 0.1m. Exceeding that threshold would mean that the addressed point is off the ground. The points that touch the ground are the ones that are pushed inwards and support the gridshell thus all the others are excluded as "Supports". In *Figure 53* There are 6 available Degrees of Freedom (DoF), 3 for Translation and 3 for Rotation. The Translational are chosen and the Rotational are omitted due to the fact that a pinned support is chosen.

The "Loads" acting on the system are the self-weight of the timber structure as well as the self-weight of the freeform panels. The latter is considered a Uniform Line because the structure tested is a gridshell rather than a continuous shell. The specific weight of the panels was unknown, so a Slider from 0 to 1kN/m is added instead to the vector pointing downwards. *Figure 56* displays the Assembled Model with the Loads and Supports.

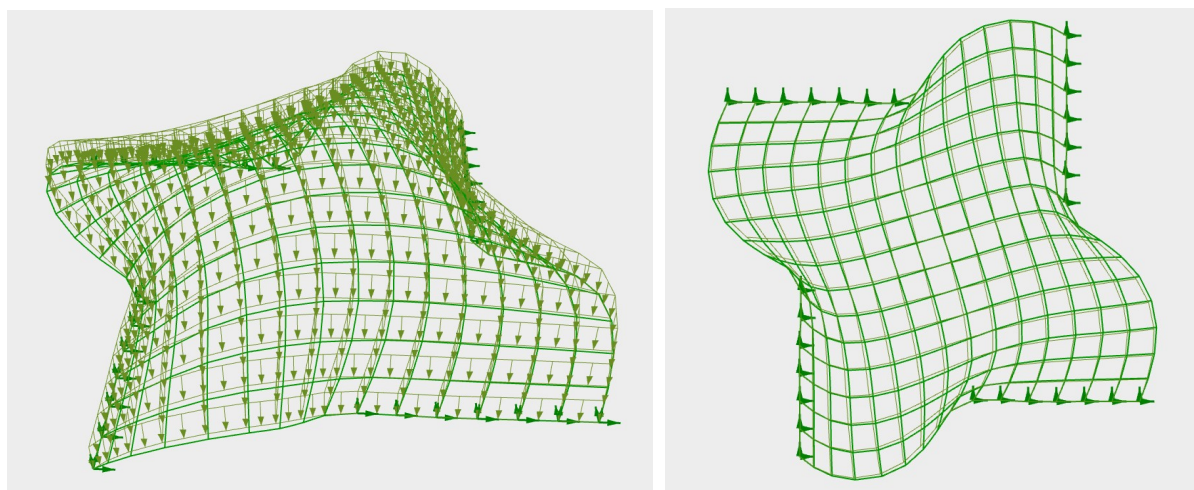


Figure 55 The Assembled Model with the Loads and Supports. Source: own illustration



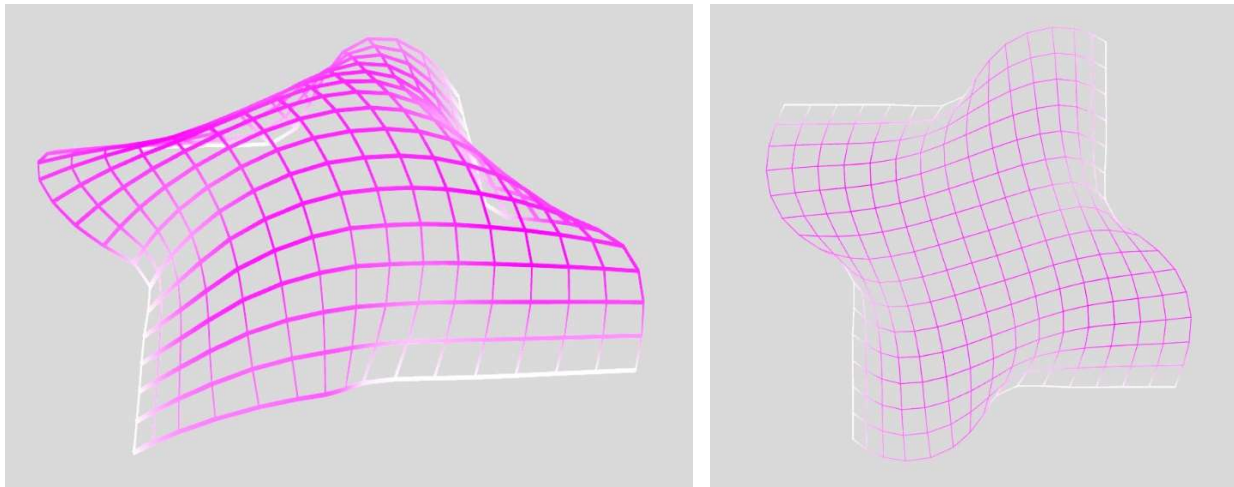


Figure 56 Deformation of the gridshell. Source: own illustration

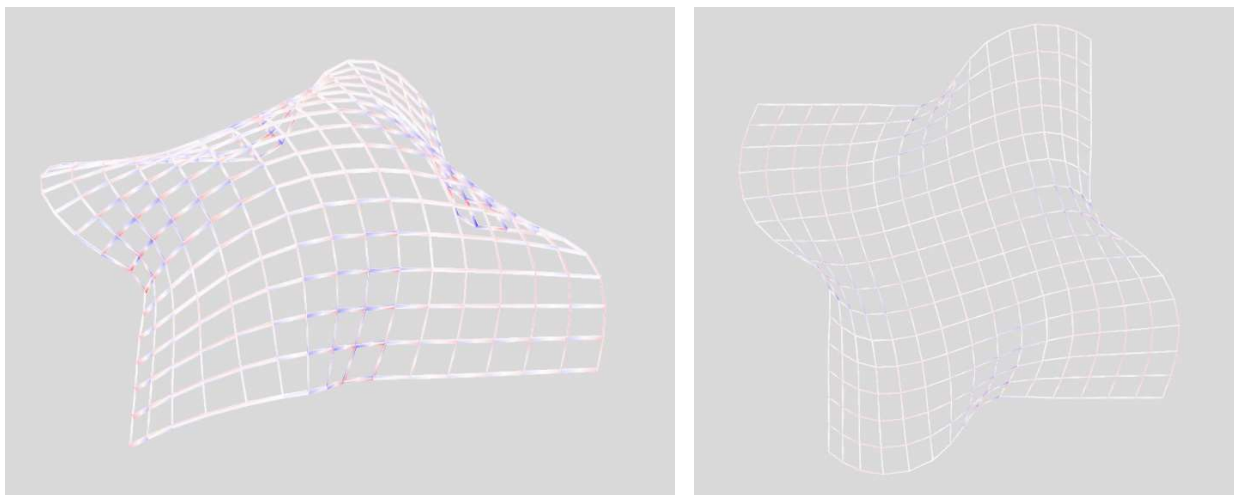


Figure 57 Axial stresses of the gridshell. Source: own illustration

*Figure 56* and *Figure 57* display the deformation and the axial stresses of the gridshell respectively,

## 5.4 Panelization of the freeform surface and Panel Rotational Correction

Once the timber gridshell's lath structure is decided, a cladding layer needs to be placed on top. That layer should take the freeform curvature of the main geometry to fit perfectly on top of it. The computational methods towards the freeform surface realization are the main objective of this chapter and the knowledge obtained in chapter 2 regarding the types of freeform rationalization is about to be put into practice.

In the current example the freeform surface will be considered as a Non-Rationalized Surface. Instead of discretizing the main freeform surface into planar quadrilateral panels, the surface is discretized into quadrilateral panels that inherit the main surface's local curvature. Note that local areas around the cladding freeform surface have a unique curvature that is inherited to the local curvatures of the panels that build it. To fabricate the individual curvature of each panel a significant number of molds would be needed. For a 13.5 by 13.5m structure in plan, considering a panel dimension of approximately 1x1m, more than 182 individual panels would be needed because the height of the structure not included. This results in more than 182 individual molds. To answer that, in the following chapters a formwork that receives each panel's unique curvature is developed and discussed. But before that, the gridshell structure needs to be panelized. Each panel is selected and moved on top of the formwork.

In *Figure 59* the flowchart of the computational method of the panelization is illustrated. A Network Surface is created by the U and V NURBS curves of the freeform obtained in chapter 5.2. In *Figure 58* the cladding surface is Offset 15cm from the central line of the cross-section (the dashed line). This distance is controlled by a Slider. Note that the lines of the panelization follow the lines of the lath network and the dimensions of the panels are approximately 1.05x1.05m. This dimension can decrease or increase depending on the local curvature of the cladding surface. This is due to the offset that occurs in one direction while the freeform surface can freely curve inwards or outwards.

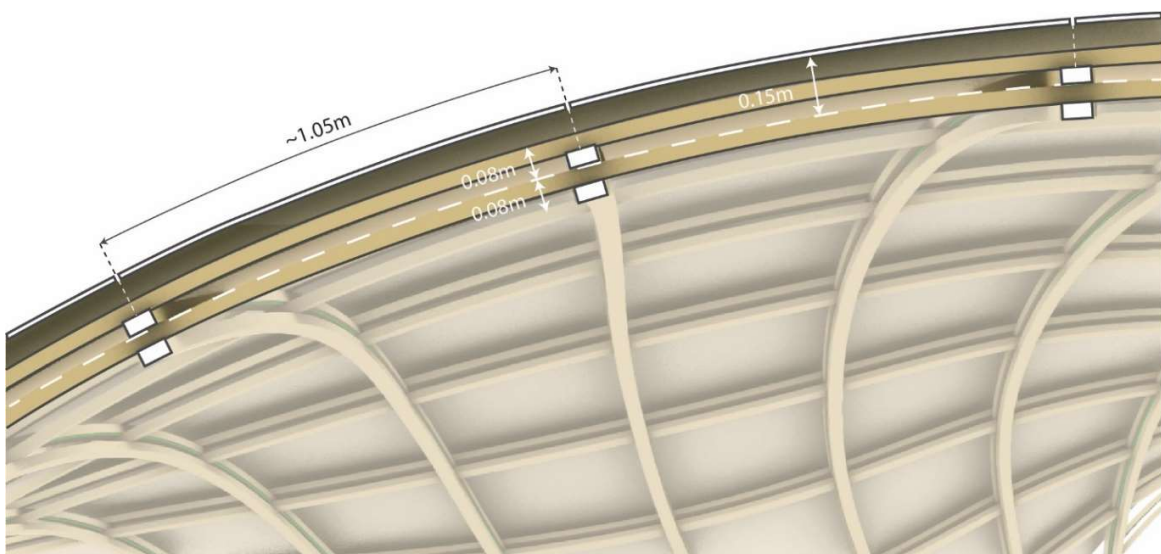


Figure 58 The Panelization lines are following the lines of the timber laths. Source:own illustration

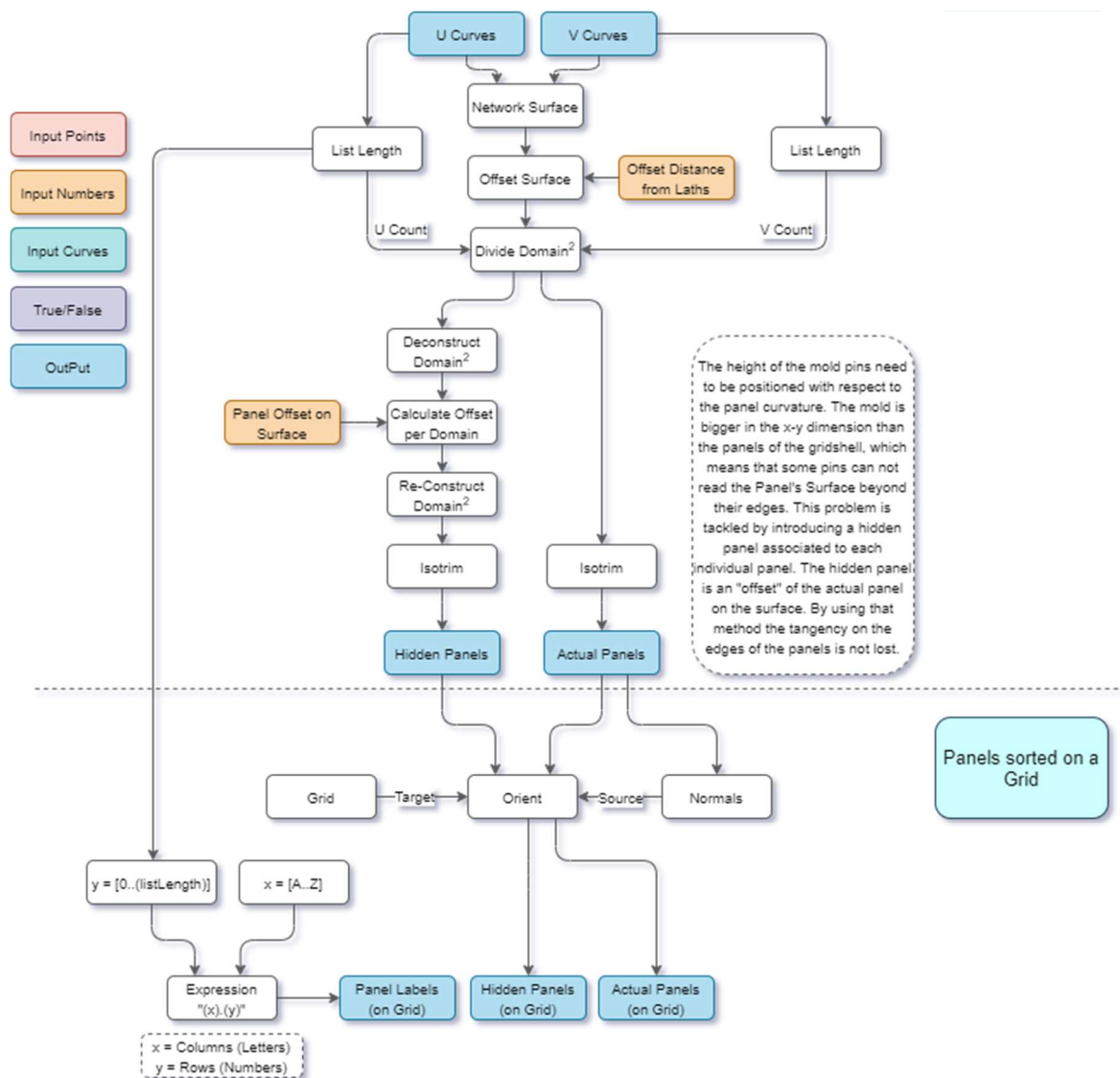


Figure 59 Flowchart for the Panelization of the freeform surface. The list of colours on the top left correspond to the different variables used within the flowchart. Source: own illustration

Computationally the division of the cladding surface is performed with the use of the "Divide Domain<sup>2</sup>". The U and V data are retrieved and fed into the component. Note that there are two lists that the panelization outputs, the "Actual Panels" and the "Hidden Panels". The first contains the isotrimmed panel geometries that are about to be 1:1 fabricated in the end. The second one contains curved geometries that are adjacent to the Actual panels and need to be read by the Re-De-Form.

To shed light into that, the mechanism of the Re-De-Form contains pins that read the curvature of each panel by translating it into positional data. Each panel's dimension is smaller than the Re-De-Form's general dimension meaning that Re-De-Form has insufficient data to process. Per panel, more positional data need to be gathered from its adjacent panels. To achieve this an offset per panel is performed on the U and V outward direction. The resultant surfaces are isotrimmed and saved under the Hidden Panel list. In other words, the tangencies beyond the panel's edges are not lost. *Figure 60* displays the relation between the lath network and the panel network.

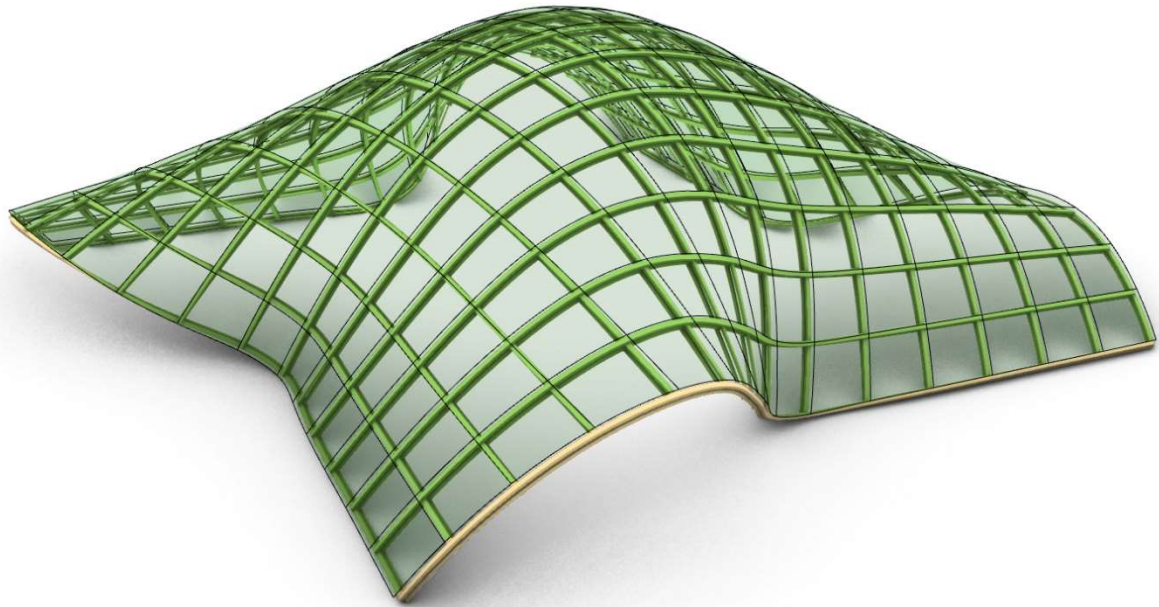


Figure 60 The panel network follows the lath network. Source: own illustration

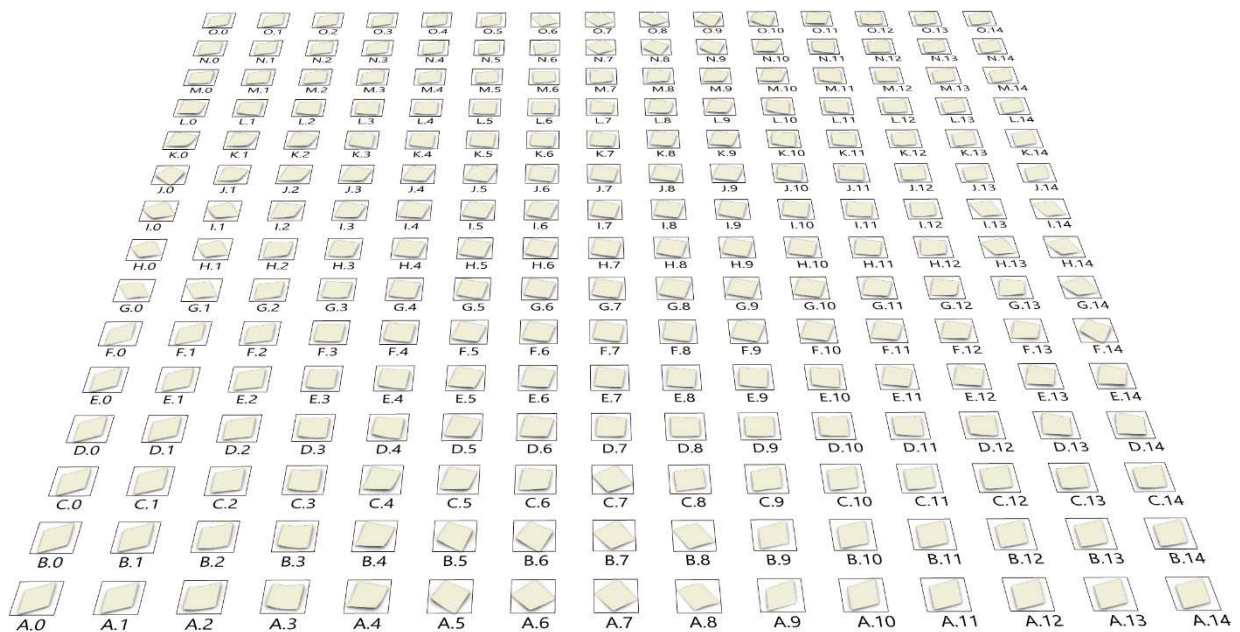


Figure 61 The panels are numbered and sorted on a grid. Source: own illustration

Once the surface is discretized the panels need to be named and placed into a grid so that they can be easily accessible for fabrication. In *Figure 61* each panel name contains a letter followed by a number. The letter represents the row and the number represents the column. On the same grid the Hidden panels are also placed so when the user selects an Actual panel the Hidden panel is also selected and sent into the Re-De-Form.



As the names indicate the Actual panel is visible and the Hidden panel is invisible. In *Figure 62*, the two panels illustrated look as if they are missing one or two adjacent faces. These panels A.13 and A.14 happen to be placed on the edges of the freeform surface, thus there are no adjacent faces to be displayed. A solution is given in section 5.5 regarding that.

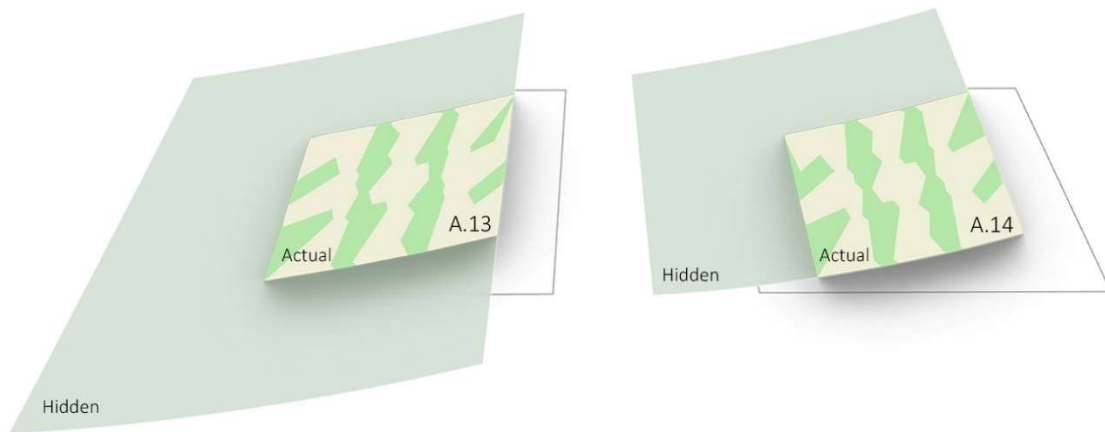


Figure 62 The A.13 and A.14 Actual and Hidden panels. Source: own illustration

In *Figure 63* the panels are visible from the top view. The 1.60x1.60m rectangle that contains them is the outline of Re-De-Form. Their dimensions parallel to the edges approximate 1.10m and their outlines are similar to parallelograms. Although their edge length remain similar, their inner angles vary. Also, once moved to the grid of points their angles of rotation with respect to Re-De-Form are random. In the following example panel A.2 fits the outline of the Re-De-Form almost perfectly, whereas panel A.5 exceeds the outline of the Re-De-Form. This means that some of the panels would require a manual rotational adjustment around their central point so that they can fit the 1.60x1.60m Re-De-Form outline before becoming ready to fabricate, a process tedious and time consuming.

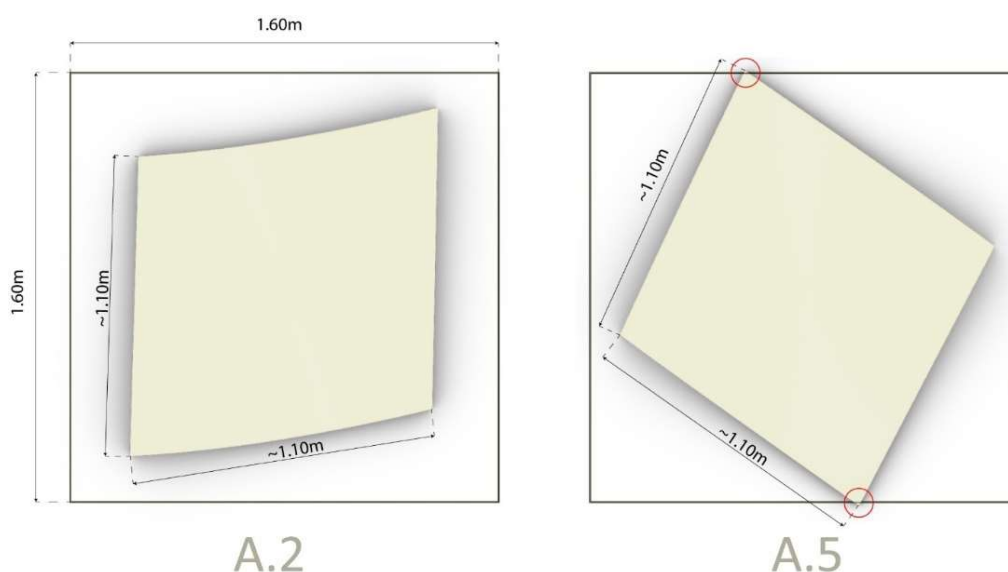


Figure 63 Panels A.2 and A.5. Source: own illustration

To answer that, an algorithm was developed that runs for all the panels and checks whether they can fit inside a rectangle and exceed the Re-De-Form outline. Inside the 0-90 range there are rotations for which the panels are rotated best. These are identified and used among the others. The script is split in two phases-refinements.

At first, a Series of numbers from 0 to 90 is connected to a Rotate component. The centroid of each panel is used as the center of rotation. The resultant 90 geometries per panel are contained inside a Bounding Box. Since most of the panels approximate parallelograms in plan and the Re-De-Form outline is a square rectangle this means that the bounding boxes of the panels can only but approximate that geometry. For each Bounding Box, two of the adjacent and perpendicular edges are retrieved and their fraction is calculated. Value 1 indicates that the two edges of the fraction have equal lengths and that their Bounding Box is a rectangle. These values are then subtracted -1 and their absolute "distances" from value 1 are saved and sorted into a list from smaller to higher. The first item of that list is picked as the best rotated panel.

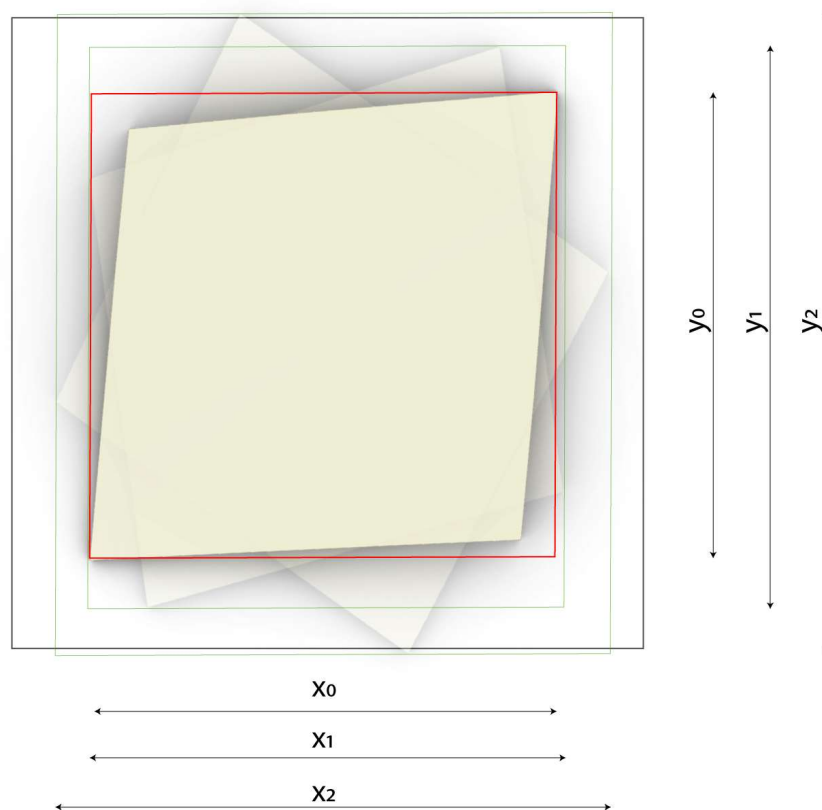


Figure 64 Different rotational options. The algorithm finds the similar length of  $x$  and  $y$ . Source: own illustration

Figure 64 illustrates panel's A.5 different rotational options.  $X_0$ ,  $x_1$ ,  $x_2$  and  $y_0$ ,  $y_1$ ,  $y_2$  are the lengths of the Bounding Box's edges calculated in the fraction. Note that  $X_0$  is almost equal to  $y_0$ . Among the other two rotational options that is the one chosen by the algorithm. Figure 65 illustrates the computational steps, included in the first phase of the algorithm.

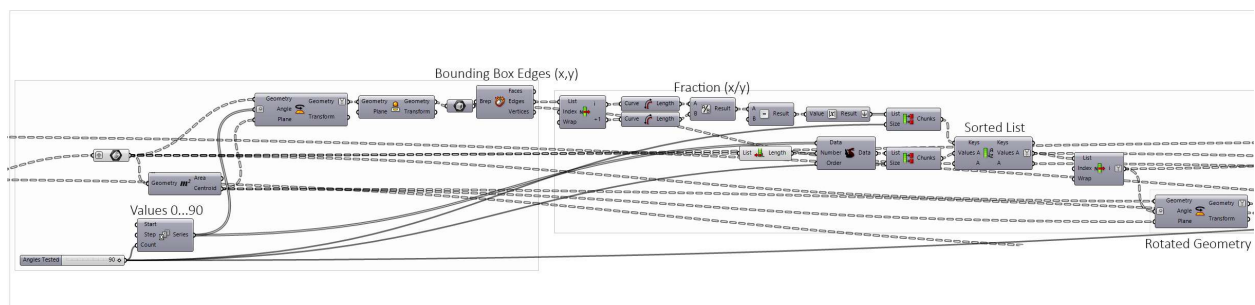


Figure 65 The first phase of the Rotational Correction Algorithm. Source: own illustration

In the second phase the algorithm checks whether the perimeter of the Bounding Box is smaller than a certain number. That number could be the perimeter of the Re-De-Form but in the current case it is a number smaller than that because the panels edges need to be as far as possible from the edges of the Re-De-Form. The value decided represents a rectangle of 1.40 by 1.40m, or in other words a 20cm inwards offset from the Re-De-Form outline. All 225 panels obtained from the first refinement should follow that rule. In *Figure 66* this can be seen.

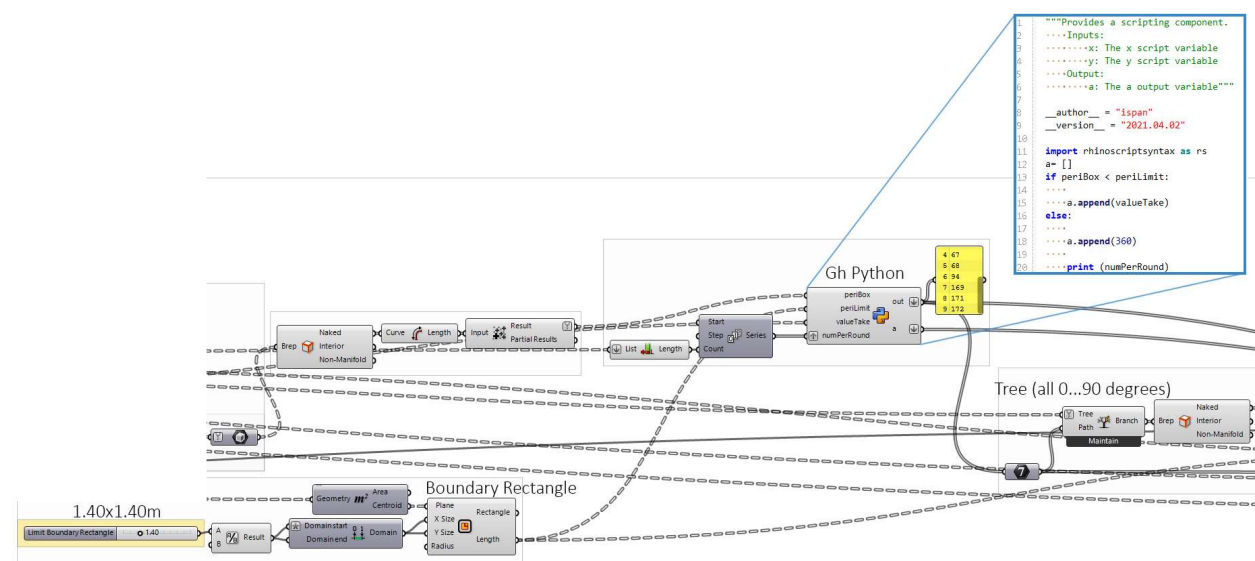


Figure 66 The 2nd refinement's 1st part. Source: own illustration

Later, a GhPython component finds the panels that do not follow that rule and an output list of indices is created. Note that in the previous phase each panel is contained inside a Branch with all the rotational options from 0 to 90 degrees. This list is retrieved and the output of the GH Python component are the Branches that need to be refined again. A "Smaller Than" expression component searches for the first panel angle, in the list of 90 values, that is smaller than the boundary of 1.40x1.40m and outputs it as the optimal rotation. The Replace Item component replaces the incorrect angles with the correct ones. The new values are assigned both to the Actual Panels and the Hidden Panels with the center of rotation the centroid of the Actual Panel. In *Figure 67* this can be seen. *Figure 68* and *Figure 69* display all the corrected panels.

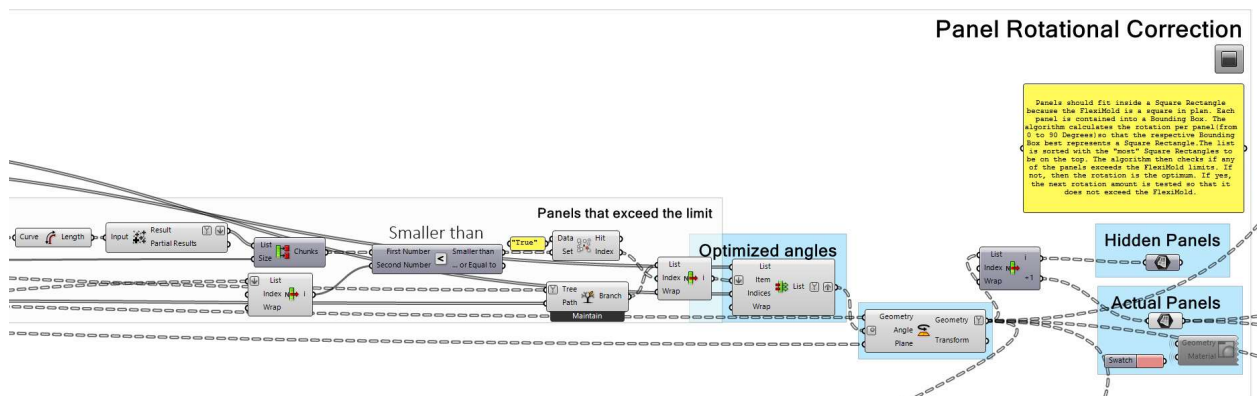


Figure 67 The 2nd refinement's 2nd part. Source: own illustration

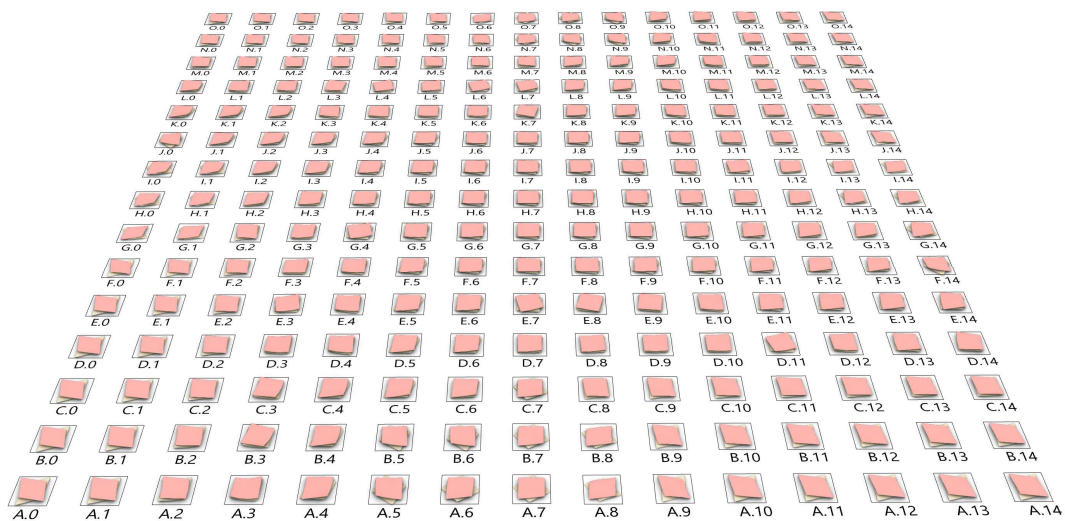


Figure 68 An overview of the rotated panels and their initial rotations. The corrected panels are marked with a pink colour. Source: own illustration

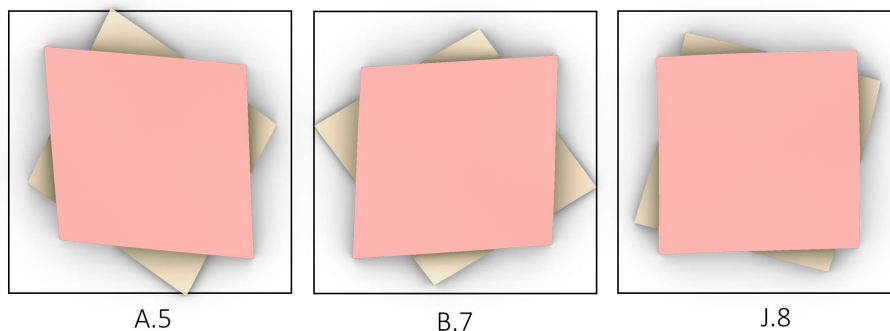


Figure 69 Orange is the initial panel and pink is the rotated one. Source: own illustration



## 5.5 The digital Re-De-Form

The digital model of the Re-De-Form is a computational tool that can be modified according to the user's requirements. The number of pins, their in-between distances, the thickness of the surface material and the timber base dimensions can change with respect to the panel's dimensions or curvature variations. In this chapter a 1:1 digital Re-De-Form is built specifically for the dimensions of the current gridshell example but since it is a parametric model these dimensions can change any time. In the next chapter a physical version of the Re-De-Form is built along with the 1:1 just by adjusting some of the Sliders and adding some lines of Code.

The 1:1 digital model consists of a timber base, pins and a flexible surface. The timber base dimensions used are just for reference. If a physical mold is about to be built, then the exact timber dimensions and cut parts should be defined in detail beforehand. The number of pins is 25 (5x5). Since the digital Re-De-Form will be used for panel fabrication the number of pins will be limited to 5x5 because the curvature of the panels is not complex. In the next chapter, 5.6.1, a detailed overview is given on what are the surface properties that this specific dimension hinders with respect to the overall dimensions of the Re-De-Form. Lastly, the flexible surface, fluctuates on top of the pins following the curvatures of the Actual and Hidden panels. The pins follow that fluctuation by changing their position on the z axis. *Figure 70* illustrates the Re-De-Form digital set up. Different panel examples are shown. *Figure 71* displays two design options with different numbers of pins and in-between pin distances.

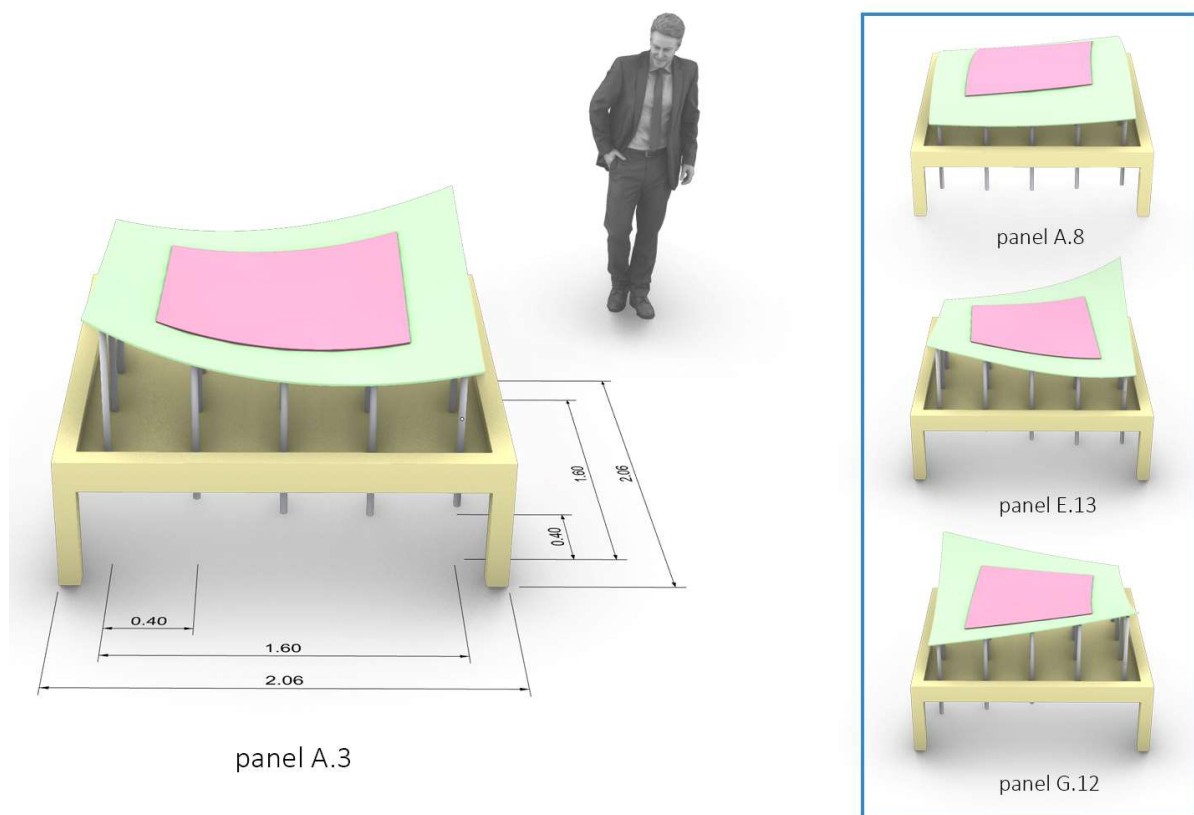


Figure 70 The digital Re-De-Form and some example panels. Source: own illustration

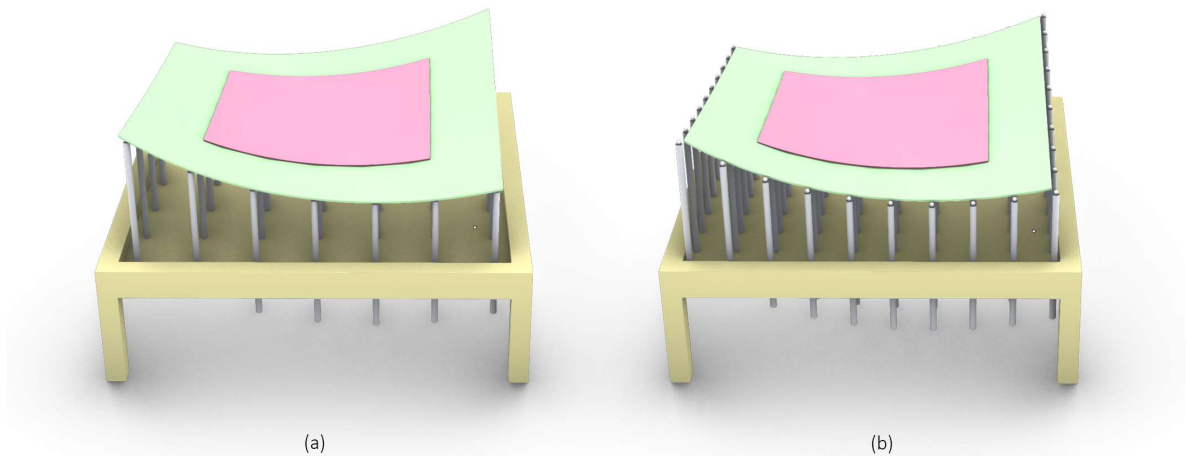


Figure 71 (a)7x7 pin Re-De-Form with in-between pin distance 30cm. (b)10x10 pin Re-De-Form with in-between pin distance 20cm. Source: own illustration

One of the challenges faced is that the panels located on the edges of the cladding freeform surface do not have adjacent faces. This means that once their respective Hidden panels are placed on the mold the algorithm is incapable of reading the rest of the surface, because it is blank. The pins that correspond to these positions can not be positioned because they are not given a z-value. An inventive method is developed to overcome this problem.

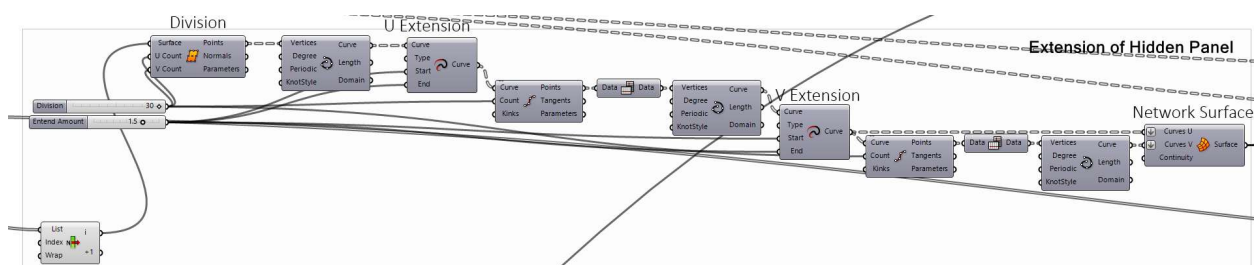


Figure 72 The extension of the Hidden panels. Source: own illustration

The Hidden panel's surface is divided into a U and V grid of points. The points are interpolated in the U and V local directions and extended outwards. A Network Surface component is used to transform the U and V curve network into a surface that can be read by the Re-De-Form. *Figure 72* illustrates the algorithm used to extend the U-V curves. *Figure 73* displays the hidden curve network above Re-De-Form.

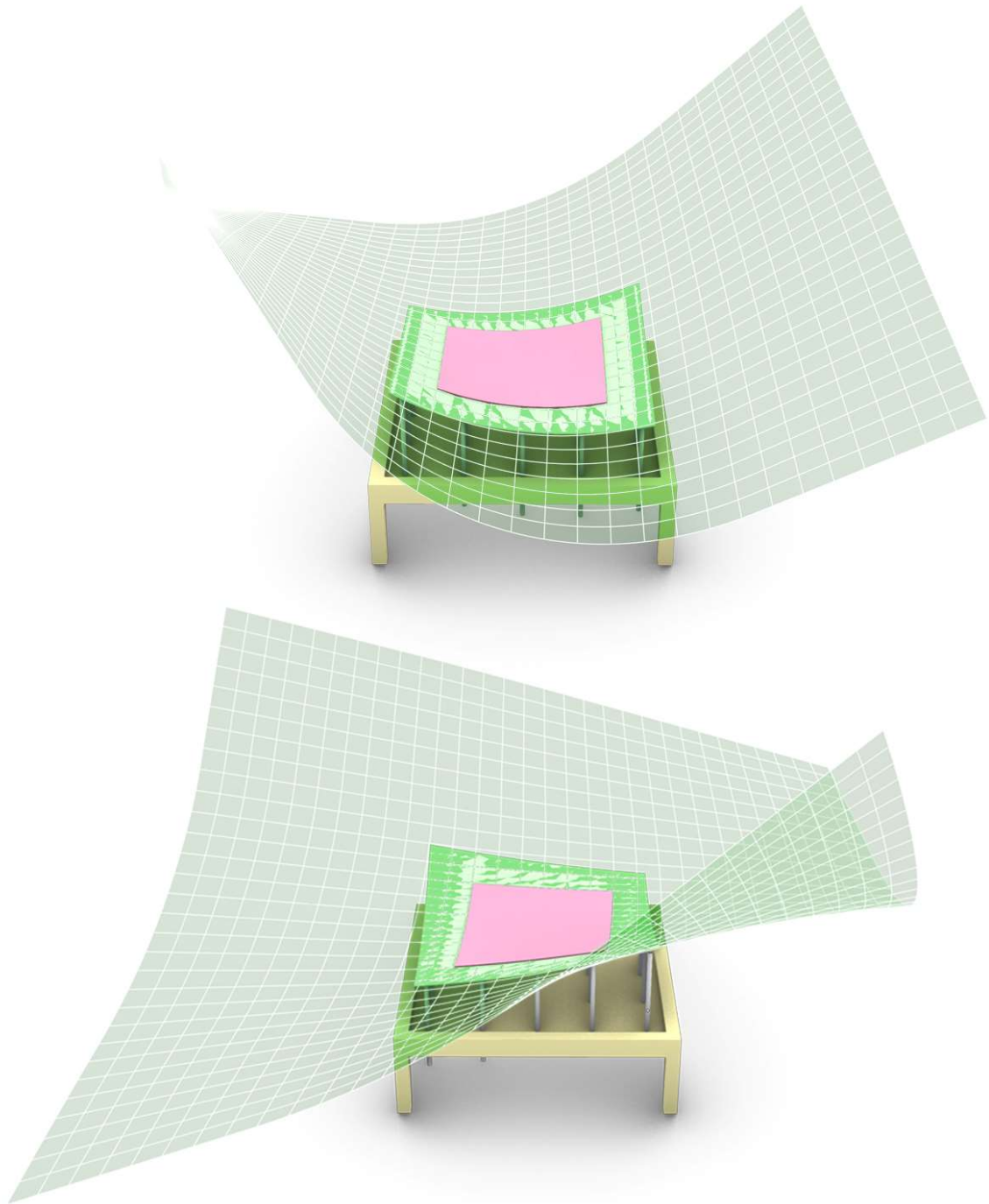


Figure 73 The extended U and V curve Networks for two different panels. Source: own illustration

Along with the digital 1:1 FlexiMold, a digital 3x3pin version is created. Its scale is 1:5 than the former, meaning that each panel has to be scaled 5 times less too. A new script is generated and is almost identical to the other one with the difference that there are some groups of components added. *Figure 74* displays the 3x3pin digital Re-De-Form.



Figure 74 The 3x3 pin Re-De-Form. Source:own illustration

In *Figure 75* the panels are scaled from the 1:1 scale down to 1:5. In *Figure 74* the pins are placed into their HOME positions (0,0,0). When Toggle "Rest Position" is True the pins are Homed and when False, panels can be cast into the mold.

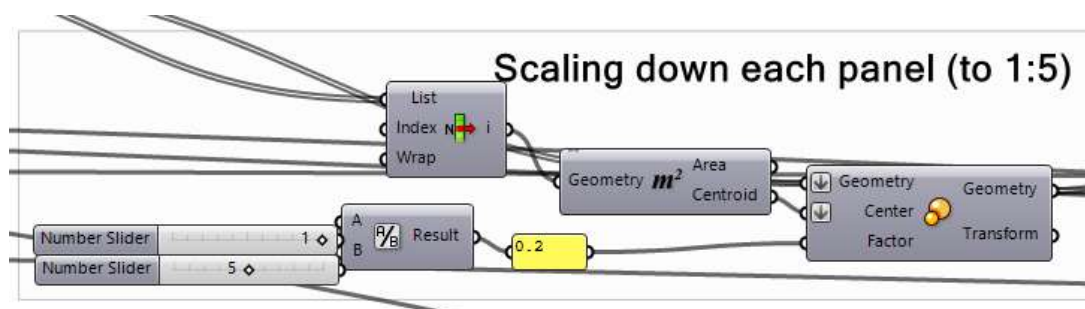


Figure 75 Scaling the panels to 1:5. Source: own illustration

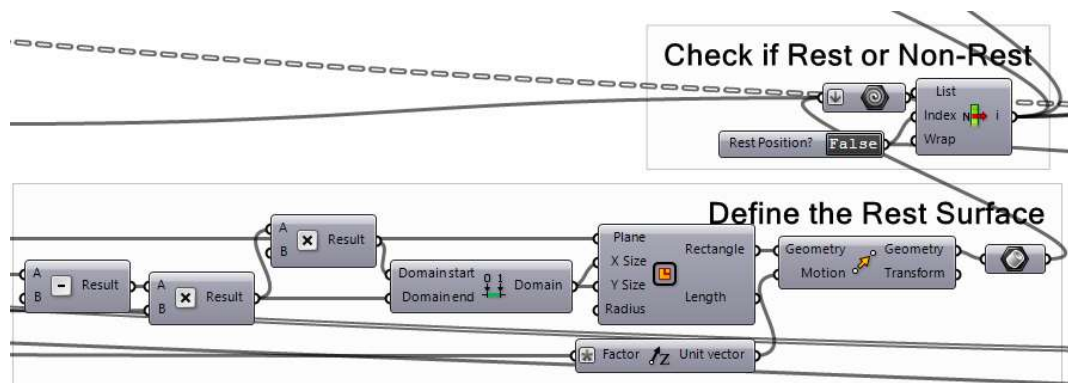


Figure 76 Place the pins into their HOME position. Source: own illustration

The last step is to connect the 3x3 digital Re-De-Form's Grasshopper Definition to the physical model built in the next chapter through the Arduino IDE. The positional values need to be converted into information that the Arduino can read to enable the steppers to move to the desired position. A more detailed overview on the physical set up is about to be given in the following chapter.

The distances the pins need to travel from their HOME position towards the curved panel are converted into centimeters. The pinion's diameter are converted into centimeters and hold a value of 1.2cm. The linear movement of the pinions is translated into rotational that the stepper motors can read. By dividing the travel distance to the perimeter of the pinion's circle and multiplying it by 360 the angles of rotation per pin are calculated. The output can be seen in *Figure 77*.

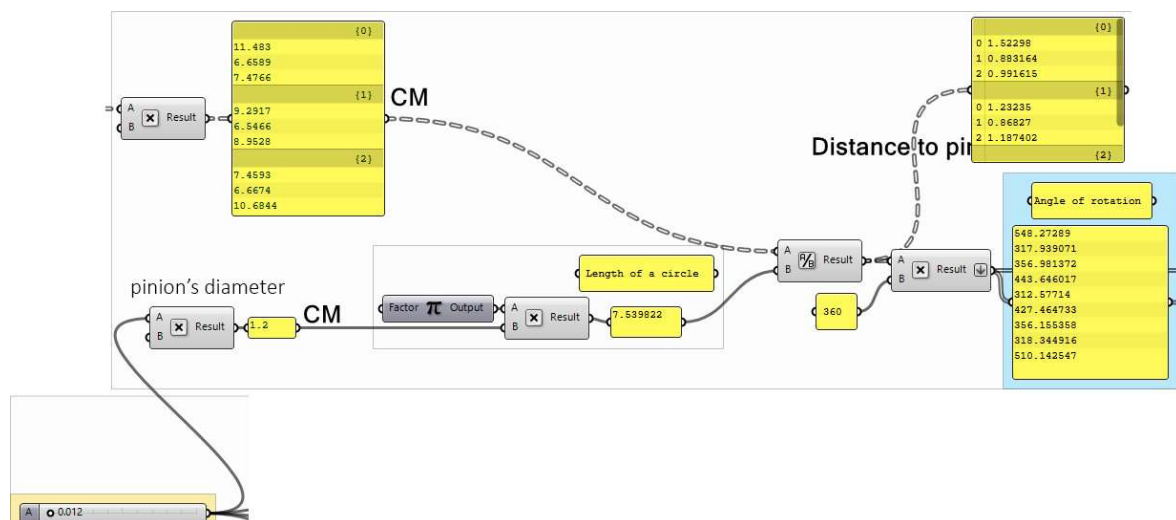


Figure 77 Angles of rotation. Source: own illustration

In *Figure 78* these values are converted to microsteps through the Firefly "Convert Degrees to Steps" component. As the name states the degrees are converted into microsteps. This is due to the fact that many stepper drivers use microstepping which breaks the microstep into smaller steps. In that case one step equals to 8 microsteps. Also, regarding that most motor drivers for one full 360 degrees rotation need 200 steps one step equals to 1.8 degrees. The internal calculation of the component is as follows: For example of the first item in the list is used, the 548. It is divided by 1.8 to find the amount of steps needed for the given degrees and then the result is multiplied by 8 for the amount of microsteps to be calculated. This value is fed to the Arduino Serial Monitor when the Simulation starts.

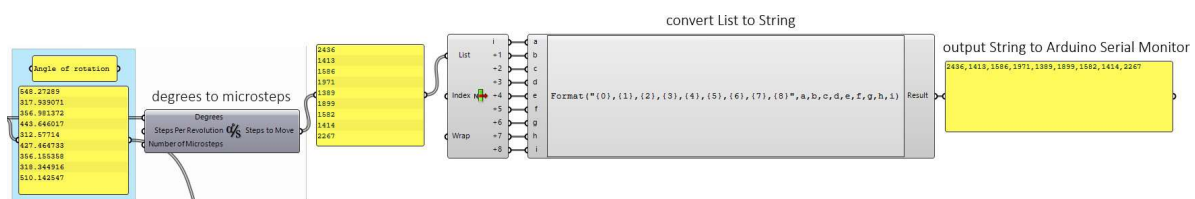


Figure 78 String to Serial Monitor. Source: own illustration

Lastly, the digital workflow of the Re-De-Form according to the input gathered previously is mainly for fabricating the panelization of the timber grishell. But its function is not only limited to that. As the examples suggest in the literature review of chapters 2 and 3 physical modelling is an important aspect when it comes to freeform surfaces and freeform gridshell structures. Reflecting upon that, an algorithm is created that changes between 2 design scales can be read by the Re-De-Form. The code used for the 1:1 Re-De-Form and 3x3 pin model is used with a few adjustments taking into account the different scaling of the gridshell's surface as well as relation to the pins of the mold.

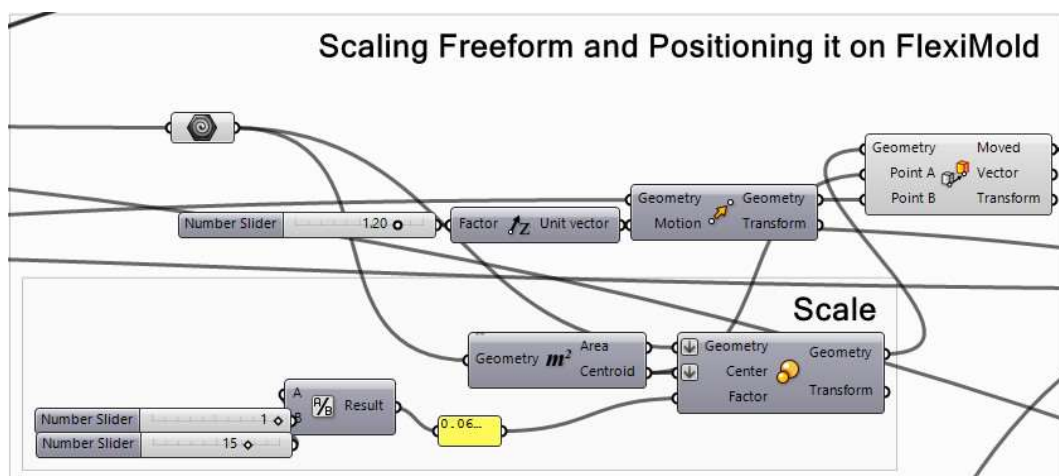


Figure 79 Scaling down the gridshell's freeform surface. Source: own illustration



The 3 scales tested are the 1:10, 1:15 and 1:20 and the number of pins has increased to 49(7x7). The curvature with relation to the scale and use are described in the next chapter 5.6.1. What is important in this face is the fact that once the freeform is scaled down and placed on the mold the same problem with the pins that can not identify the surface on the edges of the mold reappears. This is tackled by a slightly different way because the curvature of the surface's tangents are steeper in their edges than these of the panels. Extending the U and V curves of the surface would cause great height differences between the pins and generate a freeform surface impossible to produce by the physical Re-De-Form.

The outline of the freeform is retrieved from the initial parts of the script and the rectangular outline of the Re-De-Form is copied and scaled two times. A "Patch Surface" is created between these two curves and the 2 surfaces, the freeform and the patch are read by the Re-De-Form for pin positioning. The script utilized is displayed in *Figure 80*.

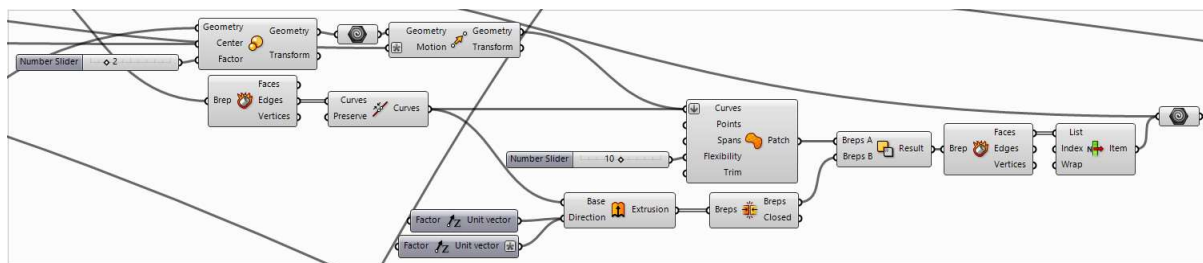


Figure 80 A patch between the freeform and a Rectangle. Source: own illustration

Re-De-Form can represent the physical model of a surface in different design scales. *Figure 81*, *Figure 82* and *Figure 83* demonstrate the different surface scales of 1:10, 1:15 and 1:20 respectively.

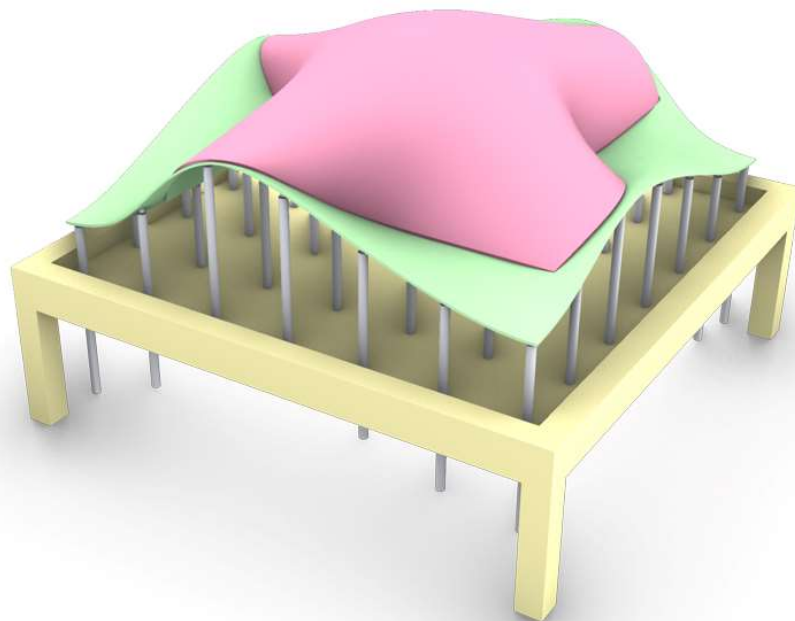
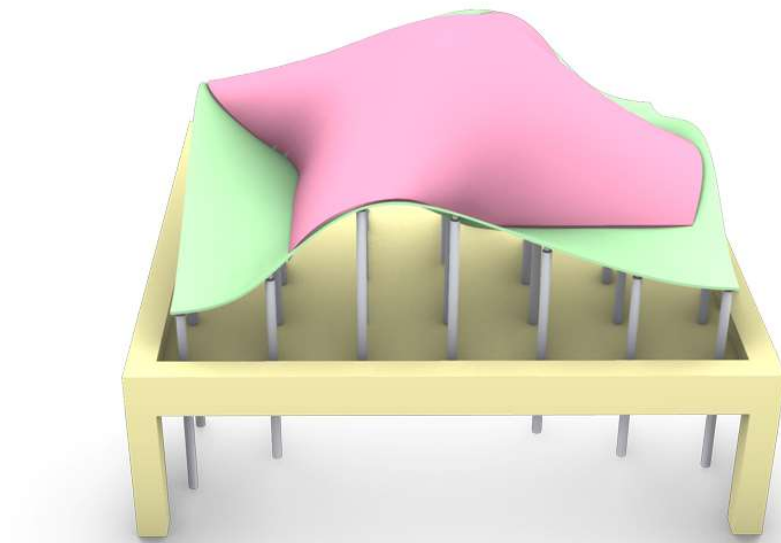


Figure 81 1:10 scale of the freeform surface on the Re-De-Form. Source: own illustration



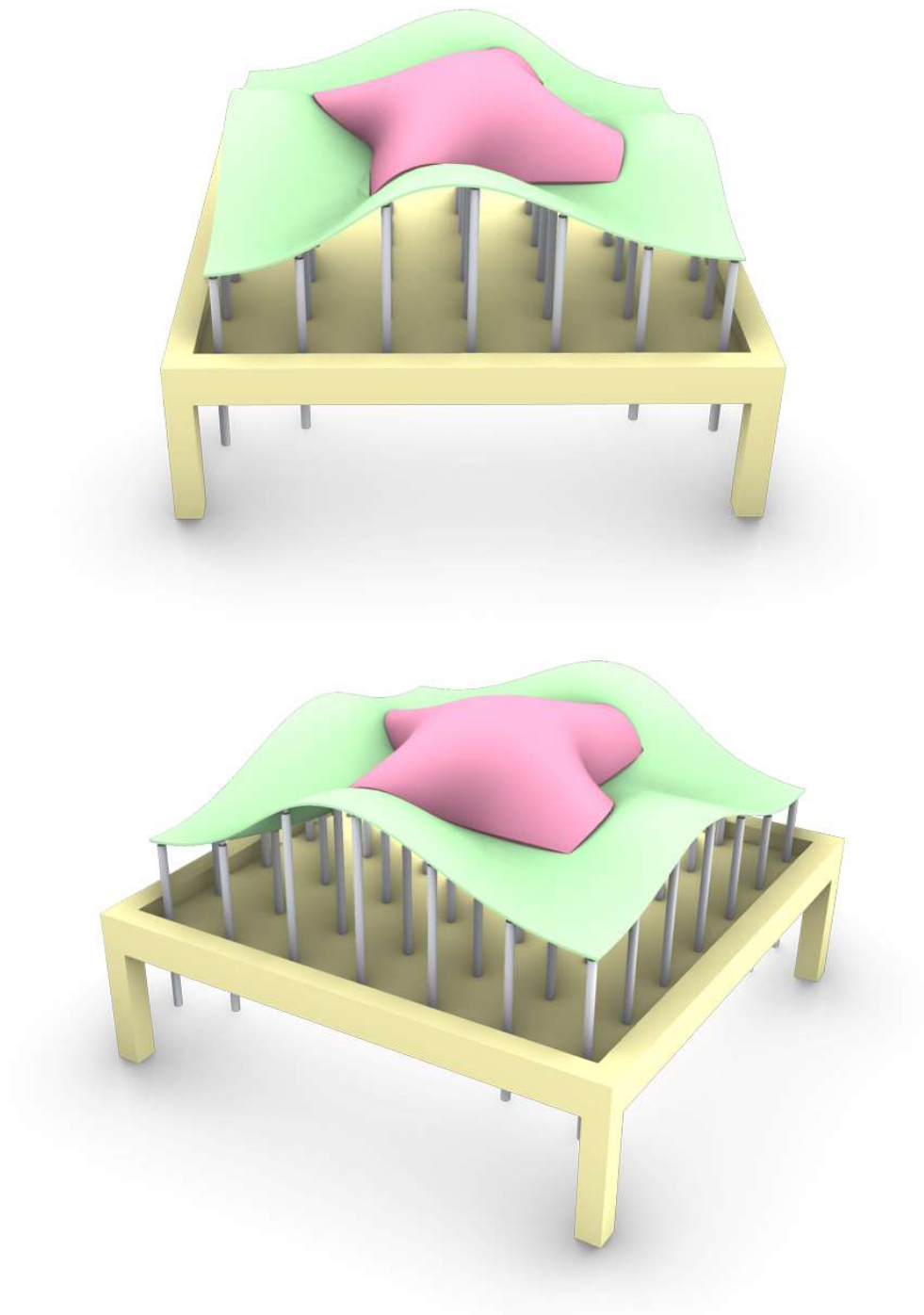


Figure 82 1:15 scale of the freeform surface on the Re-De-Form. Source: own illustration

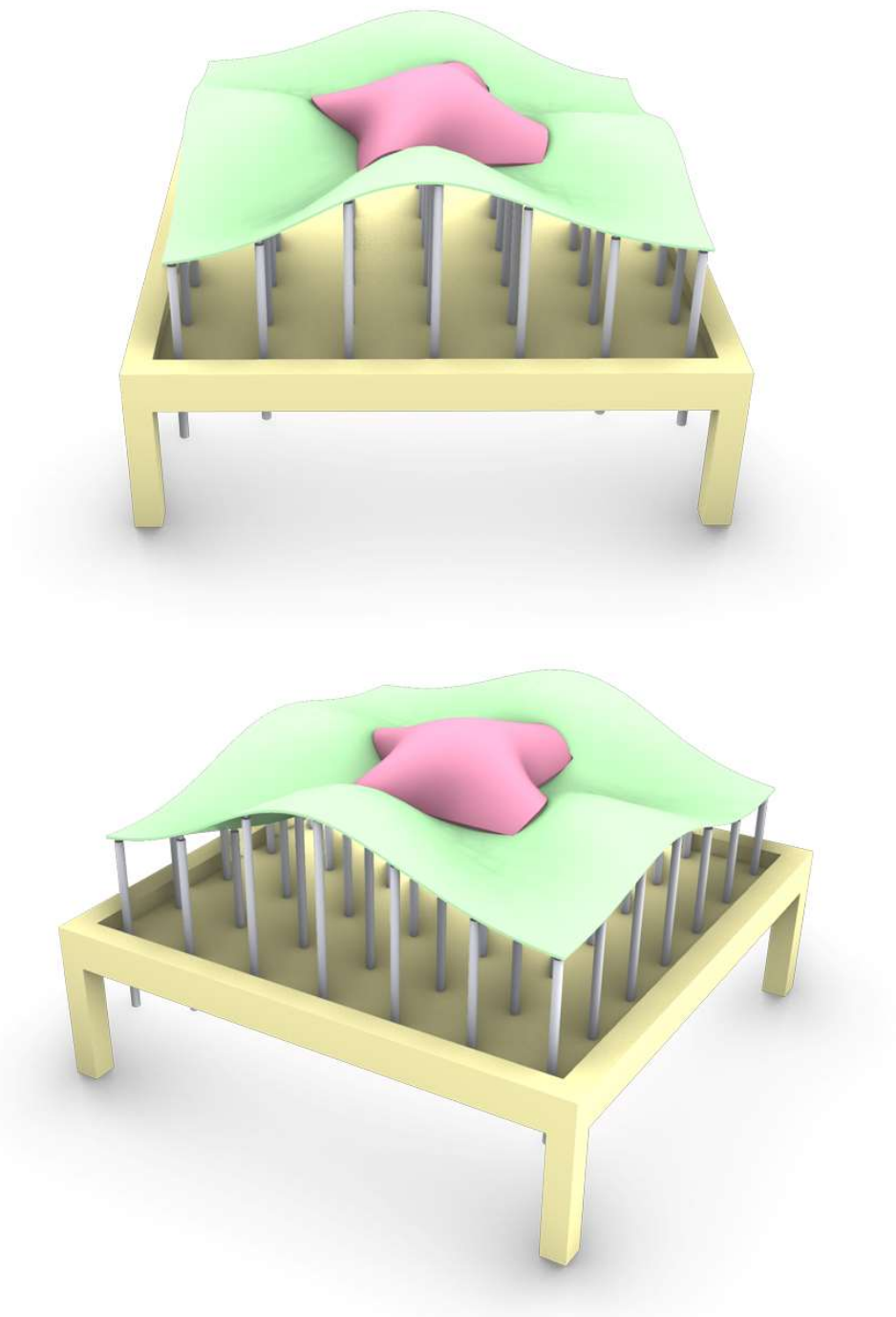


Figure 83 1:20 scale of the freeform surface on the Re-De-Form. Source: own illustration

## 5.6 The Re-De-Form prototype

### 5.6.1 Brainstorming

Re-De-Form is a mechanism that has two main functions: a) to physically represent a freeform surface as a physical model and b) to fabricate the double or single curved components of the discretized freeform surface. These require a flexibility between the scales of study. In the digital environment of Rhinoceros the computer model of a freeform surface can easily be discretized and change scales. On the other hand, moving from digital to physical scaling the model up and down on the Re-De-Form depends on the physical components the Re-De-Form consists of, such as the number of pins, the maximum heights per pins or the elasticity of the flexible formwork and surface. The change in scales between surfaces relies on the capability of the Re-De-Form as a physical mechanism to "copy" these surfaces. The accuracy of the system is also crucial.

The concept of the Re-De-Form as a) a physical representation of a surface and b) as a fabrication, mechanism and the relation of the different scales to the accuracy is understood by the following illustration. The assumption made, is that the profile c of the freeform surface is studied in comparison to the flexible surface, f lying underneath. The curve f is a curve interpolated through a variety of control points  $p_0, p_1, \dots, p_n$ , and its curvature complexity depends on the amount of those points. Generated by the digital model curve c can have various degrees of complexity while curve f's main purpose would be to as accurately as possible resemble it. Ideally, the number and position of the control points of curve f need to match those of curve c for maximizing the accuracy of the system.

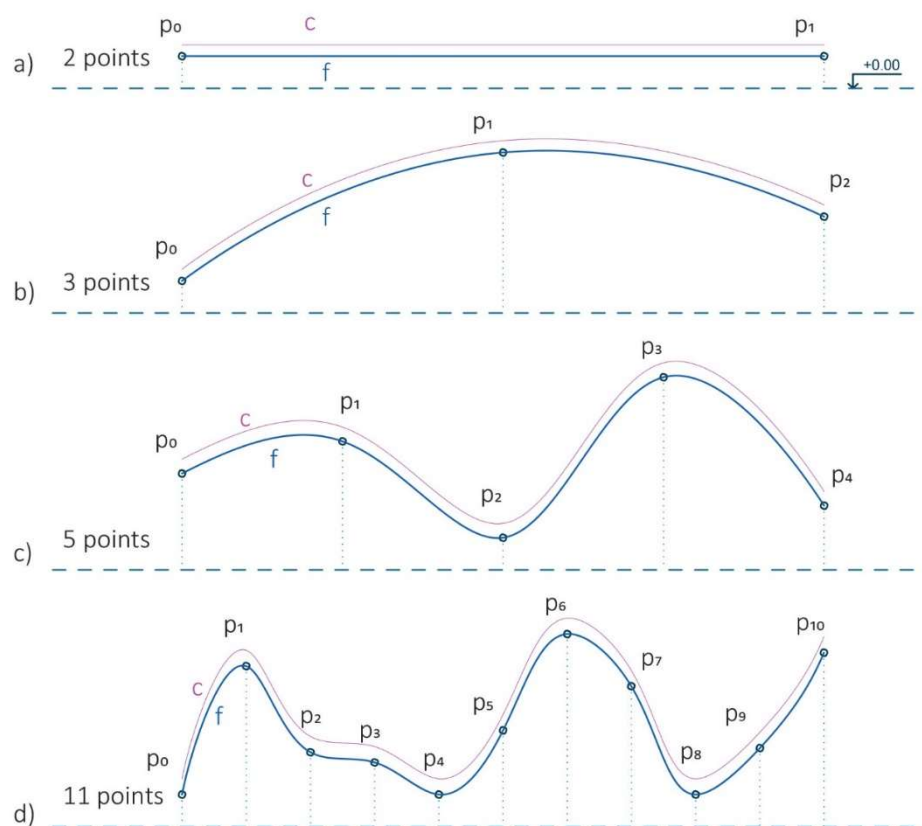


Figure 84 The flexible surface of Re-De-Form with respect to the freeform surface it represents. Source: own illustration

On the 1<sup>st</sup> example curve  $p_0$  and  $p_1$  are the only control points needed for curve  $c$  to be represented accurately. On the next examples it can be seen that the complexity of curve  $c$  increases while the number of interpolated points for curve  $f$  needs to increase too. Higher curvature examples  $b$ ,  $c$ ,  $d$  require 3, 5 or 11 points  $p$ , respectively to be realized. On a three-dimensional set up as the Re-De-Form the number of points would be 9 (3x3), 25 (5x5) and 121 (11x11) respectively.

Prototyping the Re-De-Form, each point of curve  $f$  should be able to move to the position of its respective point on curve  $c$ . Each point is linked to an actuator that would enable that movement in the  $z$  direction. More points imply more actuators which in return mean better accuracy. Greater curve complexities are achieved but on the other hand, more actuators would exponentially increase the overall the cost of the system. Thus, a reasonable amount of actuators should be chosen and the limitations associated with it should be discussed.

By assuming that the Re-De-Form digital model is 160x160cm in a scale of 1:1 and that its dimensions for creating a physical model are big for the purposes of a Graduation Project in relation to time and budget, the original model is scaled down. A 1:5 prototype of 32x32cm is built instead. The number of actuators that would fit inside the dimension  $d$  would determine the accuracy and the cost of the overall system as well as the ability to represent the design in various scales. In the illustration above it can be seen that for a constant dimension  $d = 32\text{cm}$ , an increased number of points  $p$  are providing greater curvature variations. A number of 11x11 points would be ideal because it would allow the formwork to change according to a variety of freeform surface scales, from physical modelling of 1:10 or 1:20 scales, to fabrication scale for each individual surface panel. A number of 5x5 pins provides with the possibility to fabricate each panel of the freeform surface accurately and would serve less accurately as a physical modelling mechanism. Lastly, a 3x3pin number provides with a satisfactory curvature resemblance towards panel fabrication but a poor performance as a physical modelling mechanism in case the freeform surfaces studied are very complex. In other words, the 3x3pin model of example (b) can never represent the surface complexity of example (d).

On the other hand, building the Re-De-Form required a lot of physical effort, brainstorming, building and experimentation of various building components. The creativity of the process required testing and sometimes failure of some of its custom components either mechanical or electrical. Towards the minimization of its components and overall costs as well as due to their failure possibility, the 3x3pin set-up is chosen to be built. The aforementioned practical reasons overweight the curvature limitation the 3x3 set up is associated with. To compensate for that, a detailed overview will be given so that in case the resulting project is successful a new Re-De-Form model with more pins and higher curvature possibility can be built.

Lastly, on the light of circularity, some of the materials used are waste from the BK Green Sector of the TU Delft faculty of Architecture so that the waste and overall cost is minimized. The model of the Re-De-Form can be fully disassembled too.

### 5.6.2 The Building Weeks

As it is an iterative process the building weeks involved sketching and prototyping of custom mechanical components. Also, an overview of the electrical components and their connections are given in the next two chapters.

The following illustration displays the 3x3 Re-De-Form in plan. The general dimensions are 32x32cm and the distances between the pins on the x-y plane are 16x16cm. The pins are connected with a grid of 3x3 steel cables that is able to deform according to the freeform surface fed and return back to their initial position when the system is at rest. The 3x3 pins are indicated with the blue circles and the 3x3 steel grid with the blue lines. In between the three consecutive steel laths two additional steel cables are placed both in the x and y direction to compensate for the smaller pin amount of the 3x3 model compared to the 5x5 one. Greater curvature accuracy is achieved while the Re-De-Form's counterparts become more unified as a system.

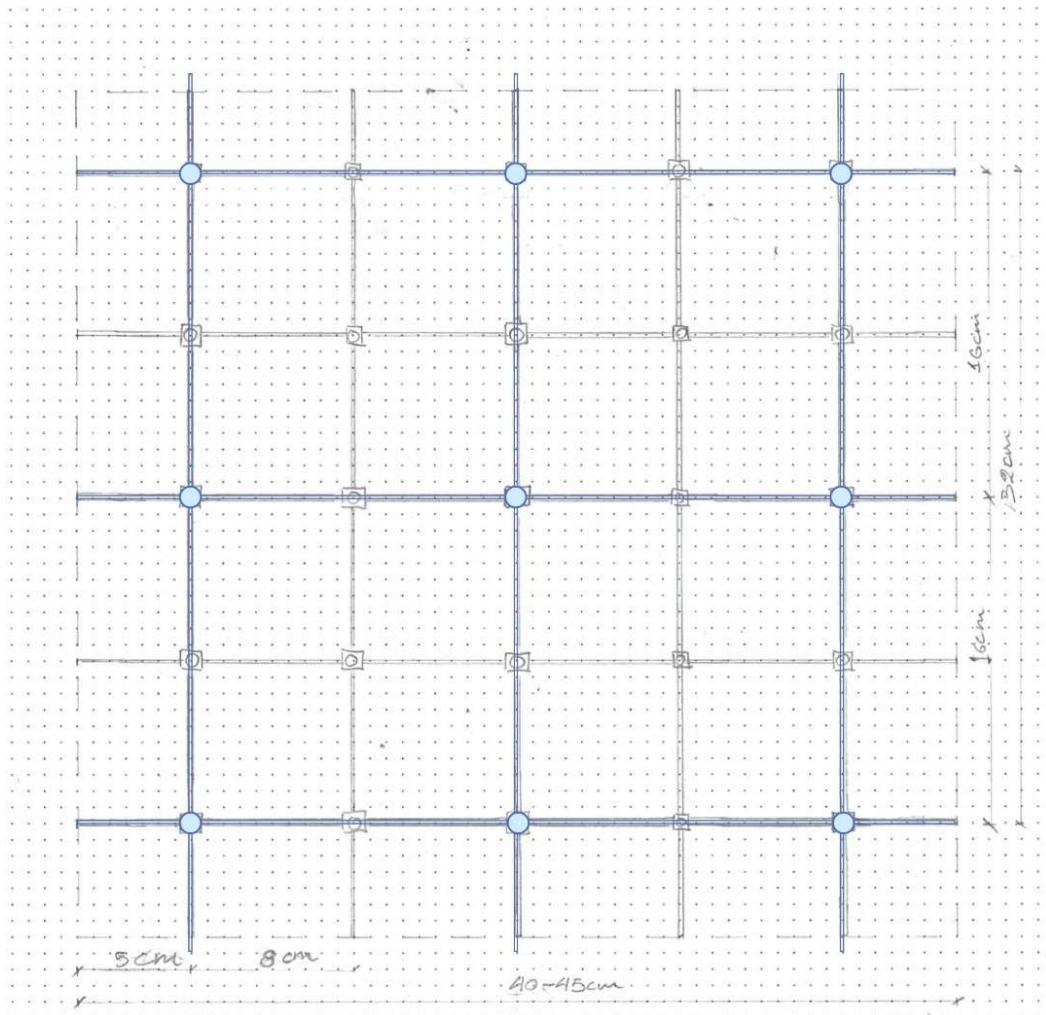


Figure 85 The plan of the Re-De-Form. Source: own illustration

The steel cable's length exceeds the general dimensioning of the mold and in this case it can vary from 40 to 45 cm. When the system is at rest the cables remain linear on the x-y plane and their area of effect is limited to 36x36cm. But when the grid takes the shape of a freeform surface the cables should increase in length due to the change in distance between the pins (>16cm). They should follow that increase by being able to slide over each other. This idea is displayed by the following figure where the cables are able to "slide" while the pins heights change.

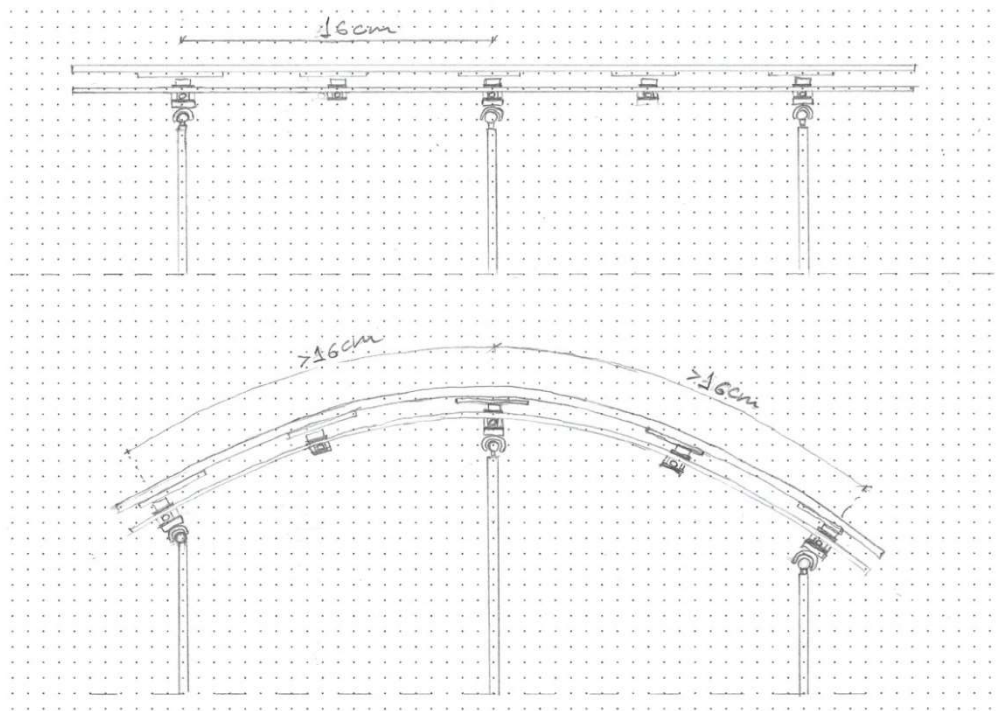


Figure 86 Re-De-Form in Section. Source: own illustration

Regarding the connections between the steel cables, they should be able to slide over each other on the local x-y plane of the grid surface. In that case, the connection enables 2 Degrees of Freedom (2DoF), the translational movement on the local x-y plane on each point where the two perpendicular steel cables intersect. In the following sketch, the resultant detail, is referred to as "wooden box" because it is made from a 3mm thick MDF sheet and is box in plan. The steel cables have a diameter of 1.5mm and when placed on top of each other perpendicularly their clear height matches the height of the MDF sheet used. The two cables penetrate the box and are able only to slide. While testing their sliding behavior, a small amount of friction was noticed. The small amount multiplied by the number of 25 wooden box connections created an increased amount of internal forces on the Re-De-Form. The connection was too tight so its internal height was increased by 0.2-0.3mm with the use of a thick waste paper found in BK Green. The 3mm high pair of cables slide inside a 3.3mm internal height box and the system is freed from the unpleasant initial friction.



The steel grid is the formwork on top of which a continuous surface needs to be placed. Without the use of the surface then it is impossible to fabricate the panels or to physical model the freeform. Here, the challenge posed is how to connect the flexible surface to the steel grid when the steel grid and surface slide locally. This is tackled by placing a magnet on top of each of the aforementioned steel cable connectors and a metal plate on the bottom of the flexible surface on the points that meet the grid connection. The magnets keep the surface in place in the z direction while maintaining the translational 2DoF movement on the local x-y plane. The ability of the flexible surface to follow the grid depends on the magnitude of the magnetic field per magnet. More advanced magnet systems would provide with a better adaptability of the freeform to the grid but in the case of the current 3x3pin Re-De-Form, board-magnets are used.

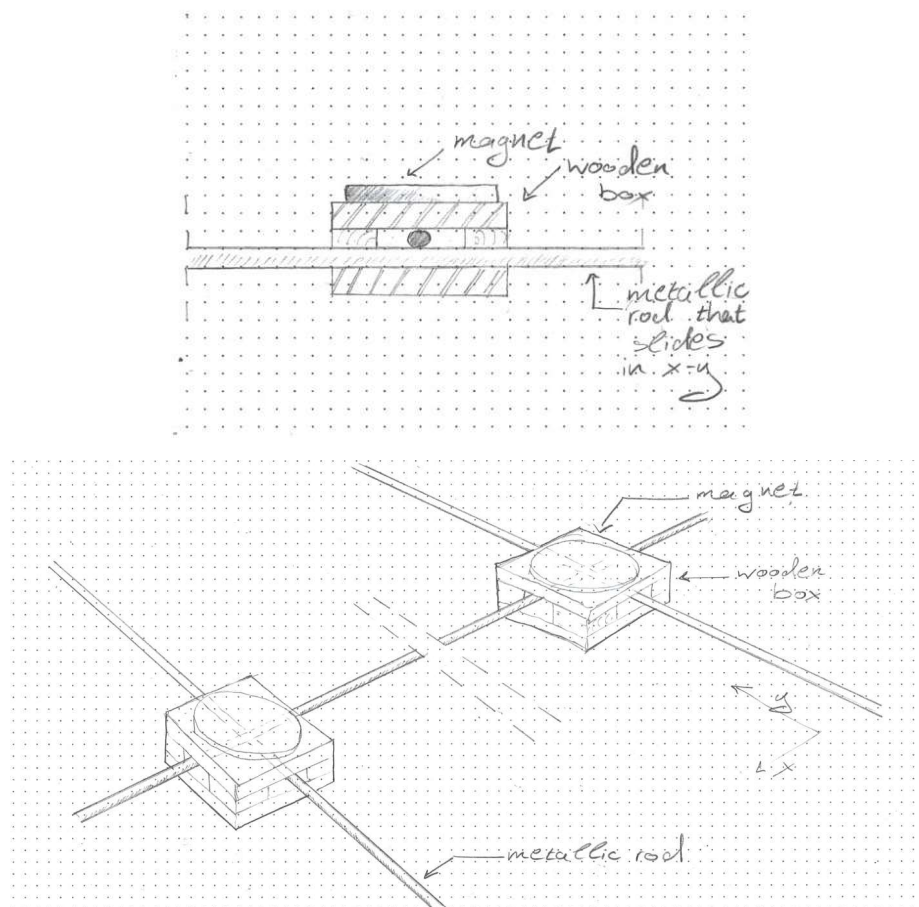


Figure 87 The wooden box and steel rod detail with the magnet on top. (a) in section, (b) in perspective. Source: own illustration

Another critical component that will be further discussed is the ball connection. The purpose of the detail is to enable rotational freedom of the cable network that the flexible surface rests upon. While the actuators move vertically the detail adapts to the change in curvature per cable and minimizes the amounts of resultant internal forces that would apply if the rotation was an anchor point.

In the first sketch of the ball connection is displayed. The ball is glued to a thin wooden piece which is then glued to a thicker pin. A "cupola" caps the ball and its shape is extended towards the ground so that it locks on the ball and does not disconnect during the vertical movement of the actuator. The detail is able to freely rotate 45 degrees on every direction. The 45 degrees are feasible due to the limited cupola extension and to the thinner wooden piece used between the pin and the ball. The cupola "just locks" on the ball while the thin wooden piece enables more travel distance on rotation. On top of that the wooden box and steel rod detail is glued while the flexible surface with its metal plate slide.

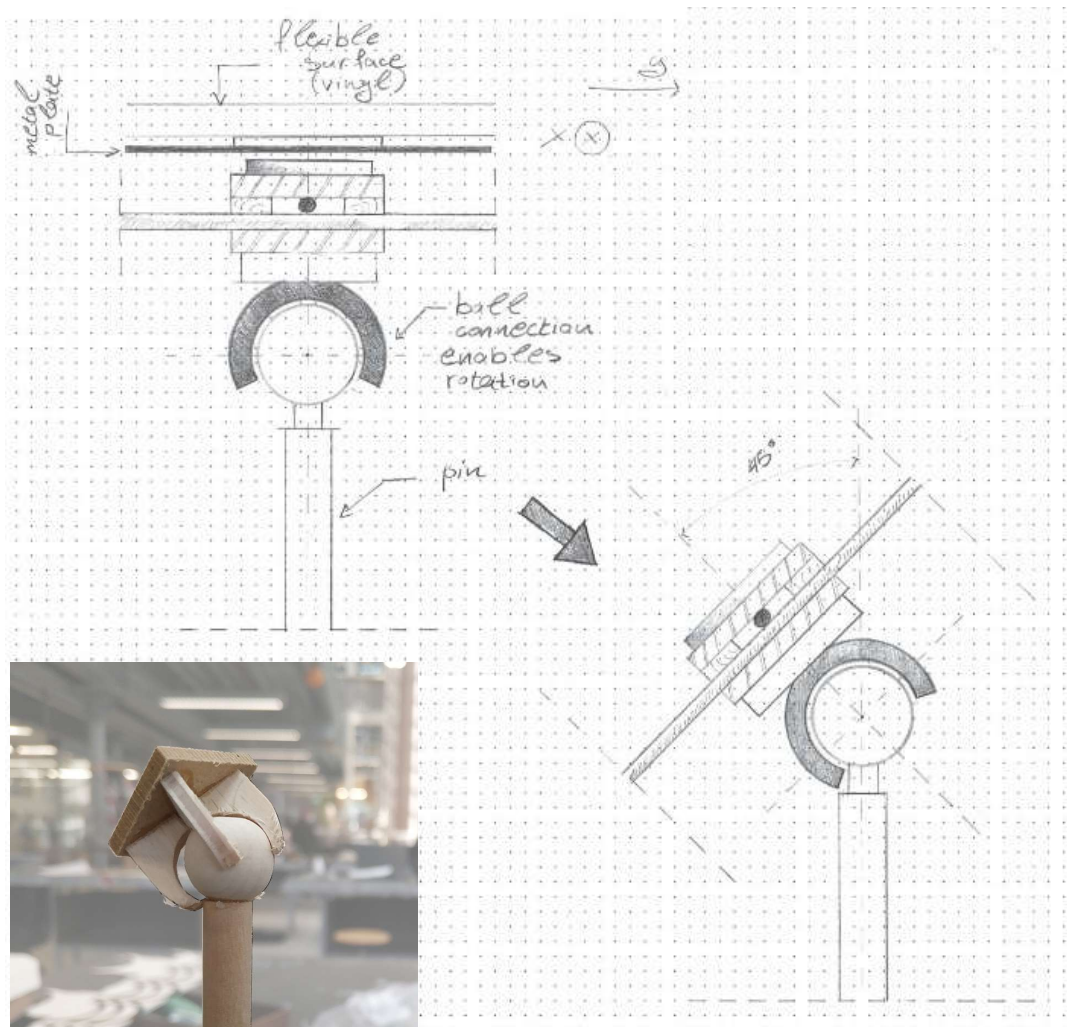


Figure 88 Ball connection sketch and model. Source: own illustration



During the building weeks the connection will change due to the difficulty in the production of the cupola and the fact that only gluing the thin wooden piece would result in a fragile detail. As can be seen in *Figure 88* the former detail was fragile while its production time is significant. The simplicity of the final ball connection radically reduced its production time. The cupola is replaced by a wooden cylinder cap whose internal depth  $d$  and width  $b$  *Figure 89* depend on the radius of the ball-bead and on the tolerance of the cap rotation around the ball. More tolerance minimizes the internal friction but undermines accuracy while the system operates and vice versa. Through prototyping and testing an intermediate solution is chosen instead for the dimensioning of the  $d$  and  $b$  values final cap. The final values are:  $d = 12\text{mm}$  and  $b = 16\text{mm}$ .

Moreover, the top of the pin was dig to a depth of 1,6cm so that part of the pinion can be glued and forced inside. The ball already had a hole in the middle and the wooden piece penetrated it and glued. Both will ensure that the detail is rigid enough to withstand loads and moments. Lastly, the diameter of the thin wooden piece is 2 times smaller than that of the pinion to ensure that greater angles of cupola rotation are possible. This can be seen in *Figure 89*.

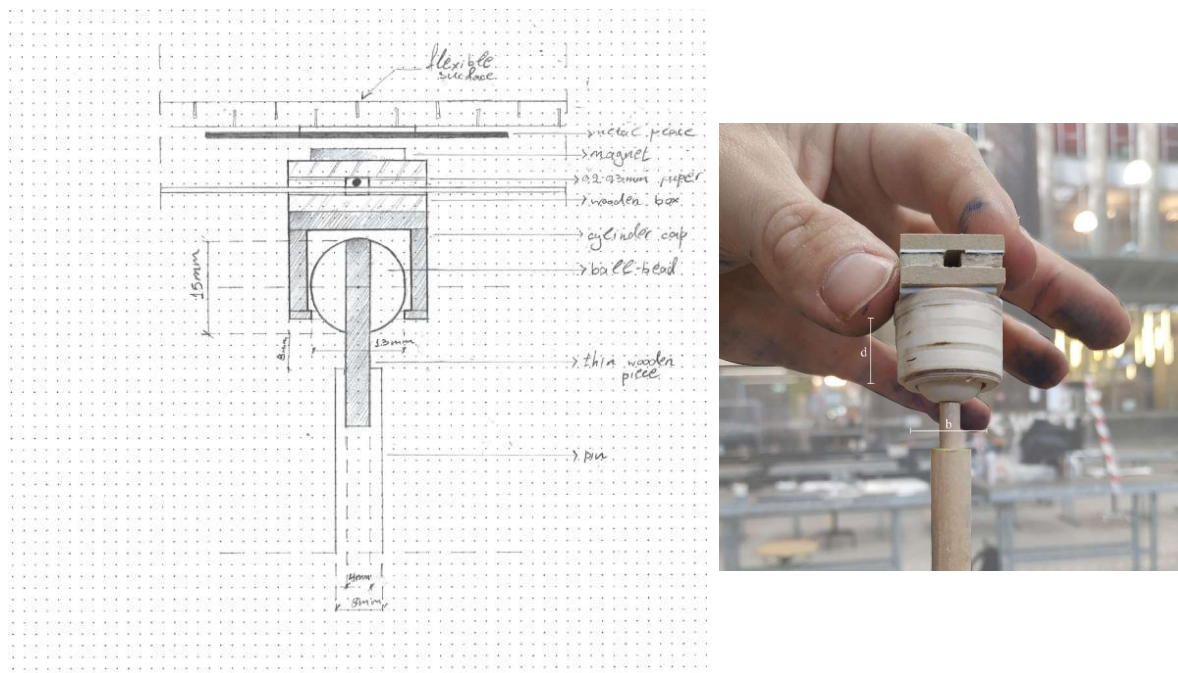


Figure 89 Final ball connection sketch and model. Source: own illustration

The next components explained are the actuators. These enable the translational freedom of the system on the z axis. Linear actuators found in the market are expensive, so a custom solution that would enable the linear movement had to be built instead. In *Figure 90* the actuator system is illustrated. It consists of racks attached to the pins and pinions connected directly to the stepper motors. The pinions and racks transform the rotational movement of the steppers to a linear one.

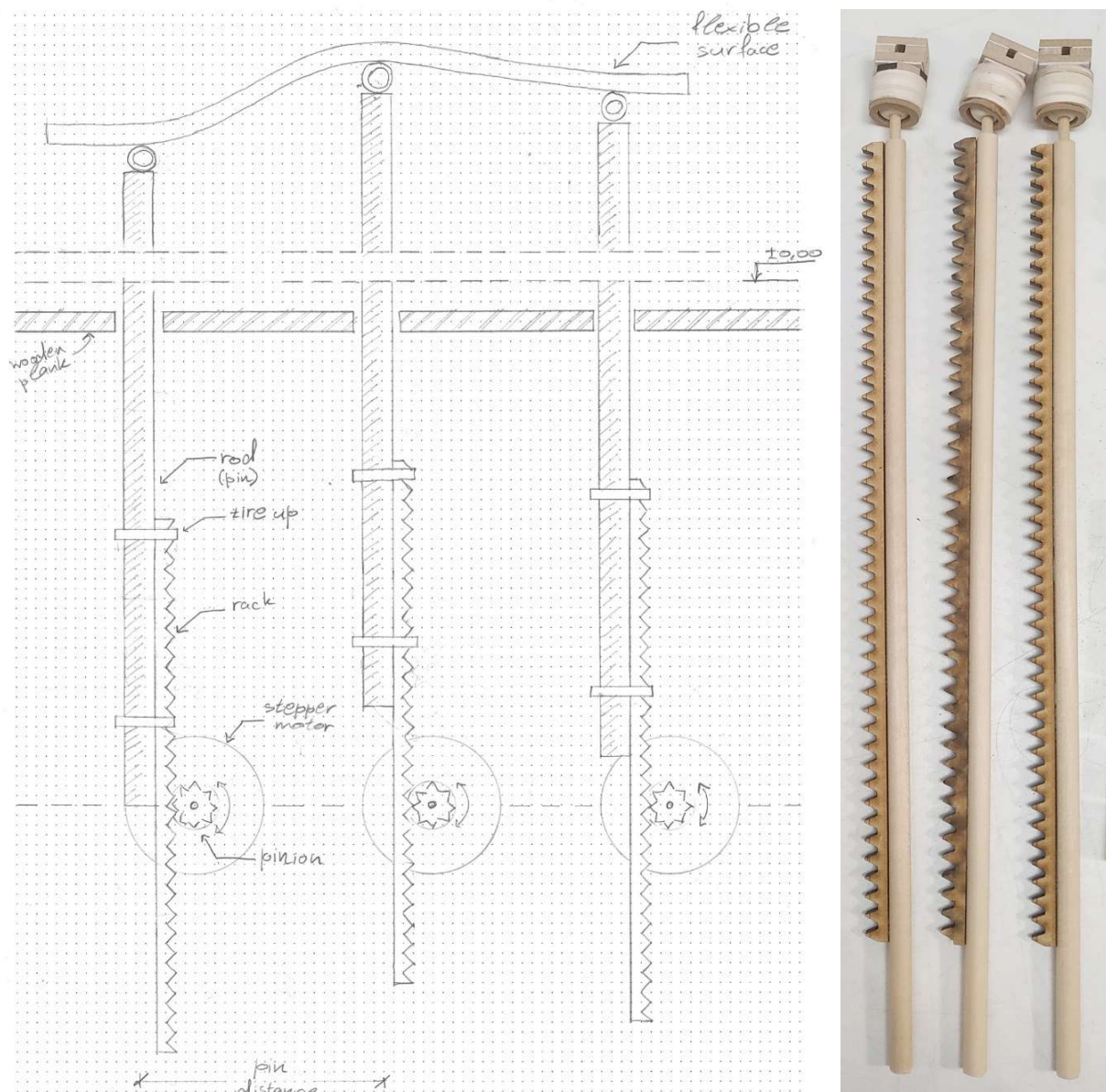


Figure 90 (a) Sketch of the actuator system, (b) The CNC-cut racks. Source: own illustration

The radius and teeth number of each pinion determines the number of steps the stepper needs to perform for the pin to move towards a specific position. A grasshopper plug-in called Gears is used for the calculation of the pinions and racks dimensions. In *Figure 91* slider A represents the radius of the pinion that is illustrated by a hidden line in and slider Teeth the number of pinion's teeth. The dimensions of the rack adjust automatically to those of the pinion.

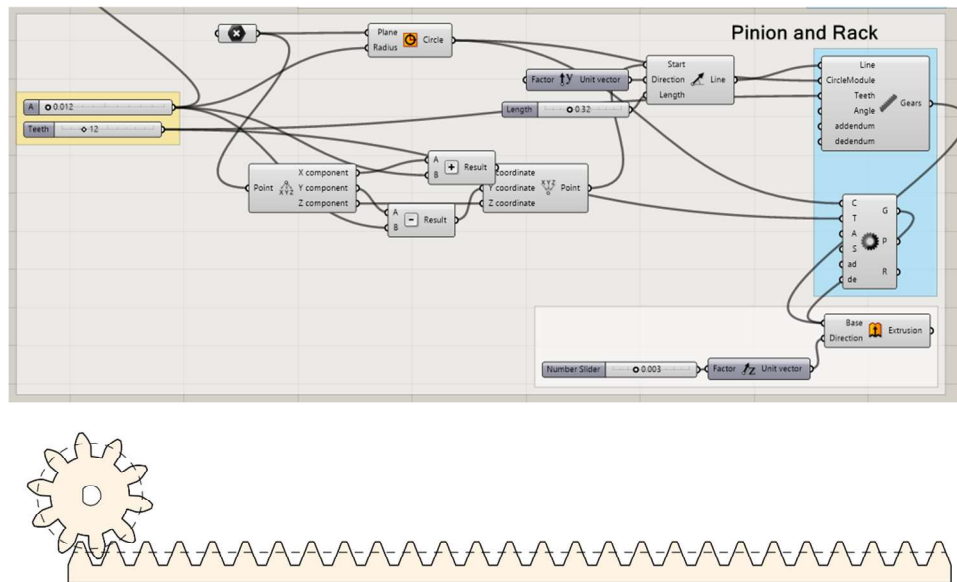


Figure 91 Pinion and rack definition. Source: own illustration

While the steppers feed the movement, the pins need to remain fixed on the x-y direction and move on the z direction only, through the use of guides. The main body of the Re-De-Form executes that. In *Figure 92* the main body consists of two 460x460x6mm MDF sheets that are drilled in the positions of the respective pins to enable their movement in z-direction. The pin's diameters are 8mm and the rack rectangular top dimensions are 4x8mm. The drilled holes should allow the pins to slide freely without enabling rotation or movement in the x-y direction.

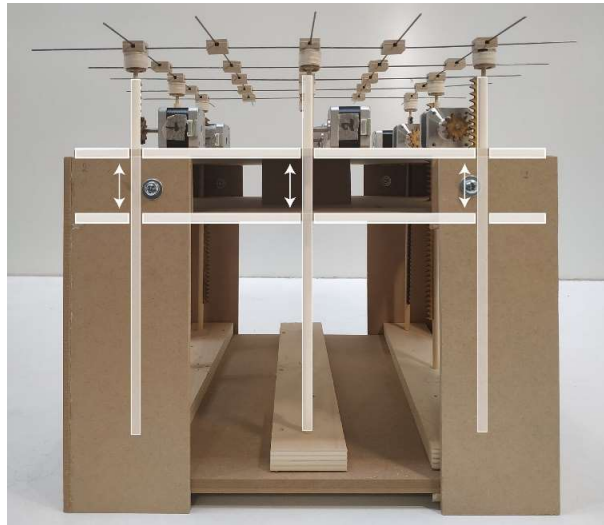


Figure 92 The guides of the Re-De-Form. Source: own illustration

During operation the wooden boxes in-between the 9 pins should slide in the x-y plane along the steel cables that run through them. The problem indicated in Figure 93(a) is that there is lack of control when Re-De-Form deforms and the in-between distances  $u_0, u_1, u_2, u_3$  and  $v_0, v_1, v_2, v_3$  change randomly. An inventive method with springs should solve that problem, but the appropriate spring size and tension could not be found in the market. Instead, a rough solution was applied. Rubber bands are glued on top of some of the wooden boxes. That method ensures that the aforementioned distances should change proportionally and when the pins are on the "HOME" position these distances remain equal.

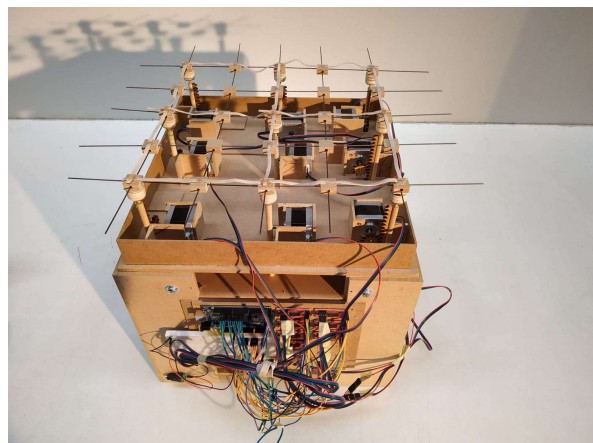


Figure 93 The  $u_0, u_1, u_2, u_3$  and  $v_0, v_1, v_2, v_3$  distances change randomly, (b) The inventive system with the rubber bands. Source: own illustration



Also another challenge that Re-De-Form poses involves the flexible surface placed on top of the steel grid. The material of the surface and the cutting pattern that the material has to undergo to produce more complex curvatures are mentioned.

For the material, a 450x450x6mm PVC sheet found in the waste materials of BK Green was used. The costs of a new PVC piece were high so a cheaper solution was chosen. Regarding the pattern, several rectangular cutting patterns between 1-3 cm were tested and 2.5cm was proved to be the most functional in terms of curvature flexibility and stiffness. CNC milling of the pattern was avoided due to high costs. A custom tool the author created was used instead. It can control the cutting depth of the sheet by changing the height of the cutting blade.



Figure 94 (a)The flexible surface on the grid, (b) The custom depth-cutting tool. Source: own illustration

### 5.6.3 The Automation

The automation involves research and testing on various electrical components, acquired from various sources. As previously stated, due to cost, the linear actuators were replaced with another system that translates rotation to linear movement. Its components and their connectivity to the digital workflow developed on chapters 5.1-5.4 are studied in this chapter.

The idea of the automation lies behind the positional data transfer from the digital workflow of the yet digital Re-De-Form to the position of each pin on the physical Re-De-Form. *Figure 95* displays the physical components needed for the data transfer of the digital mold through the Arduino board, the stepper drivers and finally to the physical mold. The transfer process is bi-directional meaning that once the pins are positioned the system is aware of it and performs the next positioning based on the previous one.

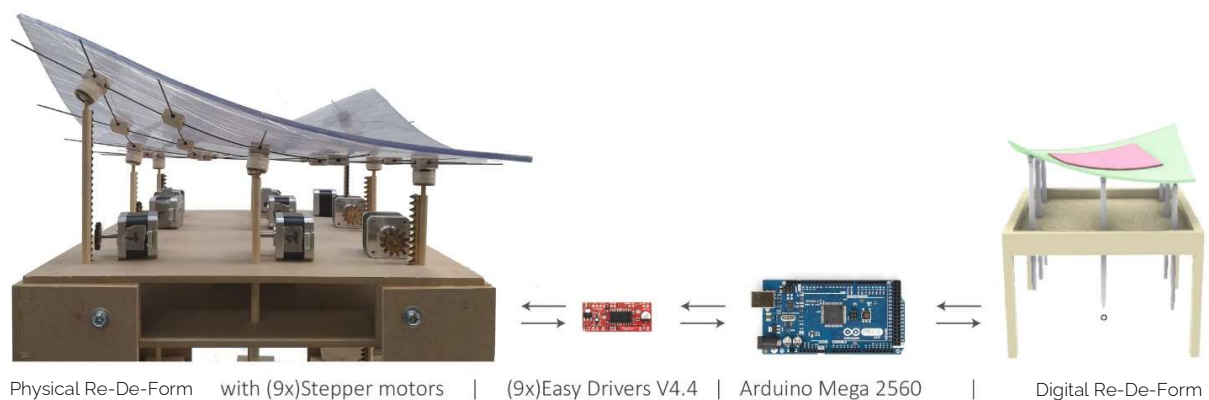


Figure 95 Digital to Physical Data Transfer. Source: own illustration

The physical components required for the Re-De-Form automation are: a) An Arduino Mega 2560 board, b) (9x) Easy Drivers V4.4, c) (9x) 12V Stepper Motors (with cables), d) a 12V-2A Power Adaptor, e) a 5.5x2.1mm DC connector, f) a 5.5x17cm Bread-Board and g) (40x) Male-Female 30cm Jumper Cables. *Figure 96* displays the connections of them in detail. Their in-between connections can be seen on *Figure 96*. Notable is the fact that, each stepper motor needs 4 cables to operate and that they are connected to a driver board directly. If the cables were connected directly to the Arduino Mega, the board's pin number would not suffice and a second Arduino Board would be needed. Through the use of a stepper driver per motor, better motor control can be achieved through a library that supports stepper drivers and will be discussed further. Each Easy Stepper Driver controls one stepper motor and needs an external power supply from 6V to 30V, 2A to power on. If the power supply is connected to the Arduino Board directly, due to the facts that it requires a lot of energy to operate and that the Arduino Board can only output up to 5V, it will drain the Arduino board damaging it completely.

The motors are placed inside the boundaries of the Re-De-Form's base. They are oriented so that the direction of rotation remains the same. When the motors rotate CCW the pins go up and when CW the pins go down.

Also, noted should be the fact that more stepper motors may require higher Voltage and more Amps than the ones used or 2 power supplies of 12V each. Higher Voltages such as 24V or 30V will cause the motor drivers to produce a lot of heat that can be tackled by a custom ventilation system, a solution that would make the overall project more complicated. Lower Voltage such as 6V or 9V cause lower torque performance by the motors. As a result, their speed decreases and are prone to missing steps causing many inaccuracies. The motors need to carry at least the weight of the wooden pins, flexible surface material, the wooden ball connections and the steel grid while operating without losing steps. The 12V were chosen as an intermediate solution that suffices for the requirements of a 3x3pin Re-De-Form. The heat produced is bearable, and the final torque is sufficient for the experiment.

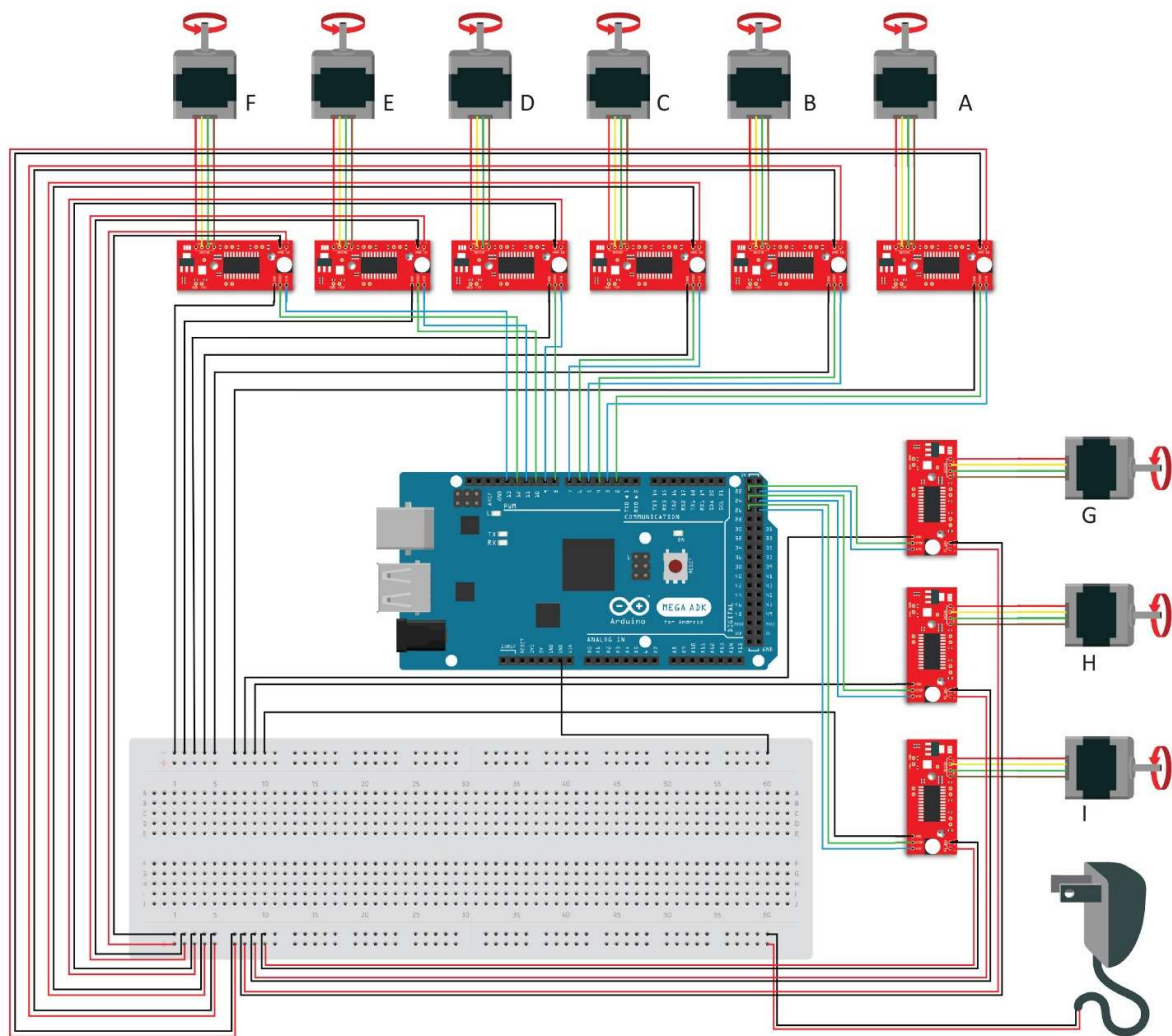


Figure 96 Circuit Connections. Source:own illustration

Moreover, special care had to be taken on soldering the Easy Drivers V4.4 before operation. Once they are plugged into the power source none of the cables that connect to the Arduino Board or the stepper motors must be disconnected or the drivers can be severely damaged.



Initially, Firefly was used for the positional data transfer from the Grasshopper file to the Re-De-Form. The plugin includes a set of tools that bridge the gap between Grasshopper, the Arduino microcontroller and other devices such as cameras, phones, sensors (Andy Payne and Kelly Johnson, 2015). An Arduino sketch (Quadstepper Firmata) associated with the plug-in is Uploaded into the Arduino Mega board and the data from the Digital Mold were fed into one of the plug-in's components called Quadstepper Component. This particular grasshopper component communicates with the Arduino board and sends the data directly to the pins connected to the stepper motors. The limitation of that component is that it can drive up to 4 motors per Serial port. Overall, for controlling the 9 motors, 3 Arduino Boards were needed and one Serial Port Open per Arduino Board. The solution does not exploit fully the extended Pin number of a Mega Board and proves to be more cost effective and complicated. Also, after some seconds of use the plug-in would give an error related to the Serial Ports that could not be resolved on time, so the automation workflow had to be revised. Instead of Firefly, the Arduino IDE will be used and the values from the Grasshopper script will be fed directly into the Arduino Serial Monitor in text form once the Simulation runs.

The "AccelStepper" library developed by Mike McCauley is integrated in the Arduino Sketch and it is the main tool that controls the steppers. It is chosen because it supports: a) acceleration and speed control, b) control of simultaneous operation of multiple motors, c) a variety of stepper motors and Arduino Boards d) small delay times if not prompted otherwise. Once it is installed and called inside the Arduino sketch the stepper motors are defined by name, type, Steps Pin, Direction Pin. In *Figure 96* the Stepper and Direction Pin connections to the Board can be seen and their correspondence to the Arduino Sketch can be read in the Arduino Sketch in the Appendix. The 12V external power source is dedicated to powering the Easy Drivers while the Arduino Board is powered through the USB port COM3. The grounds of the stepper drivers are connected to the ground of the Arduino Board.

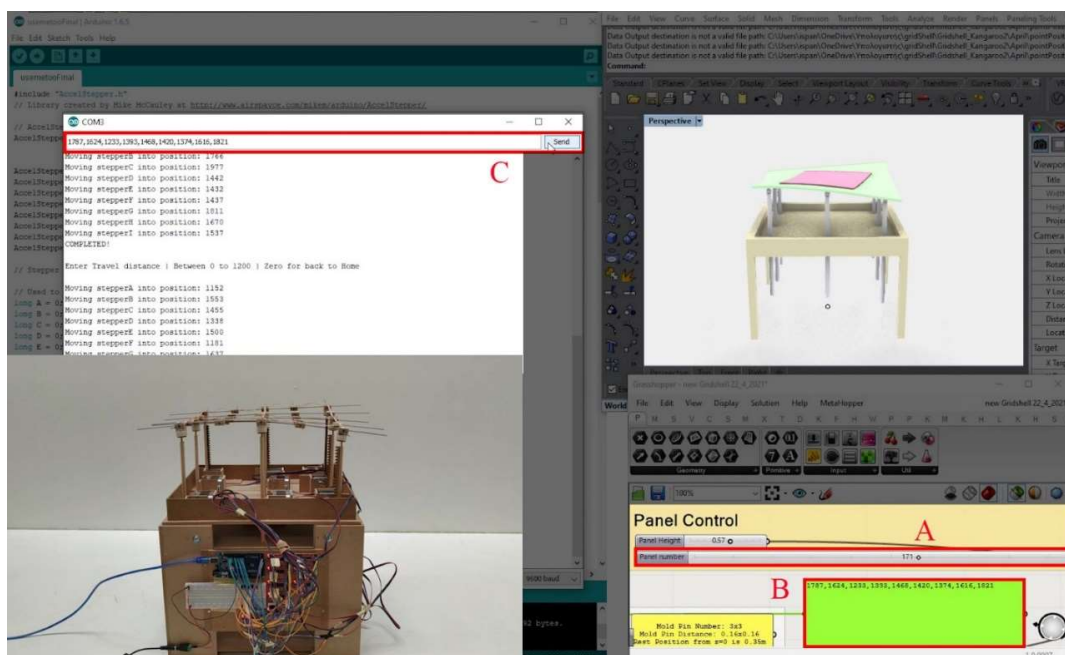


Figure 97 The steps to use the Re-De-Form. (A) Pick a panel number, (B) Copy the values from panel, (C) Paste into the Serial Monitor and hit ENTER. Source: own illustration

The process the designer needs to follow to link the Grasshopper data to the Arduino IDE involves partial manual control. To overcome this the positional values of each pin would be exported into a text file and the Arduino board would read them and adjust the pins respectively. Although promising, this idea was skipped because the grasshopper script lagged when updating the export to txt file component and the fact that there is not straightforward connection between Arduino and a text file supported by the default Arduino IDE. The Serial Monitor of the Arduino IDE is used instead as a communicator between the automated Re-De-Form and the designer.

According to *Figure 97* the designer needs to follow these steps to use the Re-De-Form: Firstly, all the physical connections should be in place as prompted in *Figure 96*. Once in the Arduino IDE the sketch needs to be Compiled and Uploaded to the Board. Then in the Grasshopper script, he/she needs to choose the panel to be fabricated. It is indicated with a panel number that corresponds to a lists of steps the stepper motor needs to execute to adjust to the respective panel position. The designer copies (Ctrl+C) the 9 values from the Grasshopper Panel and pastes (Ctrl+V) to the Arduino Serial Monitor. By hitting "ENTER" the motors drive the pins to the positions prompted. The next list of values can be immediately fed by following the same process from the point were the user changes the panel number. Once finished the pins can return to the "HOME" position, by typing "0" in the Serial Monitor and hitting "ENTER".

The "HOME" position is set 2.5cm higher than the lower level of the Re-De-Form with the use of a 30x7x2.5cm removable wooden piece. Placing the piece ensures that the motors start moving from the same height. In case the stepper motors lose steps during operation Homing them could solve the problem. Once the system is Powered Off the motors can be adjusted manually to the Home Position. This increases the accuracy of the system.

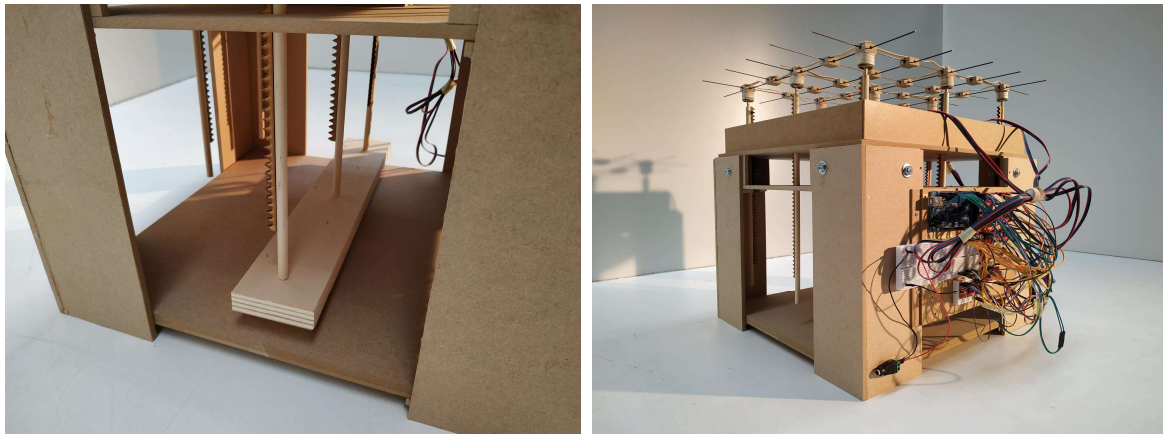


Figure 98 (a) A wooden piece is used for the initial Homing of the pins. (b) he pins of Re-De-Form are Homed. Source: own illustration

A diagram of the equipment needed for the creation of the prototype with their respective number of components and prices is given. In case a replica of the Re-De-Form is built in the future the diagram provides with useful information regarding that.

The main electrical parts are replicas from Chinese manufacturers since the originals would be at least 3 times more expensive to buy. The stepper motors are replicas of the NEMA 17 stepper motor, the driver boards are similar to the Easy Driver v4.4 drivers and the microcontroller board is the Chinese version of the Arduino Mega 2560. Also, the linear motors are replaced by stepper motors and drivers so that the overall cost does not exceed the 150 euros budget.




	Picture	Number	Cost (Euros)
Arduino Mega 2560		1	15
Male-Female Cable		40-80	4-8
Breadboard		1	5
Stepper Motor		9	54
Motor Driver		9	36
12V Power Adaptor		1	8
DC to terminal block adaptor		1	2
MDF sheets, steel cables, wooden pins, CnC cut		~	25
Total Cost			155

Figure 99 An overview of the Re-De-Form components with their respective number and prices.  
Source: own illustration

#### 5.6.4 The final product and its capabilities-limitations

The use of the Re-De-Form prototype was envisioned as a physical modelling and fabrication mechanism that can generate a freeform design in various scales. Therefore, as explained in chapter 5.5.1 the prototype capabilities come with certain limitations. These mainly rely on the number of pins that fit into the 36x36cm rectangular base of the mold base and the 15-20 cm maximum height difference between the two consecutive pins.

A detailed overview of Re-De-Form's components are given in case an upgraded version of Re-De-Form is about to be built. Hardware such as greater number of pins, steel ball connections, higher Power Adaptor Voltage or new surface cutting patterns can ensure a better curve representation making physical modelling and fabrication feasible.

However, the 3x3pin system ensures an overall smaller cost compared to the other options such as the 5x5 and 11x11pins but does not fully answer to both objectives. It is capable of accurately producing freeform panels in a scale of 1:1 while its use is limited as a physical modelling mechanism to very basic freeform shapes. A future upgrade would be the implementation of more pins and motors.

The ball connection on the top of each pin enables the surface to curve more freely and accurately. The internal stresses are minimized because when the pin moves the formwork does not cause high resistance. there. There is still a possibility that the steel cables are replaced by smaller radius cables or that the internal height of the wooden box increases. This would enable more pin height variations but it may be prone to buckling of the formwork in case high loads are applied.

What could be studied further is the nature of the surface material placed on top of the formwork as well as the cutting pattern used to make it more flexible, An implication is given in chapter 5.6.2 but still requires testing.

Also, the magnet system that connects the cable formwork to the flexible surface needs to be applied. The study of the magnets will ensure that the flexible surface follows the curvature of the formwork accurately,

Another upgrade would be to directly connect the digital model in Grasshopper to the physical formwork without the use of the Serial Monitor of the Arduino IDE. The pin system although automated still needs a small manual adjustment regarding the transferring of the values form the digital to the physical model with the Ctrl+C and Ctrl+V commands. This is a limitation that needs to be further tested as a future upgrade.

Lastly, through testing, the critical height difference between two consecutive pins is narrowed to 15-20cm. One possible upgrade would be for the algorithm to check whether this value exceeds 15cm. If it exceeds then a message would inform the designer that the curvature he/she is feeding can not be fabricated by Re-De-Form. This would result in Re-De-Form not missing steps during operation and would improve the design's accuracy. The designer would have to modify the design for Re-De-Form to be able to fabricate it.



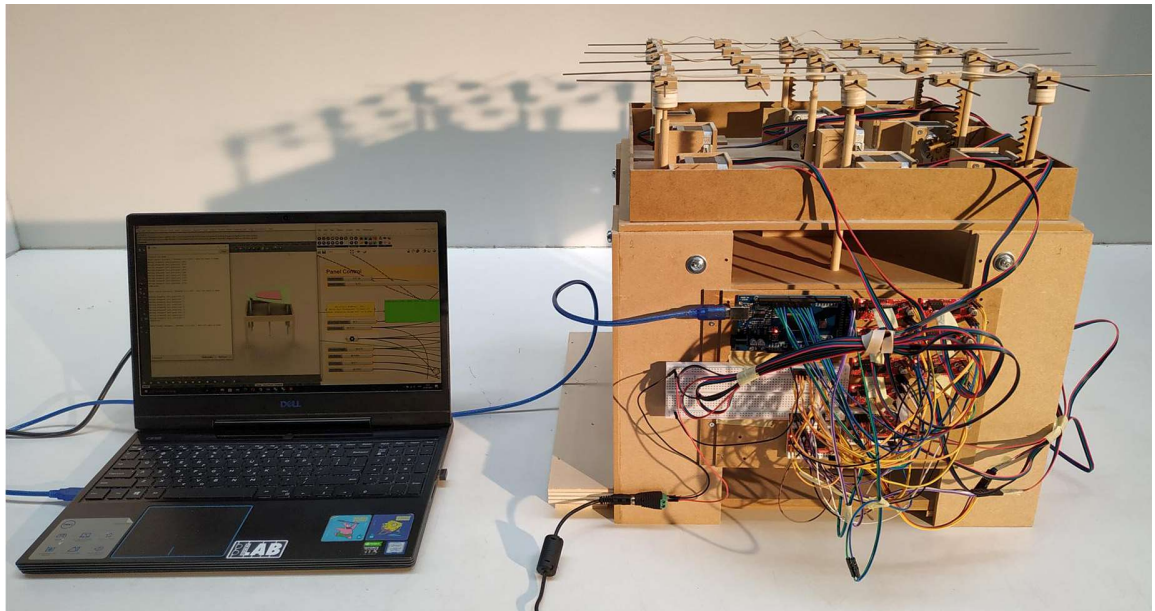


Figure 100 The Re-De-Form prototype connected to the laptop. Source: own illustration

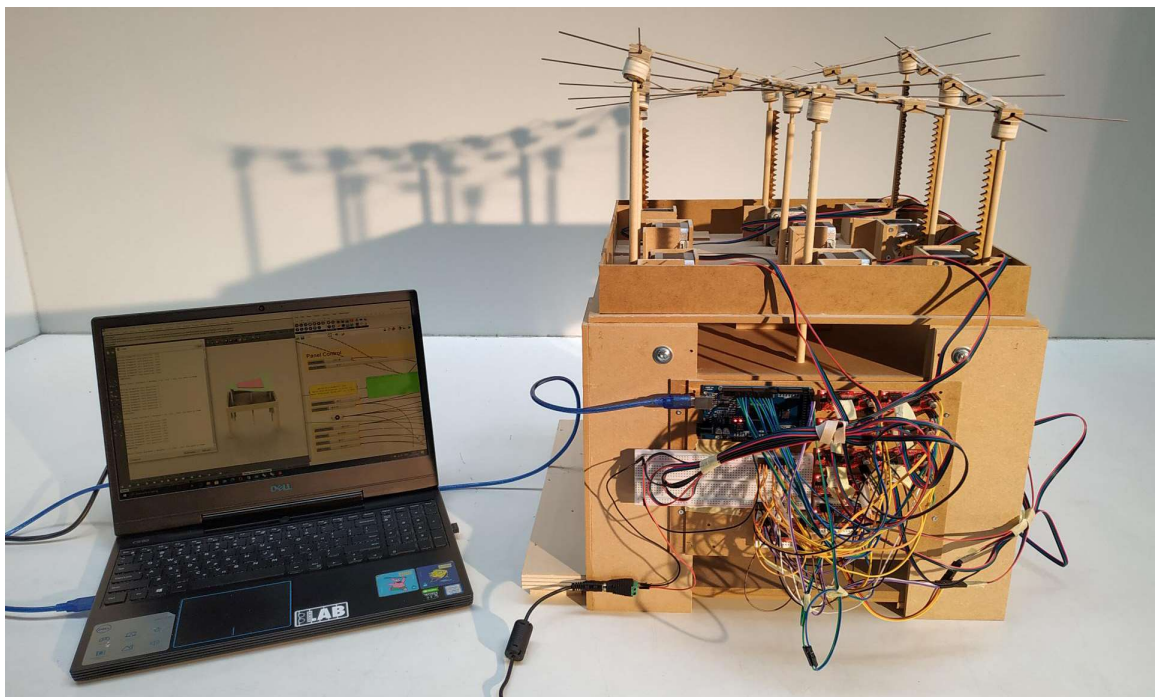


Figure 101 Re-De-Form takes the shape of a panel fed from the Serial Monitor of Arduino IDE. Source: own illustration

(End of chapter)



# 6

## Conclusion and Reflection

## 6.1 Conclusion

The purpose of this thesis was to answer the main research question: Developing a “design to fabrication” workflow that corresponds to the design process and materialization of a timber grid-shell structure, while also establishing an automation process to provide the Re-De-Form with more accuracy/precision in producing freeform surfaces.

The main research question is followed by sub-questions that indicate the main aspects that need to be answered. These are the freeform surface design, timber gridshell study and design, project relevance to freeform and timber gridshells, prototyping and automation of Re-De-Form,

At first, the literature review, provides with the necessary knowledge to understand these aspects. Later on, the design of the Re-De-Form workflow is based upon that feedback and as it evolves in chapter 5 its relevance in architecture, engineering and fabrication can be seen in *Figure 102*.

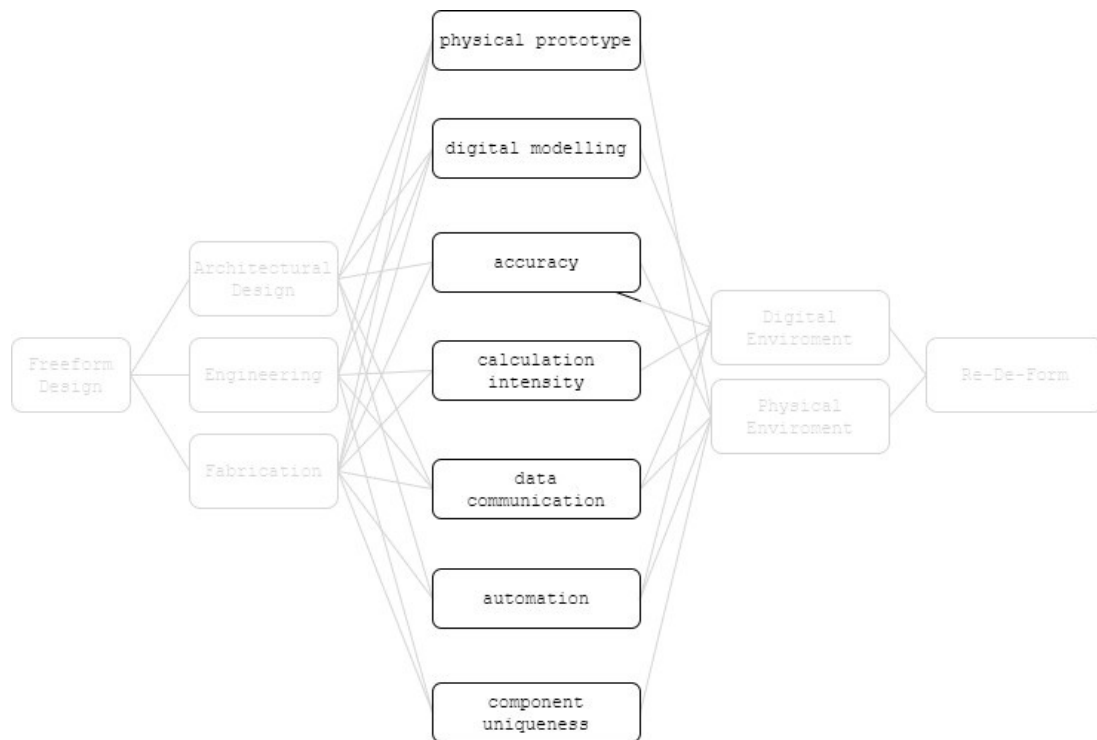


Figure 102 Re-De-Form responds to the Freeform Design's challenges . Source: own illustration

The project starts with form finding of a freeform surface. The computational method utilized is the Particle-Spring-Method by the Physics Engine of the KangarooV2 plug-in. It simulates the physical behaviour of a freeform geometry under certain constraints. For the form finding of timber gridshells physical modelling is necessary. It starts from a flat sheet of laths that are pushed towards the center and when the final form is decided the structure is fixed in place. Here, the suggestion is that instead of creating a new physical model every time minor changes happen, a digital simulation will run on the computer.



Then, the initial freeform surface is used to generate a timber gridshell geometry. The structural analysis performed provides with useful feedback about the behaviour of the structure in several load-case scenarios. The designer avoids manual, time-consuming and complicated structural calculations needed during the structural analysis of a timber gridshell structure. Re-De-Form facilitates these through the use of the Karamba 3D plugin.

What is more, the designer can decide certain design aspects of the timber gridshell after the form finding is performed. These are the cross-section type and dimensions or the distance of the panels from the main lath structure. A possible future upgrade would be the application of a nodal connection at the intersection points of the laths. The designer would be able to customize the nodal connection according to his needs.

Furthermore, the panelization of the gridshell is studied through Re-De-Form. The surface of the panels is an offset from the main surface of the laths meaning that its local curvatures are dependent on the local curvatures of the surface underneath. In the future this could be more customizable based on the structure's demand for daylight, transparency or the designer's intent. For example, each panel could undergo removal of material or some of its edges would lift from the main surface's curvature for more light to enter the interior of the structure. In this case, Re-De-Form is the foundation for a digital modelling mechanism that touches the fields of architecture, engineering and fabrication.

The demand for component uniqueness in Freeform Design is also addressed in Chapter 5. Since the studied surface is not discretized into a mesh for panel fabrication, the curvature of each panel is different. To fabricate these a huge amount of molds would be needed. Instead the physical prototype of Re-De-Form can be used multiple times for panel fabrication since it can receive these curvatures. The automation of the system replaces the manual adjustments of former formworks to a more accurate and fast mechanism for panel production.

Also, the data communication between the digital and physical will allow for the use of the formwork during the form finding phase as a physical modelling mechanism. That possibility needs to be tested further, mainly due to certain physical limits of the prototype. Some of them are: the critical height difference between the pins, the pin number and in-between distances, the surface material, the surface's cutting pattern, the magnet connections.

Overall, Re-De-Form is a mechanism that can be used for physical prototyping. It is packed with a digital modelling software that helps the designer generate freeform gridshells and structurally analyze them, while replacing the intensity of manual calculations. The formwork is used for freeform designing in different scales, from the 1:1 scale, panel fabrication to 1:10 or 1:20 scale, physical modelling. And lastly, its automation has provided with the accuracy and speed required for freeform surface study and panel fabrication.

## 6.2 Reflection

My thesis is fulfilled within the Building Technology, Sustainable Graduation Studio. The main idea is to create a digital and physical workflow that utilize a flexible formwork capable of adapting to the complex curvature of a freeform surface. Contemporary freeform architecture has been a challenging practice due to the fact that after panelization, a great amount of molds is needed for fabrication. The formwork proposed aims to overcome that problem by enabling the reuse of the same mold for all unique panels of the structure.

The topic is related to ongoing architectural practice and academi research that has been on the forefront for the last 60 years. Particularly, Re-De-Form is the upgrade of the FlexiMold, a project developed by Asut and Meijer (2016) for the Technoledge Design Informatics course. FlexiMold, a flexible formwork required the use of manual pin adjustment after reading their height values from the computer. Re-De-Form is an automated formwork that positions the pins by reading the values from the computer without manual adjustment per pin. The formwork developed will be used as a physical modelling mechanism for gridshell surfaces and panel fabrication.

On the scope of Design Informatics, computational methods were developed that make use Rhinoceros, Grasshopper, Firefly, Karamba3D and Kangaroo V2 and connect the Re-De-Form's physical and digital environment. On the scope of Building Product Innovation, the Re-De-Form workflow was related to the building environment as a physical modelling and fabrication mechanism and its prototype was built in the faculty of Architecture, BK. Prototyping involved an iterative research by design process from component conceptualization towards, creation, testing and failure or success.

Through the process I acquired a lot of knowledge regarding Computational Design methods, prototype building and project application in the building environment. The skills I have acquired in computation through TU Delft and model making from my previous studies in NTUA, helped me design the digital and physical environment. Also, I was not familiar with the Arduino microcontroller technology but I was eager to learn about it through my thesis. I am very content that in the end it worked out and that I managed to narrow down the possible future upgrades the system. It gives me a sense that I understand the project and I am capable of communicating it.

What is more, I came across several difficulties that are also caused by the Covid-19 pandemic. Some of the rooms of the BK faculty were closed and I was not able to get the equipment needed for the prototype. As I was delaying with the building of the prototype, I realized that I need to acquire the components needed myself and not depend on their availability in the faculty. Also, at the start of my project the meetings of my mentors were held online and sometimes I sensed that if they were held physically I would be more capable of understanding the feedback they gave me. Hopefully, Olga proposed that we have a walking talking session after P2 and that helped me structure the scope of my project.

To conclude, my project has been very creative and educative from the start. I was introduced to new technologies, building design methods and had the chance to experiment through prototyping in the Modelling Hall of BK. Until the P5 I have been working on context of the report and the connection of Re-De-Form to the built environment. The detailing of the prototype and the future upgrades have been thoroughly analyzed in the case a similar project is developed in the faculty. They can be used as feedback for the production of a possible upgrade. (End of chapter)



## Bibliography

Adapa (n.d.) *Adapa-AS-User-Manual-D100-300-English-05.2021-Web.pdf*. Available at: <https://adapa.dk/wp-content/plugins/pdf-poster/pdfs/web/viewer.php?file=https://adapa.dk/wp-content/uploads/2020/11/Adapa-AS-User-Manual-D100-300-English-05.2021-Web.pdf&download=true&print=true&openfile=false> (Accessed: 26 June 2021).

Adriaenssens, Block, Veenendaal and Williams (2014) 'Shell Structures for Architecture - Form Finding and Optimization', in *Shell Structures for Architecture*. doi: 10.4324/9781315849270.

Andy Payne and Kelly Johnson (2015) *Firefly Experiments, Firefly Experiments*. Available at: <http://www.fireflyexperiments.com> (Accessed: 13 May 2021).

Asut and Meijer (2016) 'FlexiMold: Teaching Numeric Control through a Hybrid Device', *undefined*. Available at: [/paper/FlexiMold%3A-Teaching-Numeric-Control-through-a-A%C2%BAut/39be5c956d343355535820be9bdb89073895739f](#) (Accessed: 18 June 2021).

Asut, S., Eigenraam, P. and Christidi (2018) 'Re-flex: Responsive Flexible Mold for Computer Aided Intuitive Design and Materialization', *Proceedings of the 36th eCAADe Conference*, 1. Available at: <https://repository.tudelft.nl/islandora/object/uuid%3Ac2799763-fb3d-4b11-9dd8-94e730a3797d> (Accessed: 22 January 2021).

Bassegoda Nonell (2000) *Antonio Gaudi: Master Architect*. Available at: [https://www.goodreads.com/work/best\\_book/881968-antonio-gaudi-master-architect](https://www.goodreads.com/work/best_book/881968-antonio-gaudi-master-architect) (Accessed: 25 February 2021).

Borgart, A. and Kocaturk, T. (2008) 'Free-Form Design as the Digital Zeitgeist'. Available at: [https://www.academia.edu/2203067/Free\\_Form\\_Design\\_as\\_the\\_Digital\\_Zeitgeist](https://www.academia.edu/2203067/Free_Form_Design_as_the_Digital_Zeitgeist) (Accessed: 16 March 2021).

Cheng, S., Zhang, X. and Tang, K. (2007) 'Shape Modification of B-Spline Curve with Geometric Constraints', in *2007 International Conference on Computational Intelligence and Security (CIS 2007)*. *2007 International Conference on Computational Intelligence and Security (CIS 2007)*, pp. 325–329. doi: 10.1109/CIS.2007.43.

Ching (2014) *Architecture: Form, Space, and Order, 4th Edition | Wiley, Wiley.com*. Available at: <http://www.wiley.com/en-nl/Architecture%3A+Form%2C+Space%2C+and+Order%2C+4th+Edition-p-9781118745137> (Accessed: 22 February 2021).

Cité de la dentelle et de la mode (n.d.) *Samples register, Google Arts & Culture*. Available at: <https://artsandculture.google.com/asset/samples-register/vQGUTf9ywfZjjQ> (Accessed: 19 June 2021).

Douthe, C., Baverel, O. and Caron, J.-F. (2006) 'Form-finding of a grid shell in composite materials', *Journal of the International Association for Shell and Spatial Structures*, 47.

Eigensatz, M. et al. (2016) *4. Case Studies in Cost-Optimized Paneling of Architectural Freeform Surfaces, Advances in Architectural Geometry 2010*. Ambra Verlag, pp. 49–72. Available at: <https://www.degruyter.com/document/doi/10.1515/9783990433713-005/html> (Accessed: 19 June 2021).

Hadjri, K. (2005) 'Assessing the Use of Contact and Non-Contact 3- Dimensional Digitization in Architectural Design Studios', p. 9.

Happold and Liddell (1975) 'TIMBER LATTICE ROOF FOR THE MANNHEIM BUNDESGARTENSCHAU', *TIMBER LATTICE ROOF FOR THE MANNHEIM BUNDESGARTENSCHAU*.

Harris, R. et al. (2003) 'Design and construction of the Downland Gridshell', *Building Research & Information*, 31(6), pp. 427–454. doi: 10.1080/0961321032000088007.

Harris, R. and Kelly, O. (2002) 'The structural engineering of the Downland gridshell', in *Space Structures 5*. Thomas Telford Publishing, p. 1: 161-172. doi: 10.1680/ss5v1.31739.0018.

Henriksson, V. and Hult, M. (2015) 'Rationalizing freeform architecture - Surface discretization and multi-objective optimization'. Available at: <https://odr.chalmers.se/handle/20.500.12380/231658> (Accessed: 19 June 2021).

Kilian, A. (2004) 'Linking Digital Hanging Chain Models to Fabrication', *Fabrication: Examining the Digital Practice of Architecture [Proceedings of the 23rd Annual Conference of the Association for Computer Aided Design in Architecture and the 2004 Conference of the AIA Technology in Architectural Practice Knowledge Community / ISBN 0-9696665-2-7] Cambridge (Ontario) 8-14 November, 2004*, 110-125.

Kolarevic, B. (2004) *Architecture in the Digital Age: Design and Manufacturing*. Taylor & Francis.

Kotnik, T. and Weinstock, M. (2012) 'Material, Form and Force', *Architectural Design*, 82(2), pp. 104–111. doi: <https://doi.org/10.1002/ad.1386>.

Kuijvenhoven, M. and Hoogenboom, P. C. J. (2012) 'Particle-spring method for form finding grid shell structures consisting of flexible members', *Journal of the International Association for Shell and Spatial Structures*, 53(1), pp. 31–38.

Lewis, W. (2003) 'Tension Structures Form and Behaviour'.

Michiels, T., Adriaenssens, S. and Dejong, M. (2019) 'Form finding of corrugated shell structures for seismic design and validation using non-linear pushover analysis', *Engineering Structures*, 181, pp. 362–373. doi: 10.1016/j.engstruct.2018.12.043.

Naicu, D., Harris and Williams (2014) *Timber gridshells: Design methods and their application to a temporary pavilion, WCTE 2014 - World Conference on Timber Engineering, Proceedings*.

Oxman, R. (2006) 'Theory and design in the first digital age', *Design Studies*, 27(3), pp. 229–265. doi: 10.1016/j.destud.2005.11.002.

Pottmann et al (2007) *Architectural Geometry*. Available at: [https://app-knovel-com.tudelft.idm.oclc.org/web/toc.v/cid:kpAG000001/viewerType:toc//root\\_slug:architectural-geometry?kpromoter=marc](https://app-knovel-com.tudelft.idm.oclc.org/web/toc.v/cid:kpAG000001/viewerType:toc//root_slug:architectural-geometry?kpromoter=marc) (Accessed: 22 February 2021).

Qin Peng Li (2018) 'A+BE | Architecture and the Built Environment, No 2 (2018): Form Follows Force'. doi: 10.7480/ABE.2018.2.

Schiftner, A. et al. (2013) 'Architectural Geometry from Research to Practice: The Eiffel Tower Pavilions', in Hesselgren, L. et al. (eds) *Advances in Architectural Geometry 2012*. Vienna: Springer, pp. 213–228. doi: 10.1007/978-3-7091-1251-9\_17.

Schipper, R. (2015) *Double-curved precast concrete elements - Research into technical viability of the flexible mould method*. doi: 10.4233/uuid:cc231be1-662c-4b1f-a1ca-8be22c0c4177.

Shelden, D. R. (Dennis R. (2002) *Digital surface representation and the constructibility of Gehry's architecture*. Thesis. Massachusetts Institute of Technology. Available at: <https://dspace.mit.edu/handle/1721.1/16899> (Accessed: 26 February 2021).

Spuybroek, L. and DeLanda, M. (2004) *NOX: Machining Architecture*. Thames & Hudson.

Tang, G., Chilton, J. C. and Beccarelli, P. (2013) *Progressive Development of Timber Gridshell Design, Analysis and Construction: Paper 1387*.

Tomiric (2013) *Freeform Geometries in Wood Construction*. Available at: <https://www.google.com/search?q=Freeform+Geometries+in+Wood+Construction+-+Marko+Tomicic&oq=Freeform+Geometries+in+Wood+Construction+-+Marko+Tomicic&aqs=chrome.69j69j60l2.615j0j4&sourceid=chrome&ie=UTF-8> (Accessed: 19 June 2021).

Toussaint, M. H. (2007) 'A design tool for timber gridshells: The development of a grid generation tool'. Available at: <https://repository.tudelft.nl/islandora/object/uuid%3A883da6d1-8f61-47db-afb8-099aa2ab536c> (Accessed: 19 June 2021).

Van de Straat, R. J. (2011) 'Parametric modelling of architectural developables'. Available at: <https://repository.tudelft.nl/islandora/object/uuid%3A9e0b4972-9fa3-4487-be81-71b5e5ada11a> (Accessed: 19 June 2021).

Williams (2014) *What is a shell?, Shell Structures for Architecture*. Routledge, pp. 35–46. doi: 10.4324/9781315849270-11.

Zellner, P. (2000) *Hybrid Space: New Forms in Digital Architecture*. Thames & Hudson.

(End of chapter)

## Appendix

### Form-Finding (KangarooV2 Physics)

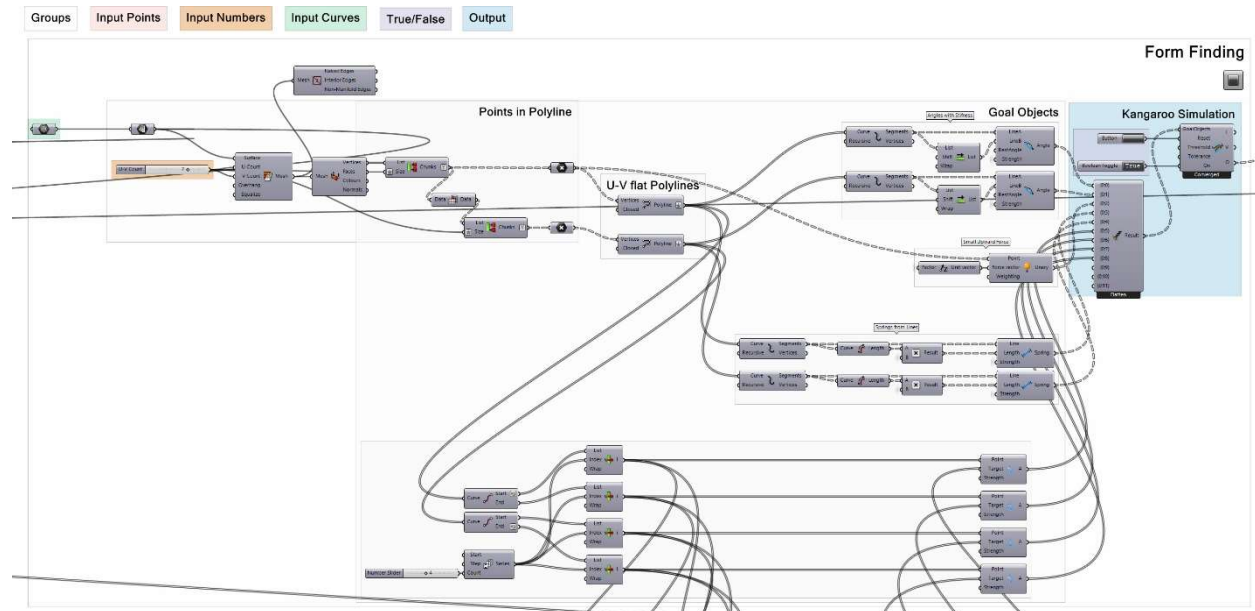


Figure 103 Form-Finding of a freeform surface. Source: own illustration

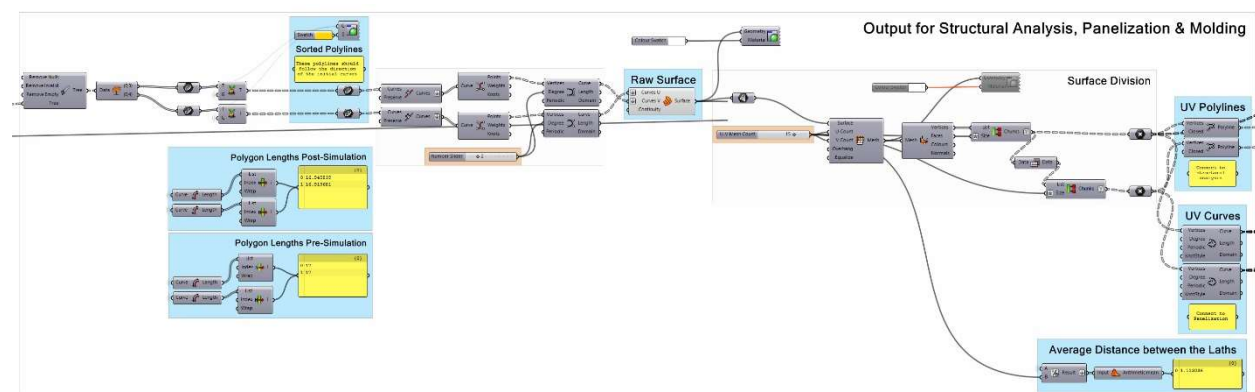


Figure 104 Output for Structural Analysis, Panelization and Molding. Source: own illustration



## The gridshell model

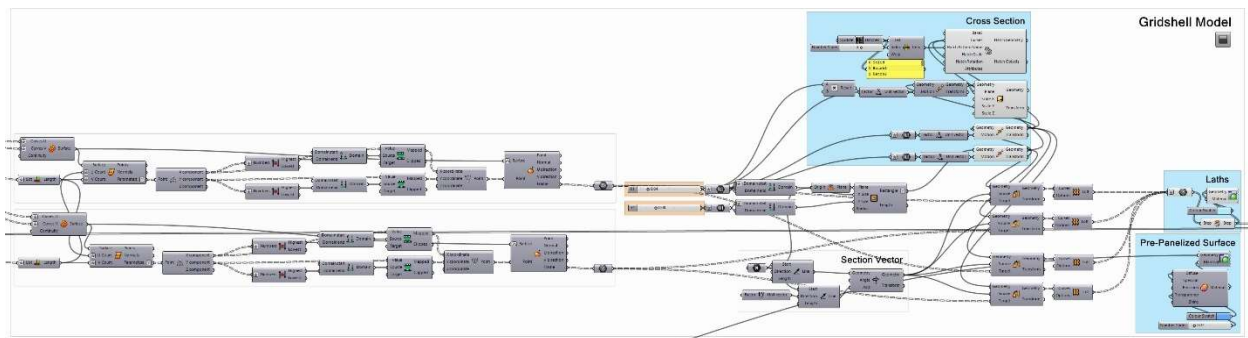


Figure 105 The gridshell. The cross-section and the pre-panelized surface are defined. Source: own illustration

## Structural Analysis

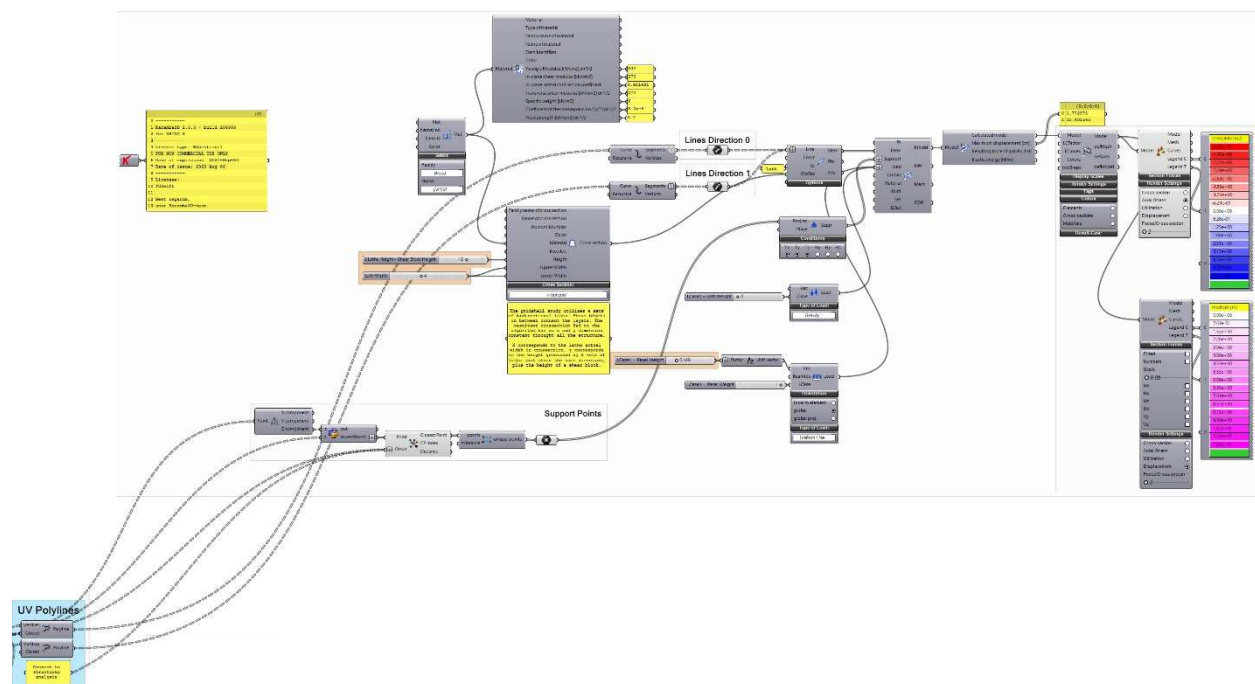


Figure 106 The structural Analysis of the timber gridshell. Source: own illustration

## Panelization and grid placement

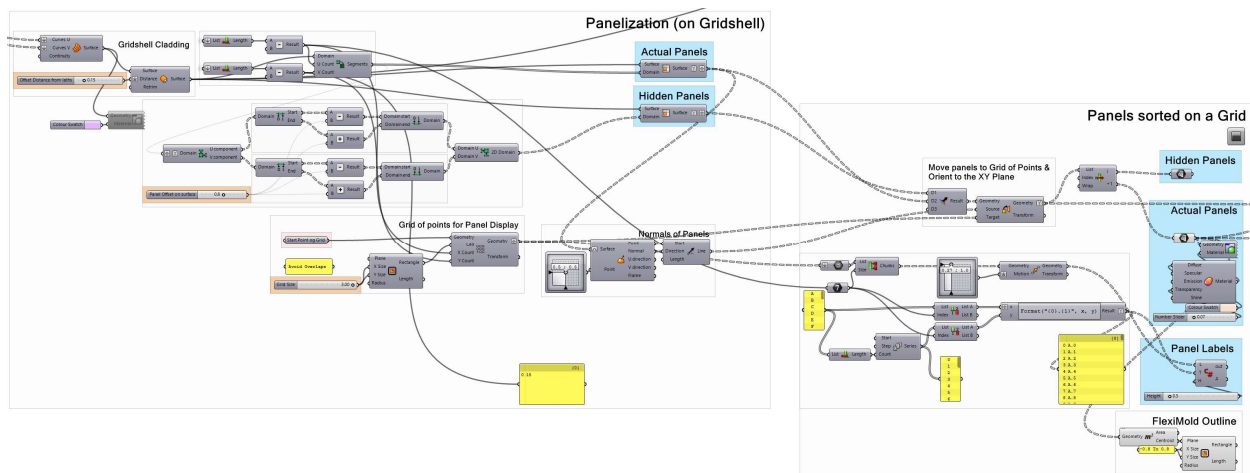


Figure 107 Source:own illustration

## Panel rotational correction



Figure 108 Source: own illustration

## Digital Re-De-Form

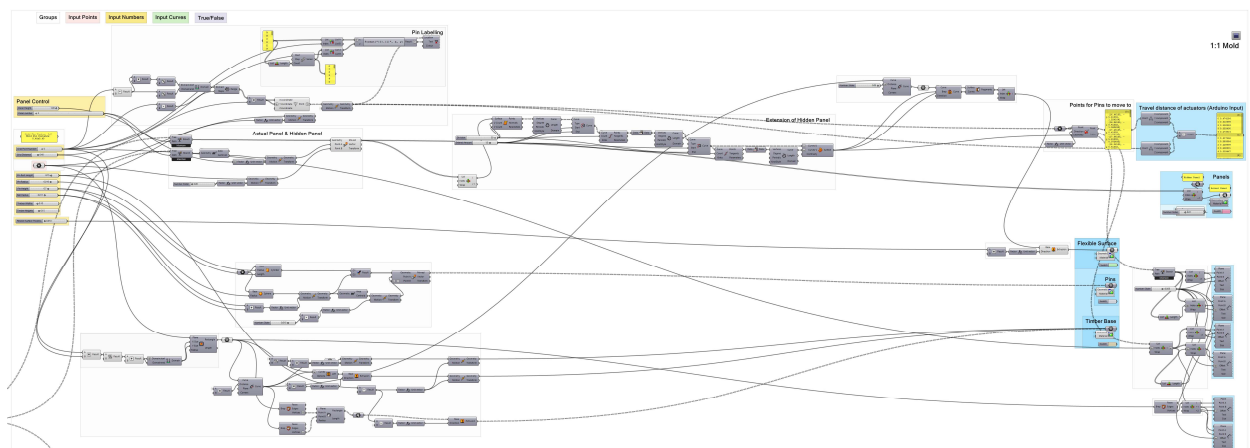


Figure 109 1:1 model. Source: own illustration

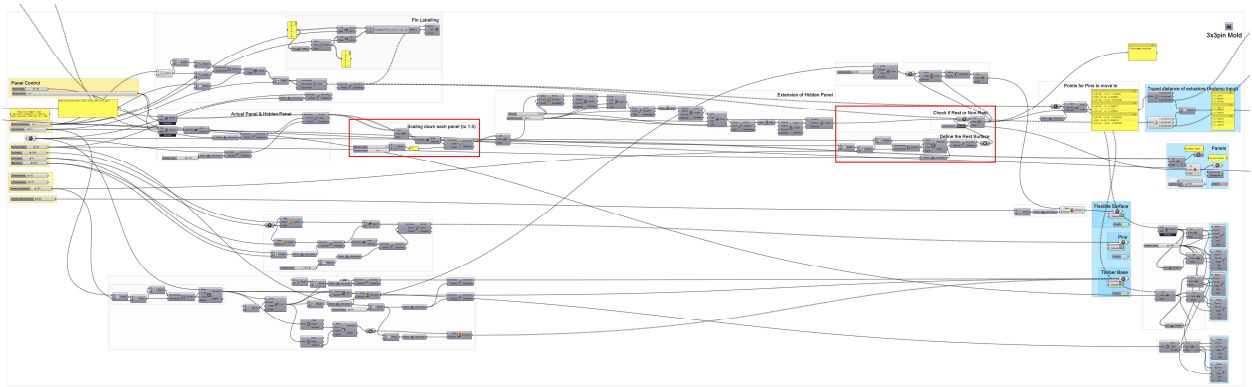


Figure 111 3x3 pin Re-De-Form. Source: own illustration

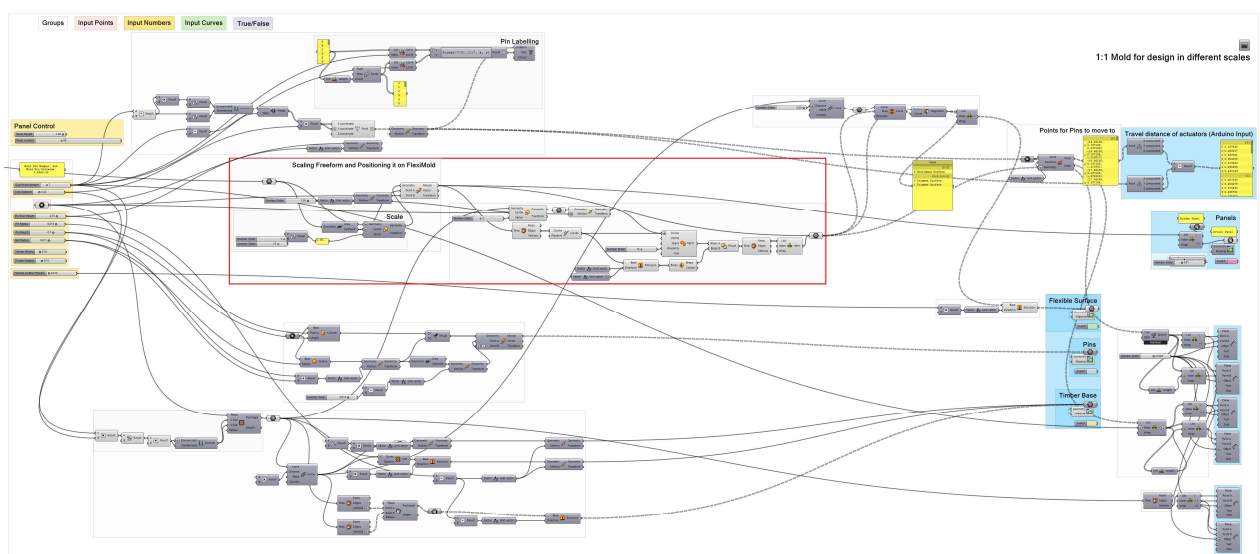


Figure 110 Design in different scales

## Output for Arduino IDE

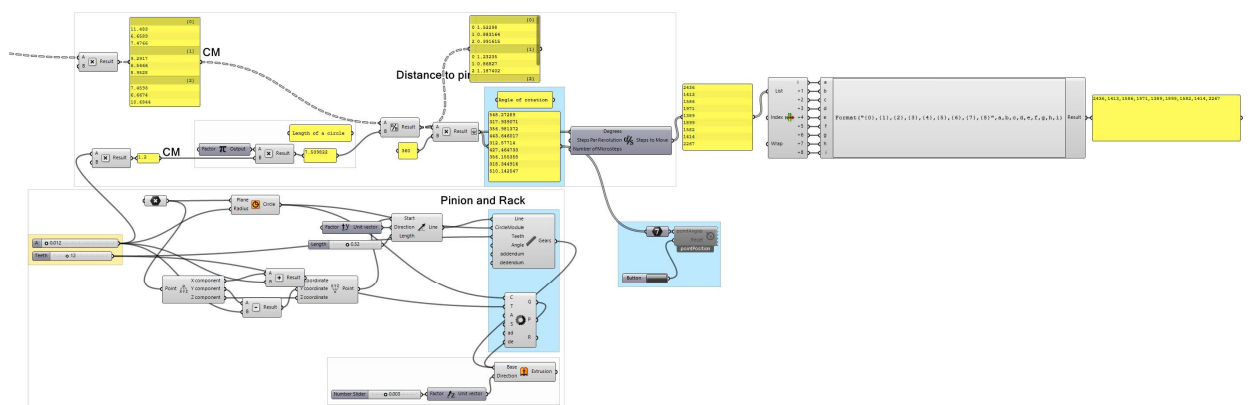


Figure 112 The output String the Arduino reads. Source: own illustration

## Arduino Sketch

```
#include "AccelStepper.h"
// Library created by Mike McCauley at http://www.airspayce.
com/mikem/arduino/AccelStepper/

// AccelStepper Setup
AccelStepper stepperA(1, 2, 3); // 1 = Easy Driver interface
                                // NANO Pin 2 connected to STEP pin of Easy
Driver
                                // NANO Pin 3 connected to DIR pin of Easy
Driver
AccelStepper stepperB(1, 4, 5);
AccelStepper stepperC(1, 6, 7);
AccelStepper stepperD(1, 8, 9);
AccelStepper stepperE(1, 10, 11);
AccelStepper stepperF(1, 12, 13);
AccelStepper stepperG(1, 22, 23);
AccelStepper stepperH(1, 24, 25);
AccelStepper stepperI(1, 26, 27);

// Stepper Travel Variables

// Used to store the X value entered in the Serial Monitor
long A = 0;
long B = 0;
long C = 0;
long D = 0;
long E = 0;
long F = 0;
long G = 0;
long H = 0;
long I = 0;

long limitMin = 0;
long limitMax = 3000;

float speedSet = 1000;
float accelerationSet = 600;

int move_finished=1; // Used to check if move is completed

void setup() {
  Serial.begin(9600); // Start the Serial monitor with speed of 9600 Bauds
  delay(5); // Wait for EasyDriver wake up

  // Steppers are Home
  Serial.print("Steppers are Home ");
  Serial.println();
}
```

```
stepperA.setCurrentPosition(0);
stepperA.setMaxSpeed(600.0);    // Set Max Speed of Stepper (Faster for
regular movements)
stepperA.setAcceleration(400.0); // Set Acceleration of Stepper

stepperB.setCurrentPosition(0);
stepperB.setMaxSpeed(600.0);    // Set Max Speed of Stepper (Faster for
regular movements)
stepperB.setAcceleration(400.0); // Set Acceleration of Stepper

stepperC.setCurrentPosition(0);
stepperC.setMaxSpeed(speedSet); // Set Max Speed of Stepper (Faster for
regular movements)
stepperC.setAcceleration(accelerationSet); // Set Acceleration of Stepper

stepperD.setCurrentPosition(0);
stepperD.setMaxSpeed(600.0);    // Set Max Speed of Stepper (Faster for
regular movements)
stepperD.setAcceleration(400.0); // Set Acceleration of Stepper

stepperE.setCurrentPosition(0);
stepperE.setMaxSpeed(600.0);    // Set Max Speed of Stepper (Faster for
regular movements)
stepperE.setAcceleration(400.0); // Set Acceleration of Stepper

stepperF.setCurrentPosition(0);
stepperF.setMaxSpeed(600.0);    // Set Max Speed of Stepper (Faster for
regular movements)
stepperF.setAcceleration(400.0); // Set Acceleration of Stepper

stepperG.setCurrentPosition(0);
stepperG.setMaxSpeed(600.0);    // Set Max Speed of Stepper (Faster for
regular movements)
stepperG.setAcceleration(400.0); // Set Acceleration of Stepper

stepperH.setCurrentPosition(0);
stepperH.setMaxSpeed(600.0);    // Set Max Speed of Stepper (Faster for
regular movements)
stepperH.setAcceleration(400.0); // Set Acceleration of Stepper

stepperI.setCurrentPosition(0);
stepperI.setMaxSpeed(600.0);    // Set Max Speed of Stepper (Faster for
regular movements)
stepperI.setAcceleration(400.0); // Set Acceleration of Stepper

stepperB.setCurrentPosition(0);
stepperB.setMaxSpeed(600.0);    // Set Max Speed of Stepper (Faster for
regular movements)
stepperB.setAcceleration(400.0); // Set Acceleration of Stepper
```

```
// Print out Instructions on the Serial Monitor at Start
Serial.print("Enter Travel distance | Between 0 to 3000 | Zero for back to
Home");
}

void loop() {

  while (Serial.available()>0) { // Check if values are available in the Serial
Buffer

    move_finished=0; // Set variable for checking move of the Stepper

    // Put numeric value from buffer in TravelX variable
    A = Serial.parseInt();
    B = Serial.parseInt();
    C = Serial.parseInt();
    D = Serial.parseInt();
    E = Serial.parseInt();
    F = Serial.parseInt();
    G = Serial.parseInt();
    H = Serial.parseInt();
    I = Serial.parseInt();

    if (A < limitMin || A > limitMax || B < limitMin || B > limitMax || C <
limitMin || C > limitMax || D < limitMin || D > limitMax || E < limitMin || E >
limitMax || F < limitMin || F > limitMax || G < limitMin || G > limitMax || H <
limitMin || H > limitMax || I < limitMin || I > limitMax) { // Make sure the
position entered is not beyond the HOME or MAX position

      Serial.println("");
      Serial.println("Please enter a value greater than zero and smaller or equal
to ");
      Serial.println(limitMax);
    } else {
      Serial.println("");
      Serial.print("Moving stepperA into position: ");
      Serial.println(A);
      Serial.print("Moving stepperB into position: ");
      Serial.println(B);
      Serial.print("Moving stepperC into position: ");
      Serial.println(C);
      Serial.print("Moving stepperD into position: ");
      Serial.println(D);
      Serial.print("Moving stepperE into position: ");
      Serial.println(E);
      Serial.print("Moving stepperF into position: ");
      Serial.println(F);
    }
  }
}
```

```

    Serial.print("Moving stepperG into position: ");
    Serial.println(G);
    Serial.print("Moving stepperH into position: ");
    Serial.println(H);
    Serial.print("Moving stepperI into position: ");
    Serial.println(I);

    stepperA.moveTo(A); // Set new moveto position of Stepper
    stepperB.moveTo(B); // Set new moveto position of Stepper
    stepperC.moveTo(C); // Set new moveto position of Stepper
    stepperD.moveTo(D); // Set new moveto position of Stepper
    stepperE.moveTo(E); // Set new moveto position of Stepper
    stepperF.moveTo(F); // Set new moveto position of Stepper
    stepperG.moveTo(G); // Set new moveto position of Stepper
    stepperH.moveTo(H); // Set new moveto position of Stepper
    stepperI.moveTo(I); // Set new moveto position of Stepper

    delay(1000); // Wait 1 seconds before moving the Stepper
  }
}

/* if (A >= limitMin && A <= limitMax && B >= limitMin && B <= limitMax && C >=
limitMin && C <= limitMax && D >= limitMin && D <= limitMax &&
  E >= limitMin && E <= limitMax && F >= limitMin && F <= limitMax && G >=
limitMin && G <= limitMax && H >= limitMin && H <= limitMax && I >= limitMin && I
<= limitMax) {
    Serial.print("Steppers are given valid numbers");
    delay(1000);

// Check if the Stepper has reached desired position
    if ((stepperA.distanceToGo() != 0) && (stepperB.distanceToGo() != 0) &&
(stepperC.distanceToGo() != 0) && (stepperD.distanceToGo() != 0)
    && (stepperE.distanceToGo() != 0) && (stepperF.distanceToGo() != 0) &&
(stepperG.distanceToGo() != 0) && (stepperH.distanceToGo() != 0) && (stepperI.
distanceToGo() != 0 )){

        stepperA.run(); // Move Stepper into position
        stepperB.run(); // Move Stepper into position
        stepperC.run(); // Move Stepper into position
        stepperD.run(); // Move Stepper into position
        stepperE.run(); // Move Stepper into position
        stepperF.run(); // Move Stepper into position
        stepperG.run(); // Move Stepper into position
        stepperH.run(); // Move Stepper into position
        stepperI.run(); // Move Stepper into position

```



```

    }
    */
    stepperA.run(); // Move Stepper into position
    stepperB.run(); // Move Stepper into position
    stepperC.run(); // Move Stepper into position
    stepperD.run(); // Move Stepper into position
    stepperE.run(); // Move Stepper into position
    stepperF.run(); // Move Stepper into position
    stepperG.run(); // Move Stepper into position
    stepperH.run(); // Move Stepper into position
    stepperI.run(); // Move Stepper into position

// If move is completed display message on Serial Monitor
    if ((move_finished == 0) && (stepperA.distanceToGo() == 0) && (stepperB.
distanceToGo() == 0) && (stepperC.distanceToGo() == 0) && (stepperD.
distanceToGo() == 0)
    && (stepperE.distanceToGo() == 0) && (stepperF.distanceToGo() == 0) &&
(stepperG.distanceToGo() == 0) && (stepperH.distanceToGo() == 0) && (stepperI.
distanceToGo() == 0) ) {
        Serial.println("COMPLETED!");
        Serial.println("");
        Serial.println("Enter Travel distance | Between 0 to 1200 | Zero for back to
Home");
        move_finished=1; // Reset move variable
    }
}

```

Figure 113 The Arduino Sketch fed into the Arduino Megaboard. Source: own illustration

## Model Pictures



Figure 114 The components of the prototype. Source: own illustration

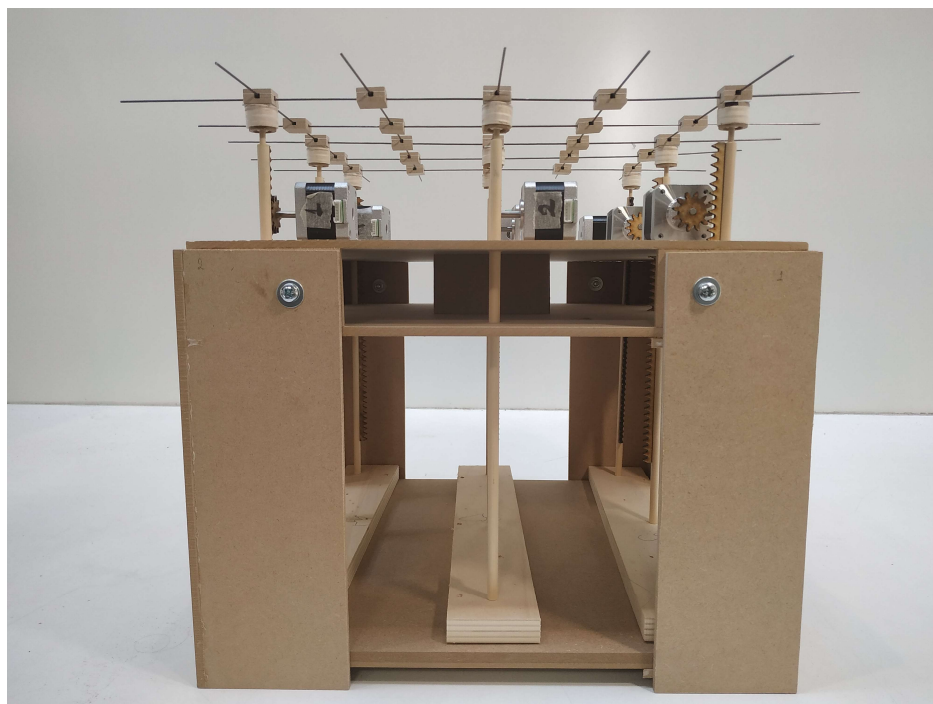


Figure 115 The prototype before the automation. Source: own illustration

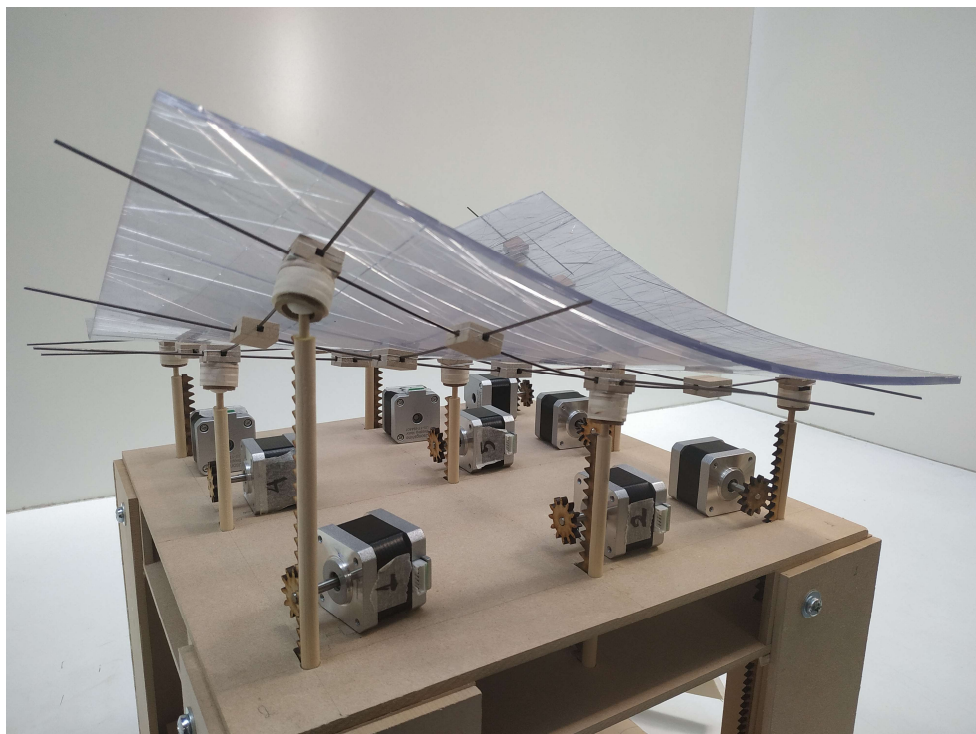
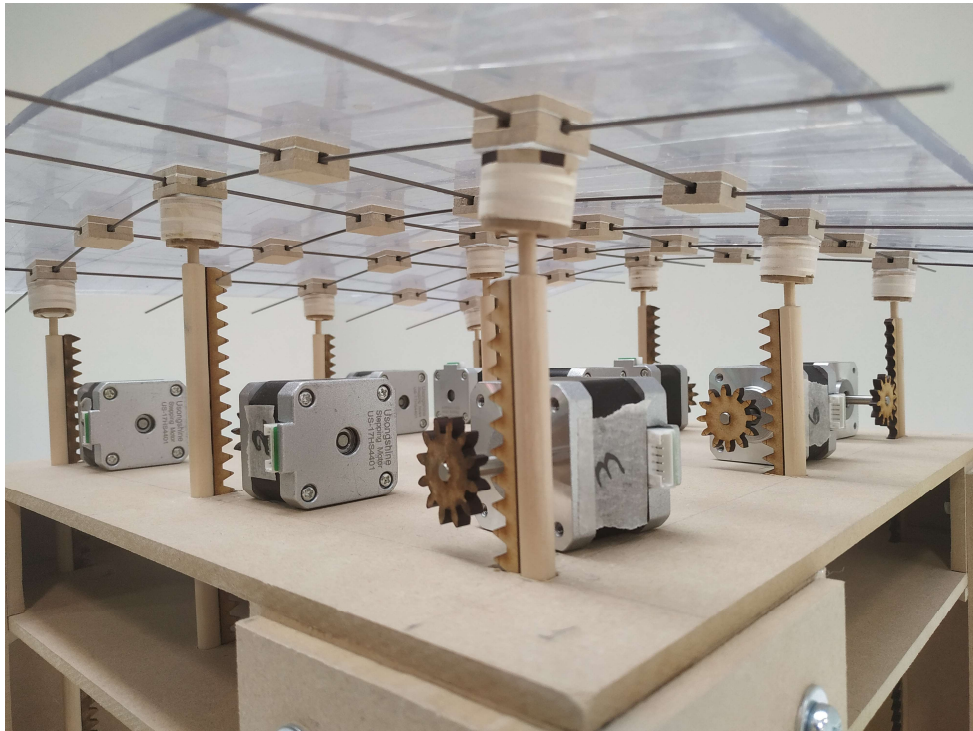


Figure 116 Testing possible curvatures with a flexible surface on top. Source: own illustration



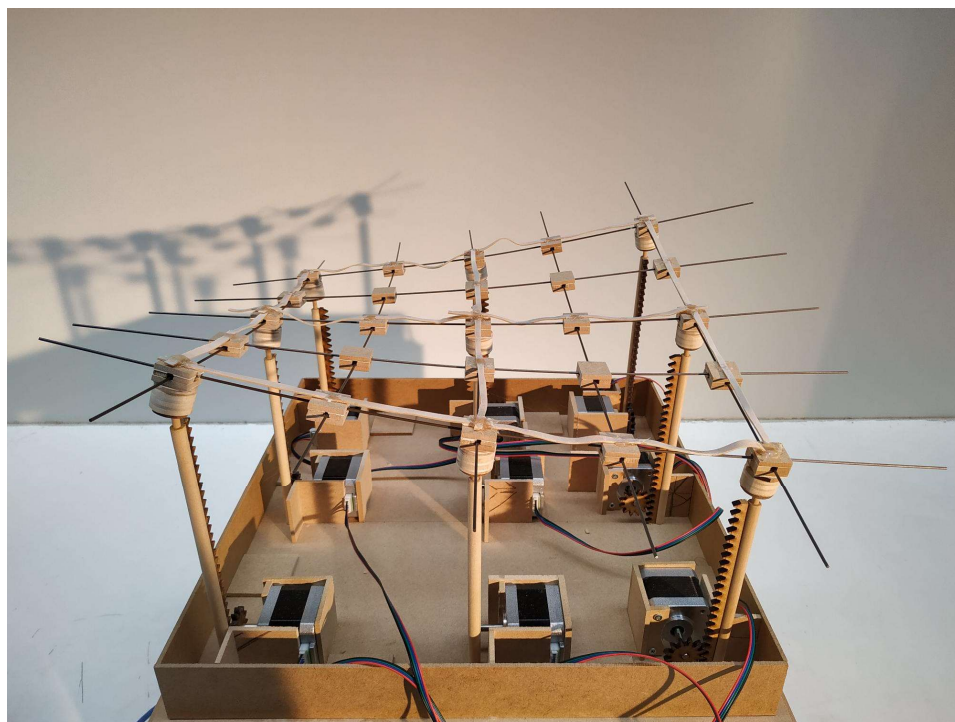
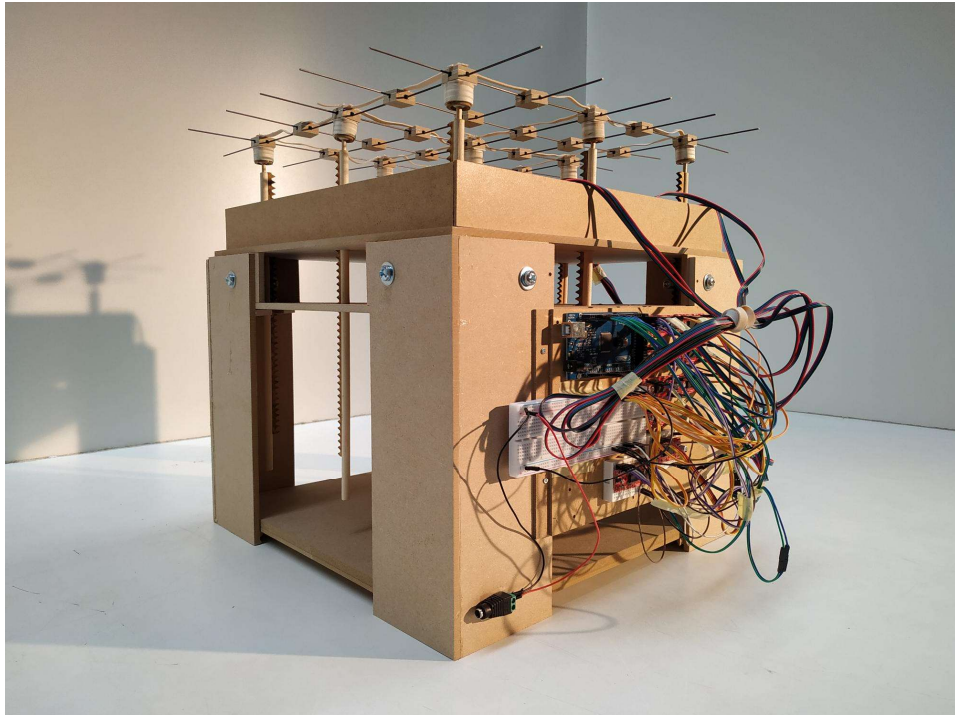


Figure 117 The automated Re-De-Form with the rubber bands added. Source: own illustration



Figure 118 Me, prototyping. Source: own illustration